

AD-423584

FEMA-Library
[Signature]
3131A

Final Technical Report

PROJECT NO. A-633

EVALUATION OF WATER CONTAMINATION FROM FALLOUT

W. N. GRUNE

T. F. CRAFT, JR.

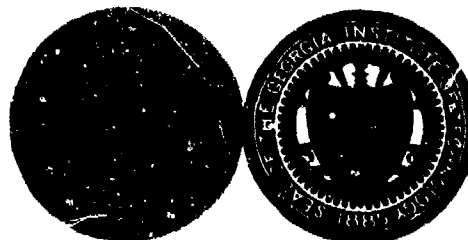
W. M. SLOAN

Covering the Period
May 9, 1962 to July 31, 1963

CONTRACT NO. OCD-OS-62-189
OCD Subtask 3131A

Performed for

OFFICE OF CIVIL DEFENSE
DEPARTMENT OF DEFENSE
Washington 25, D. C.



Engineering Experiment Station
GEORGIA INSTITUTE OF TECHNOLOGY
Atlanta, Georgia

82 06 03 003

Qualified requestors may obtain copies of
this report from Defense Documentation
Center, Arlington Hall Station, Arlington,
Virginia.

Final Technical Report

PROJECT NO. A-633

EVALUATION OF WATER CONTAMINATION FROM FALLOUT

by

W. N. GRUNE

T. F. CRAFT, JR.

W. M. SLOAN

Covering the Period

May 9, 1962 to July 31, 1963

CONTRACT NO. OCD-OS-62-189

OCD Subtask 3131A

Performed for

OFFICE OF CIVIL DEFENSE
DEPARTMENT OF DEFENSE
Washington 25, D. C.

This report has been reviewed in the Office of Civil Defense and approved for publication. Approval does not signify that the contents necessarily reflect the views and policies of the Office of Civil Defense.

ABSTRACT

Methods for obtaining ionization rate contours, fractionation numbers, atom-concentration intensity ratios, and particle size distribution from the Miller fallout model are given. Included are complete computer programs for estimating sublimation pressures, ionization rate contours, and particle size parameters.

Graphical integration of activity from fallout over the watersheds serving Houston, Texas and New York City is described. Maximum levels of selected contaminants at the water intake for these cities under most adverse wind conditions were calculated and reported in $\mu\text{c/ml}$ as follows: New York City; Sr-89, 6.8×10^{-3} ; Sr-90, 5.9×10^{-5} ; Ru-106, 7.1×10^{-4} ; I-131, 7.6×10^{-2} ; Cs-137, 4.4×10^{-5} ; Ba-140, 5.8×10^{-2} . Houston; Sr-89, 1.9×10^{-2} ; Sr-90, 1.9×10^{-4} ; Ru-106, 2.5×10^{-3} ; I-131, 2.5×10^{-1} ; Cs-137, 1.0×10^{-4} ; Ba-140, 1.9×10^{-1} .

It is concluded that the contribution of induced radioactivity to the contamination of water supplies would not be significant.

Many commercially available instruments of the survey type can be used to detect adequately the presence of substantial concentrations of radioisotopes in water under emergency conditions. For more accurate measurement of such concentrations down to safe levels more sensitive equipment or methods of preconcentration of the samples are needed. Such methods or instruments should extend the range of sensitivity by a factor of the order of 100 and should be readily adaptable for field use. Outlines of procedures for the analysis of radioactivity in water are given. Efficiency of water decontamination by various methods is discussed.

Body burdens of individual radioisotopes may be determined from a consideration of the rate of ingestion, the effective decay rate, and the

affinity for the isotope of the critical organ. It is believed that uptake of radioactive isotopes may be reduced or prevented by selective blocking of critical organs with stable isotopes.

TABLE OF CONTENTS

	<u>Page</u>
ABSTRACT	iii
LIST OF FIGURES	vii
LIST OF TABLES	viii
I. INTRODUCTION	1
II. SUMMARY OF ANALYSIS OF THE O.C.D. FALLOUT MODEL	5
A. Basic Assumptions of the O.C.D. Fallout Model	5
B. Formation and Geometry of Stem and Cloud	6
C. Particle Size Parameter and Ionization Rate Contours	7
D. Condensation of Fallout and Fractionation Numbers	14
E. Conversion between Intensity and Activity	25
F. Biological Availability and Atom-Concentration Intensity Ratio	34
G. Ionization Rate Contour Ratios and Particle Size Distribution	35
H. Conclusion - The Reality and Applications of the O.C.D. Model	39
III. COMPUTATIONAL METHODS OF THE FALLOUT MODEL	41
A. Ionization Rate Contours	41
B. Fractionation Numbers	59
1. First Period of Condensation	59
2. Second Period of Condensation	61
3. Gross Fractionation Number	65
C. Activity-Concentration Intensity Ratio	66
D. Particle Size Distribution	69
IV. INDUCED RADIOACTIVITY IN SOILS	75
V. TRANSPORT OF FALLOUT PARTICLES BY SURFACE WATER	85
VI. EVALUATION OF MUNICIPAL WATER SUPPLY CONTAMINATION	95
A. Introduction	95
B. Calculations	95
C. Conclusions	103
VII. ANALYSIS OF RADIOACTIVITY IN WATER	105
A. Radiochemical Methods	105
1. Introduction	105
2. Procedures for the Determination of Specific Radionuclides	106
a. Radiostrontium	106
b. Radiocesium	110
c. Radioiodine	113
d. Total Rare Earths	114
e. Miscellaneous Radionuclides	115
3. Summary of Radionuclide Analysis	120

	<u>Page</u>
B. Instrumentation	122
1. Preconcentration Methods	125
2. Detector Development	126
3. Summary	128
VIII. DECONTAMINATION OF WATER SUPPLIES	133
IX. BODY BURDEN FROM CONSUMPTION OF CONTAMINATED WATER	137
X. REFERENCES	155
XI. GLOSSARY	165
XII. STAFF	171
APPENDIX A - Excerpts from Quarterly Technical Report #3	173
F. Preliminary Evaluation of Water Supply Contamina- tion for Selected Cities	173
I. Decontamination of Water Supplies	182
APPENDIX B - Distribution List	195

LIST OF FIGURES

		<u>Page</u>
Figure 1	Geometry of Stem and Cloud.	8
Figure 2	Typical Ionization Rate Decay Curve for Very Close-In Fallout.	13
Figure 3	Computer Program for Estimating Sublimation Pressure. . .	15
Figure 4	Intensity versus Distance Curve	42
Figure 5	Computer Program for Ionization Rate Contours	44
Figure 6	Selected Ionization Rate Contours	60
Figure 7	Computer Program for Particle Size Parameters	72
Figure 8	Falling Velocity for Spherical Particals Falling from Various Altitudes to Sea Level	74
Figure 9	Total Activity of Soil.	77
Figure 10	Integrated Neutron Flux as a Function of the Slant Range in Air of 0.9 Sea-Level Density for a 1-Kiloton Explosion	79
Figure 11	Total Activity Percentage in Relation to Particle Diameter.	87
Figure 12	Particle Diameter versus Downwind Distance (Maximum and Minimum Curves)	88
Figure 13	Idealized Stream Section.	90
Figure 14	Method of Graphical Integration Used for the San Jacinto Watershed Serving Houston, Texas.	97
Figure 15	Relation of Dose Rate to Nuclide Concentration.	133
Figure 16	A_n versus Time for Iodine 131	149
Figure 17	A_n versus Time for Strontium 89	150
Figure 18	A_n versus Time for Strontium 90	151
Figure 19	A_n versus Time for Ruthenium 106.	152
Figure 20	A_n versus Time for Cesium 137	153
Figure 21	A_n versus Time for Barium 140	154

LIST OF TABLES

		<u>Page</u>
Table I	Cumulative Mass-Chain Yields of Fission Products	27
Table II	Air Ionization Disintegration Multipliers for the Fission Product and Other Radionuclides	32
Table III	List of Symbols	53
Table IV	Data Table for Ionization Rate Contour Program	56
Table V	Decay of Normal Fission Products from U-235, U-238, and Pu-239	67
Table VI	Atom Concentration Intensity Ratio	68
Table VII	Particle Size Distribution at Various Downwind Distances for 5 MT Weapon Yield	73
Table VIII	Composition of the (NTS) Soil Assumed	76
Table IX	Radioactivity in Soils ($\mu\text{C}/\text{MT}$)	78
Table X	Calculated Activities of Various Nuclides in Soil	80
Table XI	Activity Concentrations for Direct Contamination of the Houston Reservoir	99
Table XII	Activity Concentrations for Direct Contamination of the New York City Reservoirs	99
Table XIII	Activity Concentrations for Cypress Creek (South Wind)	101
Table XIV	Activity Concentrations for Contamination from Runoff for the Houston Watershed	102
Table XV	Activity Concentrations for Contamination from Runoff for the New York City Watershed	102
Table XVI	Summary of References to Radionuclide Analyses	121
Table XVII	Capabilities of Portable Survey Instruments	130
Table XVIII	Equipment Manufacturers	131
Table XIX	Approximate Minimum Detectable Concentrations in Water	124
Table XX	Selected Values of f_w for Various Organs	148

I. INTRODUCTION

The purpose of this study was to evaluate and summarize available information on the problem of water contamination by radioactive fallout in the event of nuclear war. Consideration has been given to the current theories of the formation and distribution of fallout and the level of fallout that might result from a possible nuclear attack.

Of the various attack models that have been recently described^(1,2) the one prepared by Technical Operations, Inc.⁽³⁾ has been selected as most appropriate for the present study. This model appears to have been well thought out and carefully developed, giving due consideration to the relative importance of various military, industrial, governmental, and power resource targets. This model assumes all detonations to be surface bursts, although perhaps a more realistic situation would include many air bursts, which would be more effective against an unhardened military or industrial target. As the type of burst has a considerable influence on the fallout produced, it must be carefully evaluated in a study of water contamination.

A thorough analysis of the fallout model of Miller⁽⁴⁾ has been made. Several important functions derived from this model have been utilized in this study and are discussed in detail in Section II, "Summary of Analysis of the Fallout Model".

Information from the Miller model has also been used in the study of possible levels of contamination by selected isotopes in the water supply systems of Houston, Texas and New York City. With appropriate consideration to the assumptions made, these results may be applied to the watersheds of municipalities other than those shown here.

This study is concerned with the effect of individual nuclear clouds, and does not consider the effects of overlapping fallout patterns. The complex problem of overlap has been treated by Technical Operations, Inc.⁽³⁾ and others, but additional studies on this subject appear desirable.

Transport of fallout by surface water has been studied. Evaluation of the effects of watershed characteristics on the concentration of radioactivity in surface water would be valuable.

Decontamination procedures, both standard and emergency, have been described previously.⁽⁵⁾ (See Appendix A) These procedures are evaluated according to their efficacies for the removal of various radioisotopes and also according to the feasibility of their use after a nuclear attack. For purposes of this study, it has been assumed that waterworks facilities have suffered only minimal damage, and that personnel will be available for operation.

A study of published methods of radiochemical analysis and existing instrumentation has been made. Due to the question of availability of personnel and facilities it appears that this information will be of more value in recognizing long-term hazards than in determining potability in the immediate post-attack period.

The biological uptake and resultant body burdens in man have been evaluated in relation to the levels of water contamination considered likely. Existing data has been put into a workable form so that the body burden of any of the selected biologically important radioisotopes may be determined at any specified time after the initiation of intake.

The internal radiation hazard resulting from nuclear attack is of importance only to those persons who survive the catastrophe for a period of several years. As a primary annihilator, it is of no consequence,

as the external dose concomitant with a lethal internal dose is more deadly by several orders of magnitude. In general, radiation from sub-lethal concentrations of internally deposited radionuclides acts slowly, and its results do not become apparent for years. Therefore, the internal radiation hazard is not among the forces debilitating the population and reducing its immediate ability to cope with a radically altered environment. Rather it has long-term effects which culminate in producing diseases such as cancer, shortening of the life span, and possibly affecting the germ plasm of mankind to a small degree."(6)

II. SUMMARY OF ANALYSIS OF THE O.C.D. FALLOUT MODEL

A. Basic Assumptions of the O.C.D. Model

During the initial phase of this project, the Postattack Research Division, Office of Civil Defense, requested that all studies be based on the fallout model as developed in "Fallout and Radiological Countermeasures"⁽⁴⁾. A thorough and quantitative study of the model was conducted because the evaluations of water contamination depend directly on previously established information concerning the distribution and properties of local fallout. The results of the detailed study are now presented in summary form.

The model was based on both established physico-chemical theories and actual test data, brought together by the scaling method. The rationality and simplicity of the basic assumptions provide this model with many advantages. The basic assumptions include:

(1) The model applies generally to a "ground surface" burst, but it can be extended to other types of detonations by suitable transformations.

(2) The required input data consist of the weapon yield and the wind velocity.

(3) The radioactive decay schemes, chemical properties and relative abundances of the fission products are based on the data developed by Bolles & Ballou⁽⁷⁾, Katcoff⁽⁸⁾, and Milier and Loeb⁽⁹⁾.

(4) The increase of the fireball volume with time is based on the adiabatic expansion of an ideal gas with the thermodynamic equations modified to include a term for the change in free energy with altitude and with the external pressure proportional to $\exp(-mgZ/kt)^*$.

* For explanation of symbols, see Glossary.

(5) The radioactive cloud is assumed to have the shape of an oblate spheroid; hence the ionization rate contours or fallout patterns under a constant wind velocity are generally cigar-shaped.

(6) All values for the dimensions and properties of the fireball and fallout patterns are scaled from test data by the scaling method to be a function of weapon yield and wind velocity.

(7) The condensation process of fallout is divided into two time periods: (a) the first period is characterized by the presence of gas and liquid phases and ends when the bulk carrier or substrate material of the particles solidifies, and (b) the second period is characterized by the existence of gas and solid phases. The temperature of 1673°K is used to divide these two periods of condensation. The radioactive material which condenses in the first period will be fused inside the fallout particles and generally becomes insoluble in water. The material which condenses during the second period will be adsorbed on the outside of the fallout particle and becomes readily soluble in water. With these basic assumptions, the model will yield the intensity, the activity and atom-concentration for a specific downwind area and other, related information.

B. Formation and Geometry of Stem and Cloud

After a surface burst, the fireball forms the shape of a sphere, and its radii, both horizontal and vertical, expand exponentially with altitude as it rises. Since the expansion coefficients are different for the two radii, the fireball grows to the form of an oblate spheroid, with a circular top-view and an elliptical side-view. When the fireball reaches its final stabilized height, it is commonly known as the "cloud". A stem is shaped by the trajectory of a continuously expanding fireball and assumes the form of an inverted exponential horn.

The initial spherical radius of the fireball, R_s , the final horizontal semi-axis, a , the final vertical semi-axis, b , and the final height of the center, h , of the cloud are related to the weapon yield, W , through empirical data as shown in the following scaling functions:

$$R_s = 2.09 \times 10^2 W^{0.333} \text{ ft.} \quad W = 1 \text{ to } 10^5 \text{ KT} \quad (1)$$

$$a = 2.45 \times 10^3 W^{0.431} \text{ ft.} \quad W = 1 \text{ to } 10^5 \text{ KT} \quad (2)$$

$$b = 1.40 \times 10^3 W^{0.300} \text{ ft.} \quad W = 1 \text{ to } 10^5 \text{ KT} \quad (3)$$

$$h = 0.66 \times 10^4 W^{0.445} \text{ ft.} \quad W = 1 \text{ to } 28 \text{ KT} \quad (4)$$

$$h = 1.68 \times 10^4 W^{0.164} \text{ ft.} \quad W = 28 \text{ to } 10^5 \text{ KT} \quad (4a)$$

At a given altitude, Z , the horizontal and vertical semi-axis of the fireball can be obtained by

$$a_Z = a_0 e^{k_a Z} \quad (5)$$

$$b_Z = b_0 e^{k_b Z} \quad (6)$$

where a_0 , b_0 , k_a , k_b can be solved from the known information of R_s , a , b , h .

The geometry of both stem and cloud is shown in Figure 1.

C. Particle Size Parameter and Ionization Rate Contours

As mentioned previously under the basic assumptions, the fission products are either fused inside or adsorbed on the outside of the dust particles and are inhaled into the fireball. The ultimate ionization rate contours, or fallout patterns, on the ground are related to the size of the falling particles. The particle size parameter, α , is defined as the ratio of wind velocity, V_w , to the average falling velocity of the particle, V_f , since it is more concerned with the falling rate than the actual physical size of a particle.

NOTE: The particles with maximum a values and particles with minimum a values which fall on point X downwind from the cloud fall along paths described by r_{\max} and r_{\min} respectively.

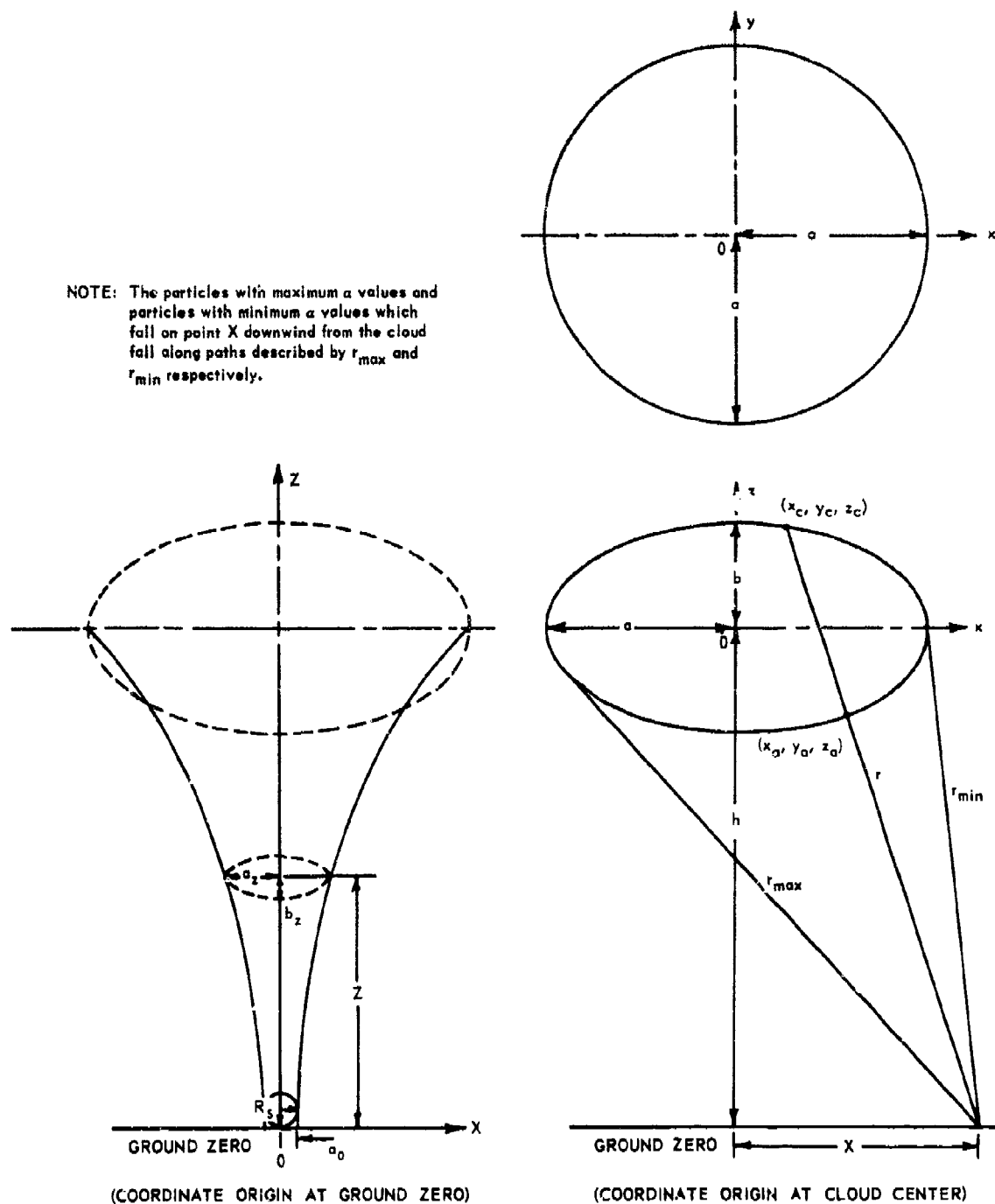


Figure 1. Geometry of Stem and Cloud

For the stem, it is assumed that the particles at a given altitude in the rising fireball are concentrated on a horizontal plane through the center of the fireball. Therefore, all particles which have equal values of α fall out of the stem starting at the same altitude. Any particle starts to fall when its instantaneous falling rate, V_Z , equals the rate of rise of the surrounding air mass, $\frac{dZ}{dt}$. There is an empirical relation between V_Z , V_f , and the fireball altitude Z :

$$V_Z/V_f = p + qZ \quad (7)$$

where $p = 0.95$, $q = 1.02 \times 10^{-5}$, where $Z = 5,000$ to $50,000$ ft

with particle diameter $d = 200$ to $1,200$ microns

$p = 0.58$, $q = 1.74 \times 10^{-5}$, when $Z = 50,000$ to $110,000$ ft

with particle diameter $d = 300$ to $1,000$ microns

There is also an empirical approximation for Z :

$$Z = Z_0 (1 - e^{-k_Z t}), \quad \text{for } t = 20 \text{ to } 480 \text{ seconds} \quad (8)$$

where Z_0 is a yield dependent multiplier*

k_Z is 0.011 sec^{-1} .

Thus,

$$V_Z = \frac{dZ}{dt} = k_Z (Z_0 - Z) \quad (9)$$

* For values of Z_0 , see Figure 5.

Therefore, the particle size parameter, α , for the particle group falling from the altitude Z is

$$\alpha = \frac{V_w}{V_f} = \frac{V_w(p + qZ)}{k_Z(Z_0 - Z)} \quad (10)$$

Moreover, it can be determined from geometry of the stem that

$$\alpha_m Z = X \pm a_Z \quad (+ \text{ for } \alpha_{\min}; - \text{ for } \alpha_{\max}) \quad (11)$$

Therefore, α_{\max} and α_{\min} may be obtained for the particles falling at a distance X from ground zero. In addition, the rising and falling time for particles of a given value of α can be determined from combining Equations (8) and (10), as shown below

$$t_r \text{ (sec)} = \frac{1}{k_Z} \ln \left[\frac{\alpha k_Z Z_0 + V_w q Z_0}{V_w p + V_w q Z_0} \right]^* \quad (12)$$

$$t_f \text{ (sec)} = \frac{\alpha(\alpha k_Z Z_0 - V_w p)}{V_w(\alpha k_Z + V_w q)} \quad (13)$$

The outer dimensions of the cloud are defined by

$$\frac{x^2 + y^2}{a^2} + \frac{z^2}{b^2} = 1 \quad (14)$$

Consequently, α_{\max} and α_{\min} for the downwind distance X can be derived, as shown by the equation

$$\alpha_m = \frac{hX \pm \sqrt{X^2 b^2 (1 - y^2/a^2) + (a^2 - y^2) [h^2 - b^2(1 - y^2/a^2)]}}{h^2 - b^2(1 - y^2/a^2)} \quad (15)$$

* This calculation usually includes the 180 sec. average delay time due to fireball toroidal circulation, which should be subtracted in order to obtain the actual rising time.

(where the sign is + for α_{max} , and - for α_{min})

Since the cloud is assumed to be stabilized, all particles with the same values of α fall along the same slope. Hence, the times of arrival and cessation for particles of a given α can be determined from the geometry of the cloud

$$t_a = \alpha (h + z_a) / V_w \quad (16)$$

$$t_c = \alpha (h + z_c) / V_w \quad (17)$$

where z_a and z_c are the smallest and largest intercepts of the slope to the outer dimension of the cloud, respectively.

$$z = \frac{\alpha(X - \alpha h) b^2 \pm ab \sqrt{(a^2 + \alpha^2 b^2) (1 - y^2/b^2) - (X - \alpha h)^2}}{a^2 + \alpha^2 b^2} \quad (18)$$

(where the sign is + for z_c , and - for z_a).

Assuming that the ionization rate, or fallout intensity, I_X , varies exponentially with downwind distance, and its distribution is closely related to α and W , also confirmed by empirical test data, a complete set of scaling functions which defines the variation of intensity versus downwind distance and the bi-elliptical outline of the ionization rate contours is tabulated in Chapter 3 of "Fallout and Radiological Countermeasures"⁽⁴⁾. Those scaling functions are not repeated in this report, but a corresponding computer program was established, as presented in Figure 5. A typical ionization rate contour for a 10 MT weapon yield and a 15 mph wind velocity is shown in Figure 6. Since the only inputs are weapon yield and wind velocity, this computer program is relatively simple to understand and to use by others to obtain the information on ionization rate contours.

It should be pointed out that these contours have been corrected to a standard reference time, $H + 1$ hour, by a decay correction factor

$$d(t, 1) = \frac{I_X(t: \text{actual time})}{I_X(1: H + 1 \text{ hour})} \quad (19)$$

This decay correction factor can be obtained directly from a typical close-in fallout decay curve as shown in Figure 2.

Knowing the ionization rate, the exposure dose, D_X , in the cloud fallout area, which is of greater interest than the stem fallout area, can be estimated by

$$D_X = \int_{t_a}^{t_c} I_X(t) dt \quad (20)$$

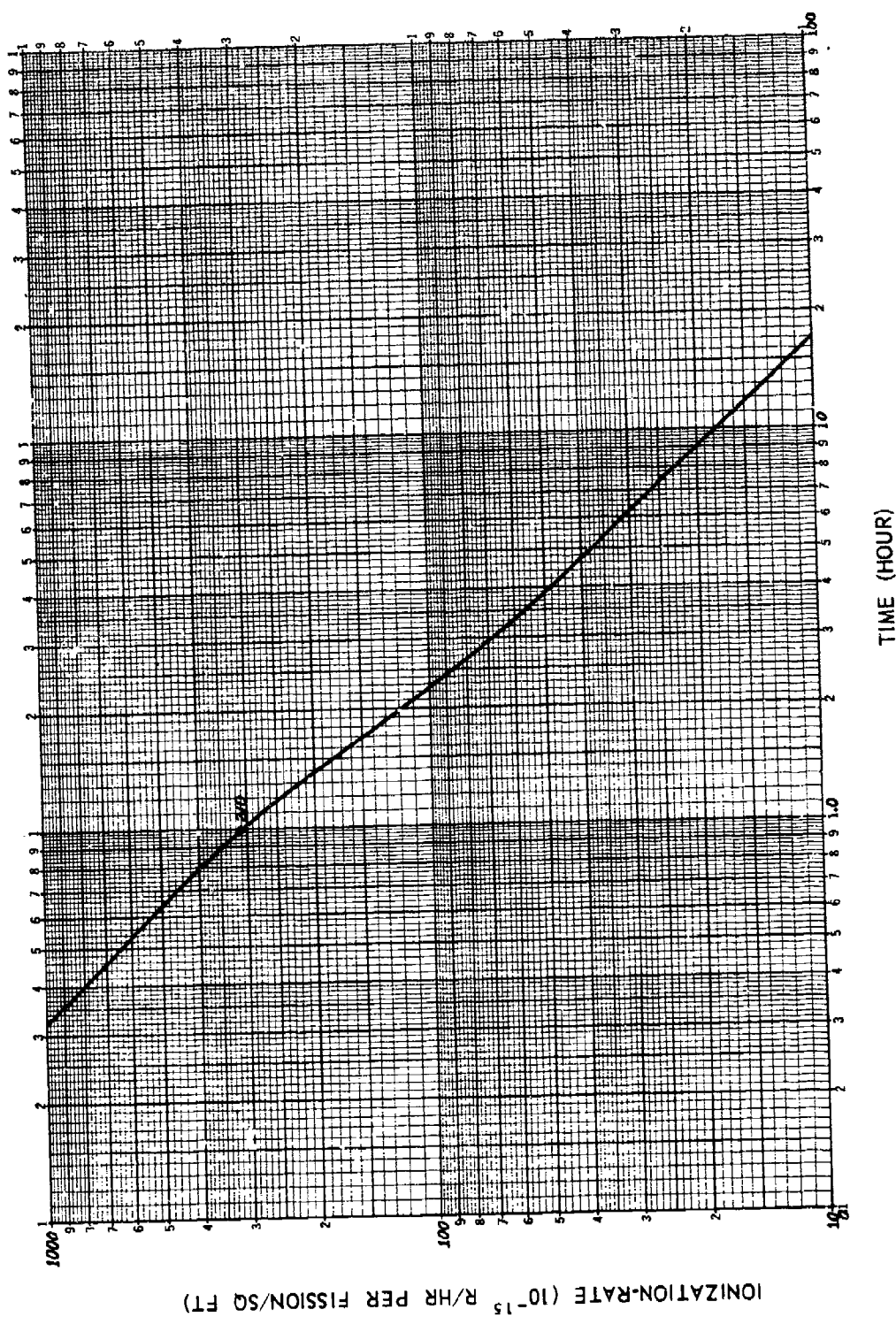


Figure 2. Typical Ionization Rate Decay Curve for Very Close-In Fallout

D. Condensation of Fallout and Fractionation Numbers

During a nuclear detonation, a tremendous amount of heat is created by nuclear fission and fusion. This heat melts and also vaporizes everything inhaled into the air mass from the ground and forms the familiar fireball. When the fireball rises, its volume begins to expand, and its temperature is assumed to drop according to the ideal gas law. The material swept inside the fireball starts to liquidify and finally solidify to particles, in or on which the fission products begin to condense. The condensation process is generally divided into two time periods as mentioned in the basic assumptions. The dividing temperature depends largely on the composition of the fireball. For a model surface burst on a soil consisting of silicate minerals this temperature is assumed to be 1673°K , as most elements will have started to solidify at this temperature. Since the two periods are characterized by the coexistence of either gas and liquid, or gas and solid, the vaporization or sublimation pressure plays an important role in the condensation process. The following formula for the evaluation of the pressure is presented in "Fallout and Radiological Counter-measures"⁽⁴⁾:

$$\log p_j = \frac{A}{T} + B + C \quad (21)$$

where p_j is the vaporization or sublimation pressure for element j ,
gm/sq. cm.,

T is temperature of the fireball, $^{\circ}\text{K}$,

A, B, C are the empirical constants for vaporization or sublimation reactions of elements contained in the fireball which were tabulated in Miller's manuscript⁽⁴⁾.

The established computer program for estimating p_j is shown in Figure 3.

Figure 3. Computer Program for Estimating Sublimation Pressure

```

0200      BAC-220 STANDARD VERSION  2/1/62
0200      COMMENT  SUBLIMATION PRESSURE. *** PIJ  BY  R. E. JAMES.      $
0200      INTEGER J,I,ABC,DEF,JK...      $  ARRAY  Q(70) , T(70)      $
0200      READ($EAA)      $
0204      WRITE($EAB,EAC)      $
0212      START.. READ($DATA)      $
0216      IF MOD(ABC,27)  EOL  0      $
0226      WRITE($EAB,EAC)      $
0230      FOR I = (1,1,DEF)      $
0241      Q(I) = EXP((2.302585)(A/T(I) + B + C))      $
0254      WRITE($EAD,EAE)      $
0262      GO START      $ CRAFT
0263      INPUT  DATA(ABC , A , B , C , JKA,JKB,JKC,JKD)      $
0291      INPUT  EAA(DEF,FOR I = (1,1,DEF) $ T(I) )      $
0315      OUTPUT EAB(FOR I = (1,1,DEF) $ T(I) )      $
0316      OUTPUT EAD(JKA,JKB,JKC,JKD,A,B,C,Q(1) )      $
0344      FORMAT EAC(B3,*IDENTIFICATION*,B11,*A*,B10,*R*,B11,*C*,B9,
0344      * PJ FOR 1673 DEG.*,170,W3)      $
0343      FORMAT EAE(4A5,X12.0,X10.3,X13.6,F20.6,W4)      $
0391      FINISH      $ CRAFT
COMPILED PROGRAM ENDS AT 0392
PROGRAM VARIABLES BEGIN AT 4230

```

Figure 3 (Continued). Computer Program for Estimating Sublimation Pressure

IDENTIFICATION			A	B	C	PJ FOR 1673 DEG.
.5	NA	700 * 1190	-16200.	8.242	.174740	.541422.-01
.5	NA	1190 * 2000	-14710.	6.977	.174740	.228639.-01
.5	K	700 * 1080	-13850.	8.193	.174740	.122800.-01
.5	K	1080 * 1800	-12580.	7.935	.174740	.389326.-01
.5	RB	750 * 974	-12090.	7.136	.174740	.121395.-01
.5	RB	974 * 1500	-11670.	6.884	.174740	.121128.-01
.5	CS	763 * 958	-11540.	7.470	.174740	.558407.-01
.5	CS	958 * 1500	-11120.	7.049	.174740	.377570.-01
	MG	923 * 1393	-38780.	11.108	.349485	.189482.-11
	MG	1393 * 2000	-38470.	10.891	.349485	.176143.-11
	MG	3075 * 3400	-28530.	7.977	.349485	.187624.-08
	CA	1123 * 1760	-41260.	10.162	.349485	.767479.-14
	CA	1760 * 2000	-41080.	10.103	.349485	.790303.-14
	CA	2860 * 3800	-37120.	9.768	.349485	.850745.-12
	SR	1043 * 1640	-38260.	9.563	.349485	.110506.-12
	SR	1640 * 2000	-37910.	9.298	.349485	.971837.-13
	SR	1640 * 2000	-32920.	7.238	.000000	.363726.-12
	SR	2730 * 3500	-31560.	8.552	.349485	.108935.-09
	RA	1000 * 2196	-36700.	8.951	.349485	.231124.-12
	RA	1000 * 2196	-20830.	6.761	.000000	.204321.-05
	RA	2196 * 3000	-37500.	9.183	.349485	.131118.-12
	BA	2196 * 3000	-20980.	6.993	.000000	.283566.-05
	ZN	298 * 2000	-24070.	10.347	.349485	.203777.-03
	ZN	1000 * 2000	-24080.	8.173	.000000	.602137.-06
	CD	1038 * 2000	-18770.	10.390	.349485	.331221.-00
1056FE		1000 * 1650	-35550.	10.642	.349056	.577836.-10

Figure 3 (Continued). Computer Program for Estimating Sublimation Pressure

IDENTIFICATION		A	B	C	PJ FOR 1673 DEG.
1056FE	1650 * 2000	-33210.	9.204	.349056	.527824,-10
1/3 FE	1000 * 1870	-39870.	12.190	.465980	.667637,-11
1/3 FE	1870 * 2000	-37640.	10.982	.465980	.890175,-11
1/2 Y	1000 * 2690	-44880.	11.895	.174740	.175259,-14
1/2 LA	1000 * 2590	-40470.	10.864	.174740	.705770,-13
1/2 PR	1000 * 2400	-38060.	9.796	.174740	.166413,-12
1/2 ND	1000 * 2350	-34810.	10.647	.174740	.103460,-09
1/2 PM	1000 * 2300	-31270.	9.913	.174740	.249325,-08
1/2 SM	1000 * 2300	-27830.	9.818	.174740	.228009,-06
AL	1000 * 2290	-47115.	11.507	.174740	.330945,-16
AL	1000 * 2290	-74020.	19.038	.698070	.126527,-26
1/2 AL	1000 * 2290	-59730.	14.343	.524220	.146180,-20
AL	1500 * 2290	-64950.	14.705	.349485	.170613,-23
1/2 AL	2290 * 3000	-47240.	11.865	.174740	.242454,-16
AL	2290 * 3800	-74690.	19.766	.698070	.679168,-27
1/2 AL	2290 * 3800	-60560.	14.708	.524220	.108087,-20
1/2 GA	1000 * 1998	-41860.	11.923	.174740	.119349,-12
GA	1000 * 1998	-42150.	14.659	.524220	.974859,-10
1/2 IN	1000 * 2000	-43390.	11.405	.174740	.440855,-14
1/2 IN	1000 * 2000	-36370.	13.940	.524220	.530677,-07
AS	730 * 1000	-3675.	5.025	.000000	.673514, 03
1/2 AS	1000 * 2000	-16670.	7.948	.174740	.144080,-01
2 SB	928 * 2000	-3894.	2.293	.000000	.923514, 00
1/2 SB	1000 * 2000	-25720.	6.716	.174740	.328973,-06
ZR	1200 * 2200	-60900.	13.468	.349485	.260503,-22
ZR	1200 * 2200	-40150.	8.656	.000000	.454147,-15
CE	1500 * 2870	-45610.	14.301	.349485	.488780,-13

Figure 3 (Continued). Computer Program for Estimating Sublimation Pressure

IDENTIFICATION		A	B	C	PJ FOR 1673 DEG.
CE	1500 * 2870	-22990.	9.384	.000000	.438752,-04
U	1500 * 2680	-53670.	12.048	.349485	.207678,-19
U	1500 * 2680	-32010.	9.594	.000000	.288873,-09
U	1500 * 2680	-11250.	4.008	.349485	.429574,-02
SI	1000 * 1950	-40130.	12.990	.349485	.225235,-10
SI	1000 * 1950	-28980.	8.905	.000000	.382671,-08
SI	1950 * 2500	-38760.	12.268	.349485	.281530,-10
SI	1950 * 2500	-27810.	8.289	.000000	.463625,-08
GE	800 * 1390	-22250.	12.620	.349485	.467759, 00
GE	1390 * 2000	-21920.	12.382	.349485	.425867, 00
SN	1300 * 1898	-28430.	12.729	.349485	.121635,-03
SN	1898 * 2500	-25940.	11.400	.349485	.175551,-03
RU	1000 * 2500	-23910.	13.997	.349485	.113447, 01
RU	1000 * 2000	-43300.	16.508	.349485	.945881,-09
1/2 RH	1000 * 2000	-13900.	6.010	-.174740	.336381,-02
1/2 RH	1000 * 1500	-12060.	1.890	-.524227	.143603,-05
SE	500 * 1000	-4539.	7.644	.000000	.852921, 05
SE	500 * 1000	-13715.	13.704	.349485	.717193, 06
SE	1000 * 2000	-16330.	12.227	.349485	.653998, 03
TE	723 * 1006	-25570.	12.889	.349485	.900666,-02
TE	1500 * 2000	-10150.	6.696	.000000	.425651, 01
2 TE	1068 * 2000	-33690.	18.278	1.307840	.345432, 00
TE	1006 * 2500	-22130.	9.860	.349485	.958851,-03
1/2 NB	1000 * 1785	-49810.	16.202	.524220	.898168,-13
1/2 NB	1000 * 1785	-30470.	11.709	.174740	.468759,-08
1/2 NB	1785 * 2500	-46330.	14.225	.524220	.113881,-12
1/2 NB	1785 * 2500	-26990.	9.732	.174740	.594354,-06

Figure 3 (Continued). Computer Program for Estimating Sublimation Pressure

IDENTIFICATION			A	B	C	PJ FOR 1473 DEG.
3	MO	800 * 1068	-17590.	14.327	.000000	.650060, 04
4	MO	800 * 1068	-20450.	17.045	.000000	.662902, 05
5	MO	800 * 1068	-23077.	18.647	.000000	.713208, 05
	MO	1068 * 2000	-51590.	13.888	.698970	.562536, -16
	MO	1068 * 2000	-34780.	10.140	.349485	.501746, -10
	MO	1068 * 2000	-17810.	7.570	.000000	.840338, -03
2	MO	1068 * 2000	-11550.	5.948	.000000	.110722, 00
3	MO	1068 * 2000	-4765.	3.389	.000000	.347394, 01
4	MO	1068 * 2000	-1168.	.490	.000000	.619231, 00
5	MO	1068 * 2000	1031.	-2.048	.000000	.370048, -01
	MO	1068 * 2000	-29210.	8.990	.000000	.339115, -08
	MO	1068 * 2000	-12240.	6.419	-.349485	.566652, -01
2	MO	1068 * 2000	-406.	3.647	-.698970	.507052, 03
3	MO	1068 * 2000	11946.	-.061	-1.048455	.107401, 07
4	MO	1068 * 2000	21110.	-4.108	-1.397840	.129482, 08
5	MO	1068 * 2000	28880.	-7.795	-1.747425	.524779, 08
	TC	1000 * 2000	-43980.	12.867	.349485	.847970, -13
	TC	1000 * 2000	-23570.	9.604	.000000	.327745, -04
	TC	393 * 585	-3059.	5.229	.000000	.251505, 04
	CU	800 * 1356	-17419.	6.514	.000000	.126521, -03
	CU	1356 * 2000	-16558.	5.881	.000000	.963406, -04
	AG	800 * 1234	-14639.	6.344	.000000	.392509, -02
	AG	1234 * 2000	-13788.	5.673	.000000	.270095, -02
	PD	1000 * 1823	-20015.	6.105	.000000	.138504, -05
	PD	1823 * 2500	-19189.	5.649	.000000	.151072, -05
	NABR	1025 * 2000	-8916.	5.346	.000000	.103908, 01
	NAI	932 * 2000	-8880.	5.660	.000000	.224993, 01

The elements in the fireball are radioactive and hence the number of moles of each species is constantly changing with time. If $y_{jA}(t)$ denotes the amount of radionuclides of element j and mass number A present at time t after fission, then the total amount of element j present at time t is

$$Y_j(t) = \sum_A y_{jA}(t) \quad \text{atoms or moles} \quad (22)$$

Correspondingly, the total amount for the entire chain of mass number A is

$$Y_A = \sum_j y_{jA}(t) \quad \text{atoms or moles} \quad (23)$$

in which Y_A is constant, except for mass chains containing neutron emitters.

For the first period of condensation, the material balance for element j between gas and liquid phase is

$$Y_j(t) = \sum_A y_{jA}(t) = \sum_A n_{jA}^o(t) + \sum_A n_{jA}(t) \quad (24)$$

where $n_{jA}^o(t)$ is the number of moles of element j with mass number A ,

which is mixed with moles from other mass chains to form n moles of vapor, and is abbreviated to n_j^o , and

$n_{jA}(t)$ is the number of moles of element j with mass number A

dissolved in the $n(\ell)$ moles of liquid carrier, which is the particle in the liquid phase, prior to solidification, and is abbreviated to n_j .

For a perfect gas, the ratio between the mole fraction of element j in the vapor phase and that in the liquid phase is

$$\frac{N_j^O}{N_j} = \frac{n_j^O/n}{n_j/n(\ell)} = \frac{n_j^O RT/p_j V}{n_j/n(\ell)} = \frac{k_j}{p_j} \quad (25)$$

where N_j^O is the mole fraction of element j in the vapor phase
 N_j is the mole fraction of element j in the liquid phase
 n is the number of moles of vapor
 $n(\ell)$ is the total moles of liquid carrier
 R is the molar gas constant
 T is the absolute temperature
 p_j is the total vaporization pressure
 V is the molar volume, and
 k_j is the Henry's Law constant

From Equation (25), the following relation between n_j^O and n_j can be obtained:

$$n_j^O = \frac{n_j k_j}{[n(\ell)/V] RT} = n_j k_j^O \quad (26)$$

where $k_j^O = k_j/[n(\ell)/V] RT$

Substituting Equation (26) into Equation (24) yields

$$\sum_A y_{jA}(t) = (1 + k_j^O) \sum_A n_{jA}(t) \quad (27)$$

The fractionation number of the first period of condensation, $r_c(A, t)$, is defined to be the fraction of the mass chain condensed, or in mathematical form

$$r_c(A, t) = \frac{1}{Y_A} \sum_j n_{jA}(t) = \frac{1}{Y_A} \sum_j \frac{y_{jA}(t)}{1 + k_j^O} \quad (28)$$

Again according to Henry's Law

$$k_j = \frac{f_j}{N_j} \doteq \frac{p_j^*}{N_j} \quad (29)$$

where f_j is the fugacity of the element in the liquid phase
 N_j is the mole fraction of the element in the liquid phase, and
 p_j^* is the partial pressure of the liquid.

However, by Raoult's Law for an ideal solution

$$p_j^* = N_j p_j \quad (30)$$

Therefore $k_j \doteq p_j \quad (31)$

The method for determining p_j has been presented in Equation (21).

The $[n(\ell)/V]$ ratio is given by a scaling function

$$[n(\ell)/V] = 5.67 \times 10^{-7} \exp[-0.510 W^{-0.373} t] \frac{\text{moles}}{\text{cm}^3} \quad (32)$$

where t , in seconds, is related to the fireball temperature, T , by

$$T = 4.66 \times 10^3 W^{-0.010} \exp(-0.546 W^{-0.373} t) ^\circ\text{K} \quad (33)$$

and the data of $y_{jA}(t)$ were calculated and tabulated as $N_j(A, t)$ by Polles and Ballou⁽⁷⁾. Hence, the fractionation number, $r_o(A, t)$, can be evaluated for the elements contained in the fireball.

During the second period of condensation, if an excess of solid surface area is present, the amount condensed at any time after solidification of the carrier, is given by

$$n_j' = n_j^o - n_j'' \quad (34)$$

where n_j' is the amount of element j condensed on the surface of the solid particles
 n_j^o is the amount of element j that has not condensed in the liquid carrier, and
 n_j'' is the amount of element j in the vapor phase.

For a perfect gas

$$n_j'' = \frac{p_j^{sV}}{RT} \quad (35)$$

where p_j^s is the sublimation pressure and may be evaluated according to Equation (21).

The material balance for element j is

$$y_j(t) = n_j(t) + n_j'(t) + n_j''(t) \quad (36)$$

Therefore, employing Equations (27) and (35)

$$n_j' = \frac{k_j^o}{1 + k_j^o} y_j - \frac{p_j^{sV}}{RT} \quad (37)$$

or

$$\Sigma_A n_{jA}' = \frac{k_j^o}{1 + k_j^o} \Sigma_A y_{jA} - \frac{V}{RT} \Sigma_A p_{jA}^s \quad (38)$$

In this equation the partial pressure of each nuclide is proportional to its abundance at any given time, and is given by

$$p_{jA}^s = (y_{jA}^o / y_j^o) p_j^s \quad (39)$$

where

$$y_{jA}^0 = (1 - r_0)y_{jA}, \quad \text{and}$$

$$Y_j^0 = \sum_A y_{jA}^0$$

The fractionation number of the second period of condensation $r'_0(A, t)$ is defined to be the fraction of the mass chain condensed up to a given time during the second period, or expressed mathematically

$$r'_0(A, t) = \frac{1}{x_A} [\sum_j y_{jA}^0(t) - \frac{V}{0.23 \text{ EWRT}} \sum_j p_{jA}^s] \quad (40)$$

or

$$r'_0(A, t) = 1 - r_0(A, t) - \frac{V}{0.23 \text{ EWRT}} \frac{\sum_j (y_{jA}^0/Y_j^0) p_{jA}^s}{\sum_j y_{jA}} \quad (41)$$

where V is the fireball volume and is given by scaling the function

$$V = 7.62 \times 10^{11} W \exp(0.510 W^{-0.373} t) \text{ cm}^3$$

B is the ratio of fission to total yield, and

0.23 is a conversion constant changing weapon yield, W , to number of fission-moles per atom.

Physically in Equation (41), $p_j^s \sqrt{V}/RT$ gives the number of moles of element j in the vapor phase and 0.23 EW_j^0 gives the total number of moles of the element produced and in existence at a given time in the second period. The combined term in Equation (41) gives the fraction still remaining in the vapor state during the second period of condensation. The $1 - r_0(A, t)$ term gives the fraction which has not condensed in the liquid carriers during their existence in the first period of condensation.

The fractionation numbers yield the information about the fractions of radioactivity condensed in, or on the particles, at any time after a burst. Therefore, the fractionation numbers not only make the conversion between intensity and activity possible, but also lead the way to the evaluation of soluble and insoluble activity which is important to biological availability and radiological countermeasures research.

E. Conversion between Intensity and Activity

The conversion between intensity (measured as ionization rate) and activity density in fissions per unit area is presented in "Fallout and Radiological Countermeasures",⁽⁴⁾ based on the simple assumption that

$$\frac{I_X(t)}{A_X} = \frac{I_X(t)(\text{ideal})}{A_X(\text{ideal})} = K_X(t) \quad (42)$$

where the conversion factor, $K_X(t)$, is further broken down into the following components

$$K_X(t) = Dq_X [r_X(t) i_{fp}(t) + i_1(t)] \quad (43)$$

in which

- D is an instrument response factor, usually assigned a value of 0.75
- q_X is the terrain shielding factor, usually assigned a value of 0.75
- $r_X(t)$ is the gross fission product fraction number, sometimes also designated as $r_Q(t)$
- $i_{fp}(t)$ is the air ionization rate per fission at 3 ft above an infinite, ideal plane for a uniform distribution of the normal fission product mixture, and
- $i_1(t)$ is the same unit for neutron induced activities.

Details about the neutron induced ionization rate, $i_i(t)$, are almost entirely classified, but generally assigned⁽⁴⁾ as 1.9% of $i_{fp}(t)$. The other components in equation (43) can be readily derived.

Detailed information about the activities of the U-235 fission products has been provided by Bolles and Ballou⁽⁷⁾. These data can be correlated to the data supplied by Katcoff⁽⁸⁾ and applied to other types of fission elements, such as U-238, Pu-239 by taking proportions of the corresponding mass number. This conversion has been systematized and tabulated in "Fallout and Radiological Countermeasures". Moreover, Miller⁽⁴⁾ translated the activity data from Bolles and Ballou into ionization rate by a disintegration multiplier, m . Both tables of correlation and of disintegration multipliers are reproduced from Miller's manuscript as Tables I and II. Therefore, the ideal or normal ionization rate of fission product mixture may be computed according to the following formula:

$$i_{fp}(t) = \sum m A_t \quad (44)$$

where A_t is the activity of the nuclide at time, t , per 10^4 fission.

In accordance with the earlier discussion, the fission products do condense and fractionate with time instead of condensing completely at the very beginning as in the ideal situation. Therefore, the real ionization rate, $i_{fp}^*(t)$, should be multiplied individually for each radionuclide by its fractionation number at any specified time. Mathematically, this may be expressed by

$$i_{fp}^*(t) = \sum m A_t [r_o(A, t) + r'_o(A, t)] \quad (45)$$

The $r'_o(A, t)$ term vanishes in the first period of condensation. As time increases, the sum of the two fractionation numbers approaches unity.

TABLE I
Cumulative Mass-Chain Yields of Fission Products⁽⁴⁾
(Values are in per cent of fissions)

Mass Number	U ²³⁵		U ²³⁸		Pu ²³⁹	
	Thermal Neutrons*	Fission Neutrons	Fission Neutrons	8-Mev Neutrons	Thermal Neutrons	Fission Neutrons
72	1.6×10^{-5}	4.6×10^{-4}	5.0×10^{-6}	-	$1.2 \times 10^{-4*}$	-
73	1.1×10^{-4}	0.0012	3.7×10^{-5}	-	2.2×10^{-4}	-
74	$(3.2 \times 10^{-4})^B$	0.0034	1.1×10^{-4}	0.001	4.1×10^{-4}	0.0011
75	(8.8×10^{-4})	0.0062	8.3×10^{-4}	0.0040	$7. \times 10^{-4}$	0.0023
76	(0.0029)	0.012	0.0012	0.0078	0.0014	0.0051
77	0.0083	0.023	0.0038*	0.014	0.0026	0.011
78	0.021	0.048	0.0095	0.026	0.0049	0.025
79	(0.041)	0.096	0.019	0.053	0.0090	0.043
80	(0.077)	0.19	0.045	0.096	0.016	0.075
81	0.14	0.21	0.088	0.18	0.030	0.14
82	(0.29)	0.50	0.20	0.35	0.056	0.23
83	0.544	0.80	0.40*	0.66	0.10	0.37
84	1.00	1.3	0.85	1.02	0.17	0.60
85	1.30	1.85	0.80	1.45	0.28	0.92
86	2.02	2.5	1.38*	1.9	0.45	1.15
87	(2.94)	3.3	1.90	2.25	0.73	1.5
88	(3.92)	4.2	2.45	2.7	1.2	1.9
89	4.79	5.1	2.9*	3.17	1.9*	2.4

Continued

TABLE I (continued)
Cumulative Mass-Chain Yields of Fission Products
(Values are in per cent of fissions)

Mass Number	²³⁵		²³⁸		Pu ²³⁹	
	Thermal Neutrons*	Fission Neutrons	Fission Neutrons	8-Mev Neutrons	Thermal Neutrons	Fission Neutrons
90	5.77	5.8	3.2*	3.7	2.4	3.0
91	5.84	5.85	3.6	4.3	3.0	3.7
92	6.03	6.0	4.1	4.8	3.7	4.4
93	6.45	6.4	4.85	5.2	4.6	5.0
94	6.40	6.4	5.3	5.45	5.5	5.4
95	6.27	6.3	5.7*	5.6	5.9*	5.6
96	6.33	6.3	5.8	5.7	5.7	5.3
97	6.09	6.1	5.7	5.64	5.6*	5.2*
98	5.78	5.8	5.7	5.6	5.4	5.4
99	6.06	6.1**	6.3*	6.2**	5.9*	5.9*
100	6.30	6.7	6.1	6.4	6.0	6.4
101	5.0	5.3	5.5	6.5	6.0	5.9
102	4.1	2.9	5.6	5.9	5.9	5.3
103	3.0	1.7	6.6	5.0	5.8*	4.6
104	1.8	0.95	5.4	3.2	5.0	3.5
105	0.90	0.54	3.9	2.2	3.9*	3.2
106	0.38	0.30	2.7*	1.5	5.0*	3.6
107	0.19	0.17	1.35	1.0	4.0	3.1
108	(0.085)	0.095	0.67	0.70	3.0	2.6
109	(0.039)	0.053***	0.32*	0.48	1.5*	1.9*
110	(0.020)	0.030	0.15	0.33	0.65	0.81
111	(0.015)	0.022***	0.073*	0.23***	0.27*	0.34
112	(0.013)	0.020***	0.046*	0.19	0.10*	0.14*
113	(0.012)	0.018	0.043	0.17	0.055	0.090

Continued

TABLE I (continued)

Cumulative Mass-Chain Yields of Fission Products
(Values are in per cent of fissions)

Mass Number	U^{235}		U^{238}		Pu^{239}	
	Thermal* Neutrons	Fission Neutrons	Fission Neutrons	8-Mev Neutrons	Thermal Neutrons	Fission Neutrons
114	(0.011)	0.017	0.041	0.16	0.046	0.075
115	0.0104	0.017***	0.040*	0.15***	0.041*	0.069*
116	<u>(0.010)^b</u>	<u>0.017^b</u>	0.039	0.14	0.039	0.065
117	(0.010)	0.017	0.039	<u>0.14^b</u>	0.038	0.065
118	(0.010)	0.017	<u>0.40^b</u>	0.14	<u>0.038^b</u>	<u>0.064^b</u>
119	(0.011)	0.017	0.041	0.14	0.039	0.064
120	(0.011)	0.018	0.042	0.15	0.041	0.065
121	(0.012)	0.020	0.044	0.16	0.044*	0.066
122	(0.013)	0.022	0.046	0.17	0.047	0.069
123	(0.015)	0.030	0.050	0.19	0.052	0.076
124	(0.017)	0.053	0.055	0.23	0.058	0.082
125	0.021	0.095	0.072	0.33	0.072*	0.14
126	(0.058)	0.17	0.175	0.48	0.175	0.35
127	(0.145)	0.30	0.39	0.70	0.39*	0.80
128	0.37	0.54	0.77	1.0	0.77	1.9
129	0.90	0.95	1.45	1.5	1.45	2.5
130	2.0	1.7	2.5	2.2	2.5	3.2
131	(2.88)	2.9	3.2*	3.2	3.8*	3.8
132	(4.31)	4.3	4.7*	4.4	5.0	4.6
133	(6.48)	6.1	5.5*	5.4	5.27*	4.9
134	(7.80)	7.3	6.6*	6.5	5.69*	5.2
135	(6.40)	6.3	6.0*	5.9	5.53*	5.1
136	(6.36)	6.4	5.9*	5.8	5.06*	5.3
137	(6.05)	6.0	6.2	5.85	5.24*	6.4*

Continued

TABLE I (continued)

Cumulative Mass-Chain Yields of Fission Products

(Values are in per cent of fissions)

Mass Number	^{235}U		^{238}U		^{239}Pu	
	Thermal Neutrons	Fission Neutrons	Fission Neutrons	8-Mev Neutrons	Thermal Neutrons	Fission Neutrons
138	5.74	5.7	6.4	5.9	5.5	5.4
139	(6.34)	6.4	6.5	6.0	5.7*	5.2
140	6.44	6.4	5.7*	5.6	5.68*	5.0*
141	(6.30)	6.3	5.7	5.5	5.2*	4.7
142	(5.85)	5.9	5.7	5.4	6.69*	4.9
143	(5.87)	5.8	5.5	4.97	5.4*	5.0
144	5.67	5.1**	4.9*	4.3**	5.29*	4.8
145	3.95	4.2	3.7	3.7	4.24*	4.4
146	3.07	3.3	3.1	3.17	3.53*	3.7
147	2.38	2.5**	2.6**	2.7**	2.92*	3.0
148	1.70	1.85	2.0	2.27	2.28*	2.36
149	1.13	1.3**	1.45	1.9**	1.75	1.86
150	0.67	0.80	1.05	1.45	1.38*	1.48
151	0.45	0.50	0.74	1.02	1.08	1.16
152	0.285	0.31	0.50	0.66	0.83*	0.92
153	0.15	0.19**	0.32	0.41**	0.52	0.60
154	0.077	0.096	0.19	0.25	0.32*	0.37
155	0.033	0.048	0.11	0.15	0.20	0.23
156	0.014	0.023**	0.066*	0.092**	0.12*	0.14
157	0.0078	0.012	0.034	0.057	0.064	0.075
158	0.002	0.0062	0.016	0.032	0.034	0.043
159	0.00107	0.0034**	0.0090**	0.017**	0.020****	0.025

Continued

TABLE I (continued)
Cumulative Mass-Chain Yields of Fission Products
(Values are in per cent of fissions)

Mass Number	U ²³⁵		U ²³⁸		Pu ²³⁹	
	Thermal Neutrons*	Fission Neutrons	Fission Neutrons	8-Mev Neutrons	Thermal Neutrons	Fission Neutrons
160	3.5x10 ⁻⁴	0.0012	0.0036	0.0085	0.0092	0.011
161	7.6x10 ⁻⁵	4.6x10 ⁻⁴ **	9.4x10 ⁻⁴	0.0044**	0.0038****	0.0051

*Seymour Katcoff, Fission-Product Yields From U, Th and Pu, Nucleonics, Vol. 16, No. 4, p 78-85 (1958)

**L. R. Bunney, E. M. Scadden, J. O. Abriam and N. E. Ballou, Radiochemical Studies of the Fast Neutron Fission of U²³⁵ and U²³⁸, Second UN International Conference on the Peaceful Uses of Atomic Energy, A/Conf. 15/P/643, USA, June 1958

***G. P. Ford, J. S. Gilmore, et al, Fission Yields, LADC-3083, 1958

****L. R. Bunney, E. M. Scadden, J. O. Abriam, N. E. Ballou, Fission Yields in Neutron Fission of Pu²³⁹, USNRDL-TR-268, 1958, Uncl.

- Parenttheses indicate estimated values or where Katcoff's value was altered in order to adjust the yields to a gross sum of 100 in each peak.
- Line indicates division of two peaks that was used for individual peak sums.

TABLE II

Air Ionization Disintegration Multipliers for
the Fission Product and Other Radionuclides (4)

<u>Nuclide</u>	$10^{-9} \frac{m}{r/hr-ft^2}$ (dis/sec)	<u>Nuclide</u>	$10^{-9} \frac{m}{r/hr-ft^2}$ (dis/sec)
Zn-72	6.75	Nb ₁ -95m	1.41
Zn-74	4.22	Nb ₁ -95	4.56
		Nb ₂ -97m	4.42
Ga-72	14.3	Nb ₁ -97	4.02
Ga-73	2.11	Nb ₂ -98	11.7
Ga-74	12.4		
Ge-75	0.216	Mo-99	0.772
Ge-77	13.1	Mo-101	6.85
Ge-78	2.74	Mo-102	0.0
As-77	0.0735		
As-78	2.51	Tc-99m	0.782
As-79	0.0	Tc-101	2.03
		Tc-102	2.45
Se ₁ -81m	0.117		
Se ₂ -81	0.0	Ru-103	2.99
Se-83	12.8	Ru-105	4.36
		Ru-106	0.0
Br-83	0.0174		
Br-84	8.12	Rh-103m	0.150
		Rh ₁ -105m	0.283
Kr-83m	0.0959	Rh ₂ -105	0.559
Kr ₁ -85m	0.973	Rh-106	1.81
Kr ₂ -85	0.0316	Rh-107	5.08
Kr-87	7.03		
Kr-88	7.40	Pd-109	0.0
		Pd-111	5.00
Rb-88	4.30	Pd-112	0.0225
Rb-89	12.0		
Rb-91	6.67	Ag-109m	0.172
		Ag-111	0.175
Sr-89	0.0	Ag-112	4.59
Sr-90	0.0	Ag-113	0.158
Sr-91	5.03	Ag-115	1.28
Sr-92	6.93		
Sr-93	1.20	Cd ₁ -115	0.187
		Cd ₂ -115	1.11
Y-90	0.008	Cd-117m	8.11
Y ₁ -91m	3.24	Cd-118	0.0
Y ₂ -91	0.0135	Cd-120	3.08
Y-92	6.56		
Y-93	0.817	In-115	1.12
Y-94	6.67	In-117	1.36
		In-118	13.5
Zr-95	4.32	In-119	0.0371
Zr-97	0.346		
		Sn-121	0.0
		Sn-123	0.0
		Sn-125	6.19
		Sn-126	0.0
		Sn-127	3.08

Table II (continued)

Air Ionization Disintegration Multipliers for
the Fission Product and Other Radionuclides

<u>Nuclide</u>	$\frac{m}{10^{-9} \text{ r/hr-ft}^2}$ (dis/sec)	<u>Nuclide</u>	$\frac{m}{10^{-9} \text{ r/hr-ft}^2}$ (dis/sec)
Sb-125	2.78	Ce-141	0.470
Sb-126	16.1	Ce-143	2.34
Sb-127	2.70	Ce-144	0.188
Sb-128	13.0	Ce-145	4.22
Sb-129	6.10	Ce-146	1.60
Sb-131	3.66		
Te ₁ -125m	0.0525	Pr-143	0.0
Te ₁ -127	0.181	Pr-144	0.163
Te ₁ -127	0.0249	Pr-145	0.0
Te ₂ -129m	0.398	Pr-146	6.42
Te ₁ -129	1.52		
Te ₂ -129	8.42	Nd-147	0.968
Te ₁ -131	2.08	Nd-149	2.31
Te ₁ -131	1.52	Nd-151	6.44
Te ₂ -132	0.790		
Te ₁ -133m	9.12	Pm-147	0.0
Te ₂ -133	7.89	Pm-149	7.25
Te ₂ -134		Pm-150	4.99
		Pm-151	2.21
I-131	2.38	Pm-152	3.79
I-132	13.0	Pm-153	4.76
I-133	3.59		
I-134	9.63	Sm-151	0.0544
I-135	9.60	Sm-153	0.455
		Sm-155	1.80
Xe ₁ -131m	0.207	Sm-156	1.20
Xe ₁ -133m	0.413	Sm-158	3.08
Xe ₁ -133	0.304		
Xe ₂ -135m	2.69	Eu-155	0.314
Xe ₁ -135	1.55	Eu-156	5.55
Xe ₂ -138	7.89	Eu-157	3.78
		Eu-158	7.21
Cs-137	0.0		
Cs-138	11.2	Gd-159	0.430
Cs-139	4.78		
		Tb-161	0.123
Ba-137m	3.65		
Ba-139	0.888	U-237	1.13
Ba-140	1.10	U-239	0.388
Ba-141	4.22	U-240	0.0
Ba-142	5.76		
		Np-239	1.11
La-140	13.0	Np-240	2.07
La-141	0.400		
La-142	11.6	Mn-56	9.40
La-143	6.67		

The gross ionization fractionation number, $r_X(1)$, is defined as the ratio between the ionization rates at $H + 1$ hour of condensed and normal fission products. It may be expressed as

$$r_X(1) = \frac{i_{fp}^*(1)}{i_{fp}(1)}$$

Thus, all the components for the condensation factor, $K_X(t)$, have been cited and derived. The intensity-activity conversion, shown as Equation (42), is very useful in fallout contamination studies and the determination of other properties of fallout.

F. Biological Availability and Atom-Concentration Intensity Ratio

The fraction of radionuclides condensed on the outside of fallout particles is potentially available for biological uptake. By an analogy to the intensity-activity conversion presented in the foregoing section, the ratio of the number of atoms condensed on the exterior of the particle to the standard intensity at $H + 1$ hour is given by the following formula

$$\frac{N_{\alpha}^*(A)}{I(1)} = \frac{Y_A r'_O(A, t)}{K_X(\tau)} \quad (47)$$

where $N_{\alpha}^*(A)$ is the number of atoms (of the end member of the mass chain and condensed on the outside of the particle) which land per square foot of ground.

The other terms in Equation (47) are the same as defined previously. The ratio N_{α}^*/I is called the atom-concentration intensity ratio.

As shown in Equation (12) the fireball rising time, t , is a function of the particle-size parameter, α . Because of time dependence this ratio is also dependent on α . However, the α can be approximated and simplified by an average value α_0 , which is

$$\alpha_o = \frac{X}{h}$$

Since α_o does not vary with cross-wind distance, the atom-concentration intensity ratio holds constant as a first approximation for all values of cross-wind distance at a given value of downwind distance $X^{(10)}$. Moreover, as shall be seen in the following section, a given value of α represents a group of particles with a small range in diameters. Therefore, the ratio N_α^*/I is essentially associated with a given particle size.

The values of $N_\alpha^*(A)/I(t)$ for six biologically important isotopes at different downwind distances for a typical 10 MT burst have been calculated as shown in Table VI.

This ratio can be applied to water contamination studies to yield the activity of soluble radionuclides in water supplies. If $r'_o(A, t)$ is replaced by $r_o(A, t)$, the ratio N_α^*/I will provide the information for the activity of insoluble radionuclides, since those radionuclides fased into the silicate particles are assumed to be not readily soluble in water.

G. Ionization Rate Contour Ratios and Particle Size Distribution

Several ionization rate contour ratios have been defined to determine special properties of fallout. They are:

(a) The mass contour ratio, $M_r(t)$, which is the ratio of the fallout mass per unit area at any downwind distance to the ideal ionization rate at that location, or mathematically:

$$M_r(t) = m_X/I_X(t) \quad (49)$$

where m_X is the mass of fallout per unit area at any downwind distance, X

$I_X(t)$ is the ideal ionization-rate at 3 ft above an extended open area covered with fallout.

The mass of fallout, m , empirically determined to be a function of both α and W , is

$$m = f(\alpha) W^{0.917} \text{ mg} \quad (50)$$

$$\begin{aligned} \text{where } f(\alpha) &= 5.33 \times 10^{-12} \alpha^{-1.25} \text{ mg/fission, } \alpha = 0.1 \text{ to } 0.9 \\ &= 5.64 \times 10^{-12} \alpha^{-0.690} \text{ mg/fission, } \alpha = 0.9 \text{ to } 2.0 \\ &= 7.14 \times 10^{-13} \text{ mg/fission } \alpha > 2.0 \end{aligned}$$

According to Equation (42), it is found that

$$I_X(1) \times \text{Area} = D(1) q_X [r_\alpha(1) i_{fp}(1) + i_i(1)] BW \quad (51)$$

Therefore, the mass contour ratio associated with $H + 1$ hour, $M_r(1)$, for a ground surface burst will be

$$M_r(1) = \frac{f(\alpha) W^{-0.083}}{D(1) q_X B [r_\alpha(1) i_{fp}(1) + i_i(1)]} \frac{\text{mg/sq ft}}{\text{r/hr at 1 hr}} \quad (52)$$

(b) The fission-product contour ratio, $FP_r(t)$, which is the ratio of the number of atoms, or moles, of fission products per unit area at any downwind distance to the ideal ionization rate at that location, or mathematically:

$$FP_r(t) = N_{fp}/I_X(t) \quad (53)$$

where N_{fp} is the number of atoms, or moles, of fission products per unit area.

From the discussion of Section 6., this contour ratio, corrected to $H + 1$ hour, for a ground surface burst may be expressed as

$$FP_r(1) = \frac{1.16 \times 10^{-24} \sum_{jA} [r_o(A) + r'_o(A)] Y_A}{D(1) q_X [r_\alpha(1) i_{fp}(1) + i_i(1)]} \quad \frac{\text{moles fp/sq ft}}{\text{r/hr at 1 hr}} \quad (54)$$

(c) The fraction of device contour ratio, $FD_r(t)$, which is the ratio of the fraction of weapon device per unit area at any downwind distance to the ideal ionization rate at that location. This ratio when corrected to $H + 1$ hour may be expressed as

$$FD_r(1) = \frac{7.1 \times 10^{-24}}{D(1) q_X BW [r_\alpha(1) i_{fp}(1) + i_i(1)]} \quad \text{r/hr/sq ft at 1 hr.} \quad (55)$$

These contour ratios predict various characteristics of local fallout, as they yield information about the mass, the number of atoms of fission products per unit area, the fraction of weapon yield per unit area and other properties of fallout at a specific location. This information is valuable for the design of fallout shelters and other radiological countermeasures. Moreover, the use of these contour ratios and their scaling functions makes possible the extrapolation of a limited amount of experimental data to cover a number of operational cases since the contour ratios are not constant but are point functions whose values depend on many variables. Furthermore, the average density of the fission products can be estimated from the ratio of $FP_r(1)$ to $M_r(1)$.

Another advantage of the O.C.D. fallout model is that particle size groups for any given downwind location can be estimated by a graphical method, provided that the particle fall-rate is known. Since the fall-rate for a given size parameter α does denote a group of particles with a range of diameters, with the fall-rate for a given particle size parameter known, the range of diameters for a group of particles can be determined, depending on the thickness of the cloud and the altitude from which the group falls.

A family of curves which shows the size of ideal, spherical particles falling through a standard atmosphere from various altitudes as a function of fall-rate was prepared by D. E. Clark⁽¹¹⁾ and appears as a sketch in Figure 8.

When estimating the particle size range at a downwind distance, it should be first decided whether the source of the particle group originates from the stem or the cloud. The origin of the particle group can be generally judged by comparing the downwind distance with the downwind range of the stem fallout. In case the distance falls within this range, the particle group predominantly originates from the stem; otherwise it is essentially derived from the cloud. Within the stem range, the maximum and minimum α values may be calculated by Equation (11), which is a laborious procedure. A computer program, as shown in Figure 7, has been established to solve this equation. The height of fall for the stem fallout is derived from Equation (10) which is

$$Z = \frac{(Z_0 \alpha k_Z - V_w p)}{\alpha k_Z + V_w q} \quad (56)$$

For particle groups falling inside the cloud range at any downwind location (X, Y) , the crosswind distance Y should first be converted to the cloud coordinate, y , according to

$$y = a \frac{Y}{Y_m} \quad (57)$$

where Y_m is the maximum half-width of the crosswind distance on a 1 r/hr contour, and a is the cloud radius.

Following this coordinate transfer, use equations (15) and (18) to determine α_m and the two extreme heights of fall, z_a and z_c . For the actual

distance of fall, the height of the cloud, h , should be added. The fall-rate is evaluated from Equation (10), which is the defining equation of α and which yields

$$V_f = \frac{V_w}{\alpha} \quad (58)$$

Therefore, with weapon yield and downwind distance known, and with the help of the fall-rate curves, the approximate particle size distribution at (X, Y) can be estimated. This information on particle size distribution is useful for studies of transport phenomena in fallout investigations.

H. Conclusion - The Reality and Applications of the O.C.D. Model

The O.C.D. fallout model mainly uses the technique of the scaling method, hence most of its formulae are derived from realistic experimental data. Therefore it serves as a very good bridge between the ideal theoretical hypothesis and practical empirical data. Moreover, this model has been applied to several real test shots, and was found to yield very satisfactory results. On the other hand, the fundamental thermodynamic theory on which this model is based is quite simple and convincing, and all the computations involved are relatively easy. Another advantage of this model is its wide application, since it gives not only information on fallout patterns but also that of activity, hence it is very valuable to radiological research. Although there are still a few defects, such as constant wind velocity, the sole dependence on weapon yield, and the cigar-shape contour assumptions, etc., this model is generally considered very realistic and applicable to the problems of fallout research. Its main applications will be radioactivity prediction, countermeasure design and biological protection.

III. COMPUTATIONAL METHODS OF THE FALLOUT MODEL

A. Ionization Rate Contours

Although the physical characteristics and the mathematical approximation for the rising stem and the cloud have been discussed in detail, little has been said about how the fallout contours are determined. Even though the available data from actual land surface shots is small and limited primarily to low weapon yields, some general conclusions have been drawn from the test data.

Because most of the observed properties of the fallout patterns are in terms of intensity, the fallout contours are usually given in units of roentgens/hour (where the time was corrected to a standard time of $H + 1$ hour). The general shape of the fallout pattern can be approximated by the overlapping of ellipses, for both the stem and cloud fallout.

The dimensions necessary for constructing the ellipses are the distances from ground zero along the downwind axis where the lateral displacement is zero, ($Y = 0$). First, to construct the intensity vs. distance curve (see Figure 4) the downwind distances of interest are the highest intensity and a preselected low intensity, which varies with wind velocity, but for a 15 mph wind is 1 r/hr at 1 hr.

For the stem these locations have been labelled as follows:

X_1 and X_4 are the upwind and downwind distances, respectively, from ground zero to the 1 r/hr at 1 hr intensity.

X_2 and X_3 are the distances to the upwind and downwind shoulders, respectively, of the intensity ridge.

For the cloud the following notation is used:

X_5 and X_9 are the arrival location for the group of particles of the the selected low intensity from the rear and front of the cloud, respectively.

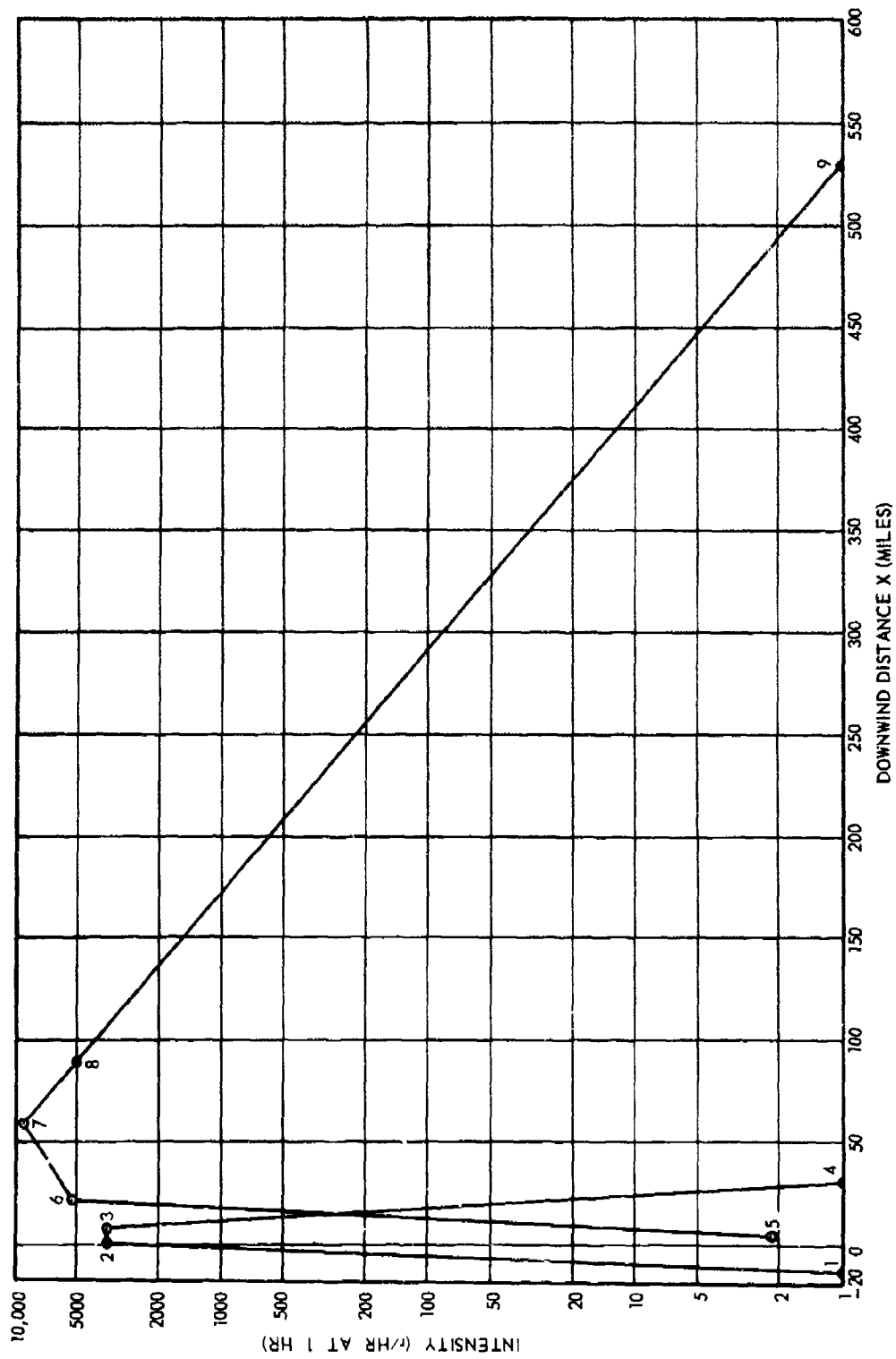


Figure 4. Intensity versus Distance Curve

- X_6 is the distance from ground zero to an intermediate point between X_5 and X_7 .
- X_7 is the downwind distance from ground zero to the peak of the intensity contour.
- X_8 is the downwind distance from ground zero where the contour intervals has a maximum half-width.

The values for these quantities are determined by equations appearing in the Ionization or Intensity rate computer program. Because of the limited characters available on the computer printer, the notation used in the analysis of the model had to be changed. The corresponding notation between the model and the computer program is given in Table III.

The following discussion describes the method for calculating the X 's and how the scaling functions can be found in the computer program in Figure 5. First, yield-dependent scaling functions for the size parameters $\alpha = \alpha_{2,3}, \alpha_4, \alpha_5, \dots, \alpha_9$ have been determined from data that has an effective, or average wind speed of 15 mph. These scaling functions are then multiplied by $\frac{V_W}{15 \text{ mph}}$ to correct for the wind velocity V_W . $I_{2,3}$, the ionization rate between X_2 and X_3 , is calculated by two formulas. For yields $W \geq 100\text{KT}$, $I_{2,3} = K_{2,3}(1) \bar{A}_{f-2,3}^0 V_W^n$ where the values for $K_{2,3}(1) \bar{A}_{f-2,3}^0$ and n were generated by fitting curves through the values of a Table in Chapter Three of Carl F. Miller's manuscript "Fallout and Radiological Countermeasures". For $W < 100$ a curve was fitted through the first three values of $I_{2,3}$ given in another table from Miller and adjusted for wind velocity by multiplying by $(\frac{V_W}{15})^{-0.79}$. The resulting equations appear on lines 0741 through 0802 in the computer program appearing in Figure 5.

In all the equations that follow the scaling function formulas and constants are given in Table IV. For any scaling function dependent

Figure 5. Computer Program for Ionization Rate Contours

```

0200      BAC-220 STANDARD VERSION   2/1/62
0200      DUMP      J      S                      TES
0400      COMMENT  RICHARD E. JAMES FOR A = 633.      S
0400      INTEGER F , G , J , P , N , EDC , Z99...      S
0400      ARRAY    ALP(9),I(9),IC(49),KAA(9),L(49),LI(9),M(49),PHI(9),X(9)      S
0400      PROCEDURE SEMI(X1,I1,X2,I2 S M,B)                      S
0404      BEGIN    C = LOG(I1)                      S
0408              D = LOG(I2)                      S
0412              M = (X2 - X1) / (D - C)          S
0422              B = (X1 . D - X2 . C) / (D - C)    S
0436      RETURN  END  SEMI()                      S
0442      FUNCTION LFF(N,W) = 2.3025851 L(N) + LW . M(N)      S
0454      FUNCTION FF(N,W) = EXP(LFF(N,W))          S
0467      FUNCTION IFF(X,MM,BB) = EXP((X-BB)/MM)      S
0478      FUNCTION SLL(I,M,B) = M.LOG(I) + B          S
0488      READ(SSQAZ) S INPUT WAZ(EDC, FOR J=(1,1,EDC) S (F,L(F),M(F))) S
0523      START.. READ(SSQBHV) S INPUT EBHV(W,VW)      S
0539      LW = LOG(W)                      S
0543      F = ( W GTR 28 )                  S
0552      G = (W GTR 9.0)                  S
0561      V = VW/15.0                      S
0565      AH = FF(39 + F , W)              S
0573      A = (2.45**3)W*0.431            S
0579      B = (1.40**3)W*0.300            S
0585      LA = LFF(3,W)                    S
0592      LARS = LFF(2,W)                  S
0599      LAS = LFF(8,W)                   S
0606      RS = FF(4,W)                     S
0613      H = FF(5+F,W)                    S
0621      KA = LARS / (W - RS)              S
0628      LA0 = LA - KA.H                  S

```

Figure 5 (Continued). Computer Program for Ionization Rate Contours

```

0632      ZS = (LAS - LA0) / KA                                $
0637      ALP23 = V.FF(7,W)                                    $
0645      I(1) = I(4) = I(9) = 1.0/V                          $
0651      FOR J = 4,5,6,7,8                                    $
0669      ALP(J) = V.FF(21+J,W)                                $
0683      ALP5 = ALP(5)                                         $
0685      Z0 = G ( 1900.0 + (ALP23 + 0.020)ZS)/A.P23 + (1-G)(H-8) $
0709      AS = EXP(LAS)                                          $
0713      X(2) = ALP23.ZS - AS                                   $
0717      X(3) = ALP23.ZS + AS                                   $
0721      X(4) = ALP(4) ( ALP(4) . Z0 - 1900.0 ) / ( ALP(4) + 0.020 ) $
0733      K12 = FF(41 + F,W)                                     $
0741      EITHER IF W LSS 100                                    $
0741      BEGIN                                                  $
0749      I023 = EXP((-0.20278297LW + 1.5887143)LW + 7.4558767) $
0754      I23 = I023 . V*-0.79                                  $
0761                                                    END $
0761      OTHERWISE $ BEGIN $
0762      VWN = -EXP( (((-7.9423586**4)LW + 0.021809740)LW $
0767      - 0.22171897)LW + 0.97745048)LW - 1.8205694) $
0776      VWSN = VW*VWN $
0781      I023 = EXP( (((-0.0017555634LW + 0.046499101)LW - $
0786      0.42765104)LW + 1.0535187)LW + 13.053862 ) $
0793      I23 = I023.VWSN $
0796      I023 = I023.15*VWN $
0802                                                    END $
0802      X(1) = X(2) - LOG(I23)/K12 $
0811      ALP5P = V.FF(11,W) $
0819      ALP(9) = V.FF(23+F,W) $
0828      EITHER IF ALP(5) GEQ AH $

```


Figure 5 (Continued). Computer Program for Ionization Rate Contours

```

0837          KAA(5) = FF(30*F,W)                                $
0841      OTHERWISE                                              $
0845      BEGIN          KAA(5) = FF(32,W)                        $
0849          ALP(5) = ALP5P                                     END    $
0851          FOR J = 6,7                                         $
0857          KAA(J) = FF(22+2J+(ALP(J) LSS AH) , W)             $
0883          KAA(9) = FF(38,W)                                   $
0890          ABSQ = FF(1,W)                                       $
0897          FOR J = 6,7,5                                       $
0907      BEGIN          EITHER IF ALP(J) LSS AH                 $
0907          QQ = ALP23                                           $
0918      OTHERWISE                                              $
0918          QQ = ALP(J) - AH                                       $
0923          PHI(J) = ((ALP(J) + AH) + SQRT(ABSQ + (ALP(J)+AH).(ALP(J)+AH)))
0937          /((QQ) + SQRT(ABSQ + QQ.QQ))                         END    $
0951          FOR J = 6,7,5                                       $
0961          I(J) = 2.A.KAA(J).LOG(PHI(J))                       $
0974          EITHER IF ALP(5) GEQ AH                             $
0974          ALP(5) = ALP5P                                       $
0981      OTHERWISE                                              $
0981          ALP(5) = ALP5                                         $
0984          FOR J = (5,1,9)                                       $
0995          X(J) = (6600 + 10200F)(W+(0.445 - 0.281F))ALP(J)   $
1021          IF ALP(5) QTR AH                                       $
1029          X(5) = X(5) - B , SQRT(ABSQ + ALP5P , ALP5P )     $
1036          ALP(5) = ALP5                                         $
1038          SEMI(X(7),I(7),X(9),I(9) $ M789,B789)               $
1054          I(8) = IFF(X(8),M789,B789)                           $
1063          Y815 = EXP(((( 9.9684814+-4)LW - 0.027025999)LW +
1068          0.22433052)LW - 0.12350012)LW + B.7992249)         $

```

Figure 5 (Continued). Computer Program for Ionization Rate Contours

```

1075      SVH = ((3.0592VW,VW/(9**5) - 3.60992VW/9000 + 0.0174592)VW
1089      - 0.346408)VW + 3.44944
1092      Y8 = Y815 , SVH
1095      I(2) = I(3) = I23
1098      FOR J = (1,1,9)
1109      LI(J) = LOG(I(J))
1117      WRITE(SSEC1,ECF1)
1125      OUTPUT EC1(FOR J = (1,1,9) $ J , FOR J = (1,1,9) $ X(J)/5280 ,
1162      FOR J = (1,1,9) $ I(J) , W , VW , Y8/5280 ) $
1192      FORMAT ECF1(I12,B113,W3,*X *,9S13-6,W4,*I *,9S13-6,W6,X35-0,* KT*,
1192      X10-0,* MPH*,B45,*Y8 **,X8,4,W6)
1213      COMMENT COMPUTATION OF VALUES WHICH WILL BE CONSTANT IN NEXT SECTIONS
1216      Y0S = FF(20,W)
1220      YS = Y0S , LOG(I23)/LOG(I023)
1233      X87 = X(8) - X(7)
1236      D = SQRT(Y8.Y8 + X87.X87)
1245      LI7 = LOG ( I(7) / I(9) )
1251      SEMI(X(1),1-0,X(2),I23 $ M12,B12)
1267      SEMI(X(3),I23,X(4),I(4) $ M34,B34)
1283      SEMI(X(5),I(5),X(6),I(6) $ M56,B56)
1299      SEMI(X(6),I(6),X(7),I(7) $ M67,B67)
1315      SEMI(0.0,I23,YS,1.0 $ MYS,BYS)
1331      SEMI(0.0,I(7),D,1.0 $ MYB,6Y8)
1347      WRITE(SSECF5) $ FORMAT ECF5(* I*,B8,*X1 - X2 X3 * X4*,
1347      B4,*X5 * X6 - X7 * X8 - X9*,B5,*Y-STEM*,B5,*Y-CLOUD*,B9,
1347      *CB*,B15,*FOCI*,W4)
1377      COMMENT WE NOW FIND THE ENDPOINTS OF THE SEVERAL ELLIPSES AND
1377      THE FOCI OF THE UPWIND CLOUD ELLIPSES
1377      READ(SSEAIC) $ INPUT EAIC(EDC,FOR J=(1,1,EDC) $ IC(J))
1405      FOR J = (1,1,EDC)

```

Figure 5 (Continued). Computer Program for Ionization Rate Contours

```

1416 BEGIN IJ = IC(IJ) $
1420 XC1 = SLL(IJ , M12 , B12) $
1429 XC3 = SLL(IJ , M34 , B34) $
1438 XC4 = SLL(IJ , M56 , B56) $
1447 IF IJ GTR I(6) $
1455 XC4 = SLL(IJ,M67,B67) $
1461 XC6 = SLL(IJ , M789 , B789) $
1470 YICS = SLL(IJ , MYS , BYS) $
1479 DPR = SLL(IJ , MY8 , BY8) $
1488 YICC = DPR . YE / D $
1493 XPRS = X(2) - LOG ( I23 / IJ ) / K12 $
1504 XX = X(3) + (X(4) - X(3))LOG(I23/ IJ )/LOG(I23/I(4)) $
1525 SA = 3.1415927((X(2)-XPRS)(X(2)-XPRS)+YS(XX+XPRS-2X(2))/2) $
1542 XXYY = LOG(I(7)/IJ) / L17 $
1550 YY = Y8.XXYY $
1553 XXC = X(7) + (X(9) - X(7))XXYY $
1558 P = 6 - ( IJ - 50 I(6)) $
1570 XPRC = X(P) + (X(P+1) - X(P))LOG( IJ / LOG I(P+1)/I(P)) $
1594 CA = 1.5708 YY ( XXC - XPRC ) $
1599 CB = (X(7) + X87.YICC / Y8 ) $
1605 ELLC = SQRT((CB - XC4)(CB - XC4) - YICC.YICC) $
1618 WRITE(SSC2,ECF2) $
1626 OUTPUT EC2(IJ,XC1/5280,XC3/5280,XC4/5280,XC6/5280,YICS/5280,
1656 YICC/5280,CB/5280,(CB-ELLC)/5280,(CB+ELLC)/5280 ) $
1680 FORMAT ECF2(X9.2,2(B2,2X11.4),B3,2X11.4,B3,3X11.4,W4) $
1691 END $
1692 Z99WINDVELOCITYMPH = VM $ Z99YIELDKT W $
1700 COMMENT HERE WE FIND THE CONSTANTS FOR A FORMULA FOR FINDING
1700 INTENSITY IN THE DOWNWIND CLOUD REGION $
1704 X7 = X(7) / 5280 $ X8 = X(8) / 5280 $ X9 = X(9) / 5280 $

```

Figure 5 (Continued). Computer Program for Ionization Rate Contours

```

1712          X87 = X8 - X7      $      X98 = X9 - X8      $
1718          MY8 = Y8 / 5280      $
1722          X44 = X98 . X98 - X87 . X87      $
1729          CI = L17 / X44      $
1733          WRITE($SEC6,ECF6)      $
1741      OUTPUT EC6(L17+LOG([I(9)]),X87.CI,X98.CI,X44/(MY8.MY8),X7      $
1770      FORMAT ECF6(W,*FOR DOWNWIND CLOUD INTENSITIES, *,W4,*,I = EXP (*,
1770          S10.9,* + (*,X12.10,*).XX7 - (*,X11.9,*).SQRT(XX7.XX7 + (*,
1770          S10.8,*Y.Y ) )*,W4 , B55,*WHERE XX7 = X - *,S10.8,B5,
1770          *, ( X AND Y IN MILES ),*,W6      $
1811          IF W EQL 10000.0      $      STOP 44645457      $
1818          GO START      $
1819          FINISH      $
COMPILED PROGRAM ENDS AT 1820
PROGRAM VARIABLES BEGIN AT 3735

```


Figure 5 (Continued). Computer Program for Ionization Rate Contours

LAST LABEL PASSED WAS	START(0001)
LABEL IN PROGRAM	NUMBER OF TIMES EXECUTED
START	0001
VARIABLE IN PROGRAM	VALUE
A	.12976754, 06
ABSQ	.34197939, 02
AM	.17021584, 01
ALP23	.62373482, 00
ALP5	.81358236, 00
ALP5P	.21183611, 01
AS	.18706619, 05
B	.22188803, 05
BYS	.66527252, 05
BYO	.37981424, 06
B12	.69421578, 05
B34	.16264538, 06
B56	.14080468, 05
B67	.29357516, 07
B789	.27881052, 07
CA	.32907063, 11
CB	.32726406, 06
CI	.47418109, -04
D	.37981425, 06
DPR	.46067330, 05
EDC	.000000008
ELLG	.21818324, 06
F	.000000001
G	.000000001
H	.76207868, 05
IJ	.30000000, 04
I23	.35456541, 04
I23	.35456541, 04
J	.000000009
KA	.46930778, -04
K12	.1271975, -03
LA	.11773117, 02
LAR8	.33663793, 01
LAS	.98366434, 01
LA0	.81966230, 01
L17	.91114921, 01
LW	.92103404, 01
MY8	.81334057, 04
MY8	.65219246, 02
M12	.88715596, 04
M34	.14943680, 05
M56	.11616057, 05
M67	.35598784, 06
M789	.27221409, 06
P	.000000005
QO	.41620270, 00
RS	.44771326, 04
SA	.40226966, 10
SVH	.10000000, 01
V	.10000000, 01
VM	.15000000, 02
VWH	.73964731, 00
VWGH	.13492961, 00
H	.10000000, 05
XC1	.16073800, 04
XC3	.43000790, 05
XC4	.10708308, 06
XC6	.60865920, 06
XPRC	.10708309, 06
XPRS	.16073805, 04
XX	.43000799, 05
XXC	.60865921, 06
XXVY	.12126946, 06
X44	.19215216, 06
X7	.58300899, 02
X8	.88649301, 02
X87	.30346402, 02
X9	.52805024, 03
X98	.43940094, 03
YICC	.41766826, 05
YICR	.13901792, 04
Y8	.66527253, 05
YV	.41766818, 05
Y8U	.66527255, 05
Y8	.34435702, 06
Y815	.34435702, 06
Z9	.3912207, 05
Z0	.3912207, 05
Z99YINDVEL	.000000012
Z99YISLDKY	.0000010000

Figure 5 (Continued). Computer Program for Ionization Rate Contours

ARRAY ALP

.00000000, 00 .00000000, 00 .00000000, 00 .42266858, 01 .81656236, 00 .14927943, 01 .40457582, 01
 .81517684, 01 .36443750, 02

ARRAY I

.10000000, 01 .35456541, 04 .35456541, 04 .10000000, 01 .21872992, 01 .52492282, 04 .90588020, 04
 .50283099, 04 .10000000, 01

ARRAY IC

.10000000, 01 .30000000, 01 .10000000, 02 .30000000, 02 .10000000, 03 .30000000, 03 .10000000, 04
 .30000000, 04 .10000000, 03 .20000000, 03 .30000000, 03 .60000000, 03 .10000000, 04 .20000000, 04
 .20300000, 04 .45000000, 04 .00000000, 00 .00000000, 00 .00000000, 00 .00000000, 00 .00000000, 00
 .00000000, 00 .00000000, 00 .00000000, 00 .00000000, 00 .00000000, 00 .00000000, 00 .00000000, 00
 .00000000, 00 .00000000, 00 .00000000, 00 .00000000, 00 .00000000, 00 .00000000, 00 .00000000, 00
 .00000000, 00 .00000000, 00 .00000000, 00 .00000000, 00 .00000000, 00 .00000000, 00 .00000000, 00

ARRAY KAA

.00000000, 00 .00000000, 00 .00000000, 00 .00000000, 00 .15523881, -04 .48640727, -01 .72945764, -01
 .00000000, 00 .42266870, -04

ARRAY L

.48600000, 00 .10700000, 01 .33890000, 01 .23190000, 01 .38200000, 01 .42260000, 01 -.50900000, 00
 .28800000, 01 .33080000, 01 .35640000, 01 -.54000000, -01 .38500000, 01 .42550000, 01 .38620000, 01
 .42880000, 01 .40050000, 01 .44100000, 01 .51900000, 01 .32020000, 01 .32230000, 01 .36440000, 01
 .40490000, 01 .13710000, 01 .98000000, 00 .27000000, 00 -.17600000, 00 .30000000, -01 .43000000, -01
 .18300000, 00 -.32860000, 01 -.28890000, 01 -.31850000, 01 .00000000, 00 -.12340000, 01 -.12290000, 01
 -.98900000, 00 -.10790000, 01 -.21660000, 01 -.43100000, 00 -.83700000, 00 -.25030000, 01 -.26000000, 01
 .00000000, 00 .00000000, 00 .00000000, 00 .00000000, 00 .00000000, 00 .00000000, 00 .00000000, 00

ARRAY M

.26200000, 00 .78000000, -01 .43100000, 00 .33300000, 00 .44500000, 00 .16400000, 00 .76000000, -01
 .34800000, 00 .40600000, 00 .31900000, 00 .95000000, -01 .48100000, 00 .20000000, 00 .58600000, 00
 .30500000, 00 .59600000, 00 .31500000, 00 .31900000, 00 .31100000, 00 .40000000, 00 .44700000, 00
 .18600000, 00 .12400000, 00 .14400000, 00 .89000000, -01 .22000000, -01 .38000000, -01 .14100000, 00
 .15100000, 00 .29800000, 00 .00720000, 00 -.40600000, 00 .00000000, 00 -.74000000, -01 -.22000000, -01
 -.37000000, -01 .20000000, -01 .55200000, 00 -.14000000, -01 .26700000, 00 -.40400000, 00 .33700000, 00
 .00000000, 00 .00000000, 00 .00000000, 00 .00000000, 00 .00000000, 00 .00000000, 00 .00000000, 00

ARRAY PHI

.00000000, 00 .00000000, 00 .00000000, 00 .00000000, 00 .17209733, 01 .15156043, 01 .16136391, 01
 .00000000, 00 .00000000, 00

ARRAY X

-.69421579, 05 .30899180, 04 .40503536, 05 .16264939, 06 .23172180, 05 .11958192, 06 .30782875, 06
 .46806831, 06 .27881053, 07

Table III

LIST OF SYMBOLS

Notation of computer program	Notation due primarily to Miller	Notation of computer program	Notation due primarily to Miller
A	a	ELLC	Distance from center to focus of ellipse of chosen contour in upwind cloud region
ABSQ	a^2/b^2		
AH	a/h		
ALP ()	$\alpha_4, \alpha_5, \alpha_6, \alpha_7, \alpha_8, \alpha_9$	F	F=1 if W > 28 KT F=0 if W ≤ 28 KT (used to differentiate scaling functions)
ALP23	$\alpha_{2,3}$		
ALP5	α_5	G	G=1 if W < 9 KT G=0 if W ≥ 9 KT
ALP5P	α'_5		
AS	a_s	H	h
B	b	I ()	$I_1, I_4, I_5, I_6, I_7, I_8, I_9$
MYS, BYS *	(0, I_7), (D, 1)	IC ()	Intensities of chosen contours
MY8, BY8 *	(0, $I_{2,3}$), (Y_s , 1)	IJ	Intensity of chosen contour $I_{2,3}^0$
M12, B12 *	(X_1, I_1), ($X_2, I_{2,3}$)	I023	$K_{2,3}(1) \bar{A}_{f,2,3}^0$
M34, B34 *	($X_3, I_{2,3}$), (X_4, I_4)	I23	$I_{2,3}$
M56, B56 *	(X_5, I_5), (X_6, I_6)	J	Dummy variable used as "i" in I_1 , etc.
M67, B67 *	(X_6, I_6), (X_7, I_7)	KA	K_a
M789, B789*	(X_7, I_7), (X_9, I_9)	KAA ()	$K_i(1) \bar{A}_\alpha, K'_i(1) \bar{A}'_\alpha$
CA	CA(I)	K12	$K_1, 2$
CB	X_c	L ()	Array containing constants for scaling functions
CI	LI7 X44		
D	D	LA	ln a
DPR	D'	LARS	ln a/ R_s
EDC	Number of contours studied	LAS	ln a_s

Table III (Continued)

LIST OF SYMBOLS

<u>Notation of computer program</u>	<u>Notation due primarily to Miller</u>	<u>Notation of computer program</u>	<u>Notation due primarily to Miller</u>
LAO	$\ln a_0$	XC6	7, 9 **
LI ()	$\ln I_1^0$	XPRC	X'
LI ₇	$\ln(I_7/I_9)$	XPRS	X'
LW	$\ln W$	XX	X
M ()	Array containing constants for scaling functions	XXC	X
P	Used in equations involving X'	XXYY	$\frac{\ln(I_7/I)}{\ln(I_7/I_9)}$
PHI	ϕ_5, ϕ_6, ϕ_7	X44	$X_{98}^2 - X_{87}^2$
QQ	$\alpha_{2,3}$ or $\alpha_1 - \frac{a}{h}$	X7	X ₇ in feet
RS	R _s	X8	X ₈ in feet
SA	SA(I)	X87	X ₈ - X ₇
SVW	S(v _w)	X9	X ₉ in feet
V	v _w /15	X98	X ₉ - X ₈ in feet
VW	v _w	YICC	Maximum cloud width at chosen contour
VWN	n	YICS	Maximum stem width at chosen contour
VWSN	$\frac{n}{v_w}$	YS	Y _s
W	W	YY	Y
X ()	X ₁ , X ₂ , X ₃ , X ₄ , X ₅ , X ₆ , X ₇ , X ₈ , X ₉	YOS	Y _s ^o
XC1	1, 2 **	Y8	Y ₈ , Y ₈ (v _w)
XC3	3, 4 **	Y815	Y ₈ (15)
XC4	5, 7 **	ZS	Z _s
		ZO	Z _o

Table III (continued)

LIST OF SYMBOLS
Continued

<u>Notation of computer program</u>	<u>Notation due primarily to Miller</u>	<u>Notation of computer program</u>	<u>Notation due primarily to Miller</u>
Z99WINDVELOCITYMPH	v_w	Z99YIELDKT	W

* The slope and intercept, respectively, for a semi-logarithmic line through the two points whose coordinates are given.

** The downwind distance (for the chosen intensity) to the fallout pattern between the points indicated.

TABLE IV

Data Table for Ionization Rate Contour Program

for	N	L(N)	M(N)	for	N	L(N)	M(N)
$(a/b)^2$	1	0.486	0.262	α_9	23	1.371	-0.124
$\ln A/R_s$	2	1.070	0.098		24	0.980	0.146
$\ln A$	3	3.389	0.431	X_4	25	0.270	0.089
R_s	4	2.319	0.333	α_5	26	-0.176	0.022
H	5	3.820	0.445	α_6	27	0.030	0.036
	6	4.226	0.164	α_7	28	0.043	0.141
α_{23}	7	-0.509	0.076	α_8	29	0.185	0.151
$\ln a_s$	8	2.880	0.348	$K_5 \bar{A} \alpha$	30	-3.286	-0.298
	9	3.308	0.496		31	-2.889	-0.572
χ_1	10	3.564	0.319	$K_5' \bar{A} \alpha$	32	-3.185	-0.406
	11	-0.054	0.095		33		
α_5'	12	3.850	0.481	$K_6 \bar{A} \alpha$	34	-1.134	-0.074
X_6	13	4.255	0.200		35	-1.225	-0.022
	14	3.862	0.586	$K_7 \bar{A} \alpha$	36	-0.989	-0.037
X_7	15	4.265	0.305		37	-1.079	-0.020
	16	4.005	0.596	$K_9 \bar{A} \alpha$	38	-2.166	-0.552
X_8	17	4.410	0.315		39	-0.431	-0.014
	18	5.190	0.319	A/H	40	-0.837	0.267
X_9	19	5.202	0.311				
	20	3.223	0.400	K_{12}	41	-2.503	-0.404
χ_s^0	21	3.644	0.467		42	-2.600	-0.337
X_5	22	4.049	0.186				

variable, for example, H (height of cloud), the program determines which formula should be used. The equation for H appears on line 0613 of the contour program.

The following chain is then started

$$H = FF(5 + F, W) \quad \text{line 0613}$$

$$FF(N, W) = EXP(LFF(N, W)) \quad \text{line 0454}$$

$$LFF(N, W) = 2.3025851 L(N) + LW \cdot M(N) \quad \text{line 0467}$$

The program then finds for $W \leq 28$ KT that $F = 0$ since W greater 28 is false and F is a Boolean variable. Therefore for $N = 5$, one finds in the Table IV that $L(5) = 3.820$ and $M(5) = 0.445$. The complete equation of H for $W \leq 28$ KT is

$$H = \exp[(2.3025851)(3.820) + \log_e W \cdot 0.445], \quad (59)$$

$$\log_e H = (2.3025851)(3.820) + \log_e W \cdot 0.445, \quad (59a)$$

or

$$\log_{10} H = 3.820 + 0.445 \log_{10} W. \quad (59b)$$

The variation of X_2 and X_3 with wind speed depends on the wind modified parameter $\alpha_{2,3}$ (lines 0713, 0717). The equations for X_1 and X_4 are then

$$X_1 = X_2 - \frac{2.303 \log_e I_{2,3}}{K_{1,2}} \quad (60)$$

$$X_4 = \frac{V_W(Z_o \alpha_4 V_W - 86.36)}{(1 + 9.273 \times 10^{-4} \alpha_4 V_W)} \quad (61)$$

or

$$X_4 = \frac{\alpha_4(\alpha_4 Z_0 - 1900)}{\alpha_4 + 0.020} \quad (61a)$$

for 15 mph wind velocity.

The equations for the distances X_6 through X_9 (line 0995) are given by

For $i = 6, 7, 8$ and 9

$$X_i = 6.60 \times 10^3 W^{0.445} \alpha_i, \quad W = 1 \text{ to } 28 \text{ KT} \quad (62)$$

$$X_i = 1.68 \times 10^4 W^{0.164} \alpha_i, \quad W = 28 \text{ to } 10^5 \text{ KT} \quad (62a)$$

The above equations also hold for X_5 when α_5 is greater than a/h . When α_5 is less than or equal to a/h , then X_5 is determined by

$$X_5 = 6.60 \times 10^3 W^{0.445} \alpha_5' - 1.40 \times 10^3 W^{0.300} \sqrt{3.06 W^{0.262} + \alpha_5'^2}; \quad W = 1 \text{ to } 28 \text{ KT} \quad (63)$$

or

$$X_5 = 1.68 \times 10^4 W^{0.164} \alpha_5' - 1.40 \times 10^3 W^{0.300} \sqrt{3.06 W^{0.262} + \alpha_5'^2}; \quad W = 28 \text{ to } 10^5 \text{ KT} \quad (63a)$$

Next the intensities I_1 , I_4 , and I_9 are set equal to $\frac{V_W}{15 \text{ mph}}$.

The equations for I_5 , I_6 , and I_7 are on lines 0951 through 0961. I_8 is determined from a semi-logarithmic line between (X_7, I_7) and (X_9, I_9) with the value of X_8 as previously calculated.

After X_1 through X_9 and their corresponding intensities have been found, a graph can then be drawn of the intensity profiles or elevations.

A plot of $\log_{10} I_X(1)$ against distance X for a 10 MT weapon is given in Figure 4. For any set of intensities the intersection (downwind distance X) of the contour ellipses with $Y = 0$ can be read off the graph.

In the computer program semilog equations were found for the Intensity vs. Distance curve so that any pre-selected intensity contour intervals were included in the computer printout.

Next, to find the lateral locations or width of the contour patterns for the stem, the half width Y_S for the stem fallout is needed. Y_S is defined as the lateral distance from the center-line of the stem pattern to the 1r/hr at 1 hr (for 15 mph wind) contour (lines 1216-1220). A semilogarithmic line from $(I_{2,3}, Y = 0)$ to $(1, Y_S)$ is then calculated on line 1315. Using this equation the lateral displacement of any intensity contour of the stem can be found.

The maximum pattern half width for the cloud, Y_8 , is the maximum distance from $Y = 0$ to the 1r/hr at 1 hr contour when the wind velocity is 15 mph. The calculation of Y_8 with its variation due to wind speed occurs on lines 1054 to 1092.

To find the lateral displacements of the contour locations between $(X_7, 0)$ and (X_8, Y_8) a semilogarithmic line from $(I_7, Y = 0)$ to $(1, D = \sqrt{Y_8^2 + (X_8 - X_7)^2})$ is calculated. In lines 1236 through 1347 the $X + Y$ and foci are then found for the ellipses. Using the information in the computer printout an ionization rate contour map can be drawn. (Figure 6).

B. Fractionation Numbers

1. First period of condensation

For a ground surface burst, the ratio of the total moles of liquid carrier to the molar volume $n(l)/V$ is computed by Equations (32) and (33) with $W = 10$ MT or 10,000 KT, and $T = 1673^\circ\text{K}$. They yield

$$t = 53 \text{ sec}$$

$$[n(l)/V]RT = 3.25 \times 10^{-2} \text{ atm.}$$

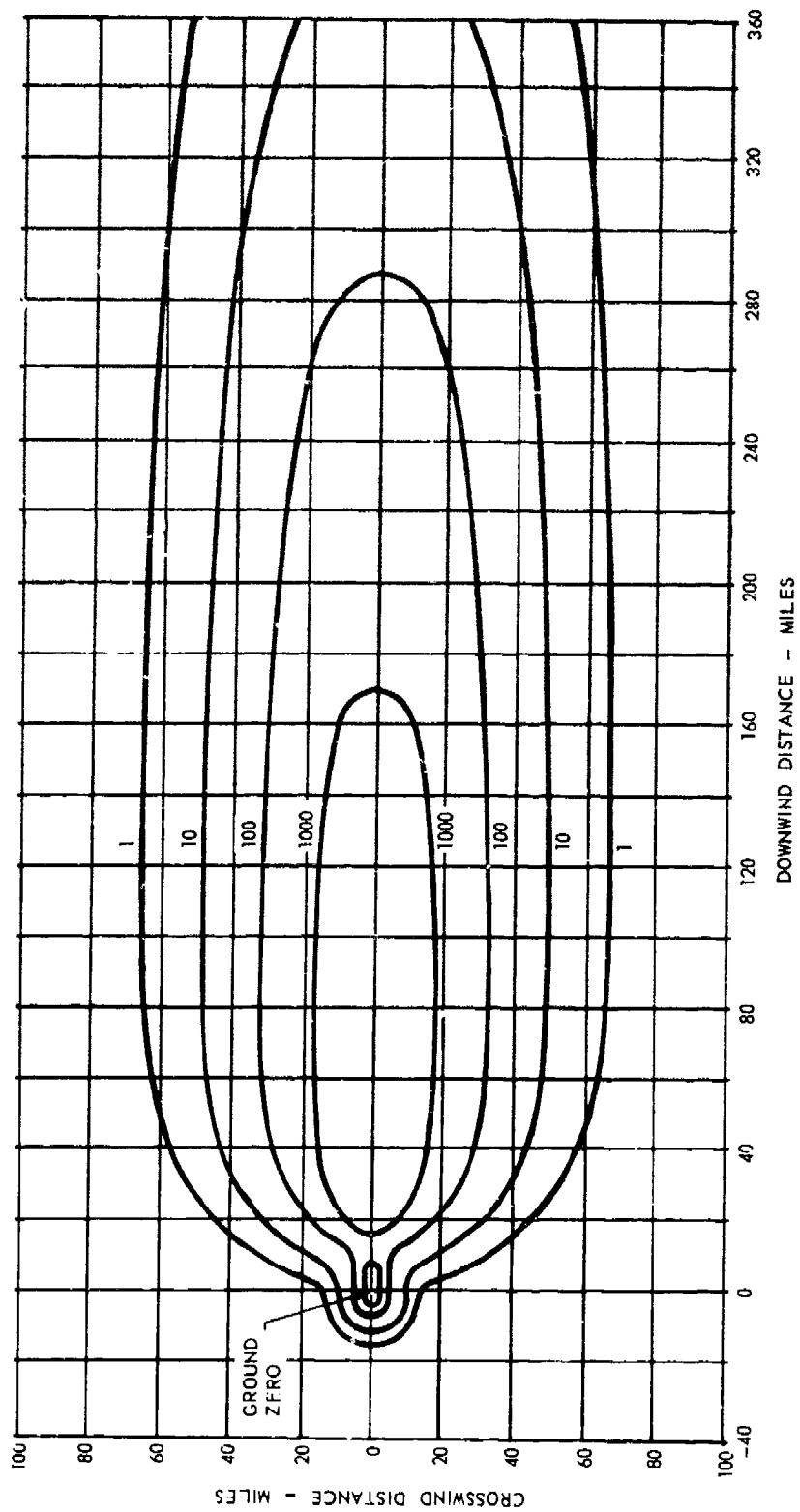
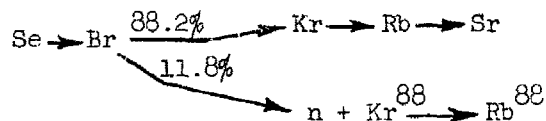


Figure 6. Selected Ionization Rate Contours

For a typical element Sr-89, the procedure of finding its fractionation number of first period of condensation $r_0(89)$ is given below:

Decay chain of Sr-89:



Here a neutron-emitter is involved. But the Bolles and Ballou data have already included this effect, hence no alteration needs to be put on the number of atoms $N(A, t)$ in their work. Moreover, the values calculated by them according to Glendenin theory are generally considered to be more reliable and also used in the following calculations.

	Se	Br	Kr	Rb	Sr
$k_j = p_j$	1.01×10^6	1.04		0.605	4.61×10^{-13}
$k_j^0 = \frac{k_j}{[N(\ell)/V]RT}$	3.108×10^7	32.00		18.62	1.418×10^{-11}
$N(A, t)$	- *	0.21	309	94	3
$\Sigma N(A, t)$	-	0.21	309.21	403.21	406.21
$\frac{N(A, t)}{1 + k_j}$	-	6.363×10^{-3}	0	4.791	3
$\Sigma \frac{N(A, t)}{1 + k_j}$	-	6.363×10^{-3}	(2) 6363	4.797	7.797
$r_0(89)$	-	0.0303	0	0.0119	<u>0.01919</u>

Note: data unlisted, usually negligible

The $r_0(89)$ for Br, Kr, Rb are the by-products.

2. Second period of condensation

The fractionation number of second period of condensation $r_1^i(A, t)$ depends very much on the time and the elements involved in the decay chain.

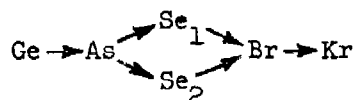
When the time is small, the sublimation pressures of most elements are still quite significant, and the values of $\frac{P_j V}{RT}$ are usually greater than those of 0.23 BWY_j^0 . In the second period of condensation a portion of each such element remains in the vapor phase. Therefore, in computing, the ratio of these two values should be set equal to unity. As time increases, the sublimation pressures of all elements except the rare gases and As and Se, decrease sharply and soon become negligible. Therefore, the second period fractionation number for a mass chain not involving the rare gases and As and Se will be greatly simplified:

$$r'_0(A, t) = 1 - r_0(A, t). \quad (64)$$

Four typical examples are given below:

(a) 10 MT ground surface burst, 60 sec after burst, Kr (83).

Decay chain:



This involves a split chain, but the Bolles and Ballou data also have taken this effect into account.

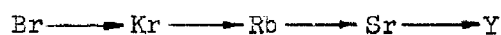
	Ge	As	Se ₁		Br	Kr
$r_0(83)$	—	0	0	0	0.0066	0.0066
$1-r_0$	—	1	1	1	0.9934	0.9934
$N(83.60)$	—	0.13	21.80	16.80	12.30	0
ΣN	—	0.13	21.93	16.93	51.03	51.03
$N^0 = (1-r_0)N$	—	0.13	21.80	16.80	12.20	0

ΣN^0	—	0.13	21.93	16.93	50.93	50.93
P_j	(2)8216	(9)3578	34.53	34.53	0.2086	
$\frac{V}{0.23BWRT} \times 10^7$	7.41	7.41	7.41	7.41	7.41	7.41
$\frac{\Sigma N''}{\Sigma N}$	—	1	1	1	0.9980	0.9980
$r'_0(83)$	—	0	0	0	0*	0

* Note: $r'_0(A, t)$ can not be a negative value, hence the smallest is zero.

(b) 10 MT ground surface burst, 1.47 min after burst, Sr(Y)(90).

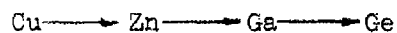
Decay chain:



	Br	Kr	Rb	Sr	Y
$r_0(90)$	—	0	0.036	0.1378	0.1378
$1-r_0$	—	1	0.964	0.8622	0.8622
$N(90,88)$	—	67	338	106	0
ΣN	—	67	405	511	511
$N''=(1-r_0)N$	—	67	325.8	91.4	0
$\Sigma N''$	—	67	392.8	392.8	392.8
P_j	(4)3050	∞	(6)4338	0	0
$\frac{V}{0.23BWRT} \times 10^8$	1.92	1.92	1.92	1.92	1.92
$\frac{\Sigma N''}{\Sigma N}$	—	1	0.9698	0.7686	0.7686
$r'_0(90)$	—	0	0	0.0936	0.0936

(c.) 10 MT ground surface burst, 1.47 min after burst, Ge(75).

Decay chain:



	Cu	Zn	Ga	Ge
$r_o(75)$	—	1	1	0.6716
$1-r_o$	—	0	0	0.3284
$N(75,88)$	—	(3)12	0.0459	0.0536
ΣN	—	(3)12	0.0460	0.0996
$N^0 = (1-r_o)N$	—	0	0	0.0176
P_j	—	0	0	(11)2288
$\frac{V}{0.23\text{BWTR}} \times 10^8$	1.92	1.92	1.92	1.92
\bar{v}_j^*	—			(3)4268
$\Sigma_j \frac{V P_j N^0}{0.23\text{BWTR}_j}$	—	0	0	0.0018
$r'_o(75)$	—	0	0	0.3266

* Note: In computing Y_j , the individual mass number dependent conversion factor $\alpha(A)$ for U^{235} to U^{238} should be multiplied to each radionuclide.

$$Y_j = \Sigma_A \alpha(A) N(A, t). \quad \alpha(A) \text{ can be calculated from Table I}$$

(d.) 10 MT ground surface burst, 6.77 min after burst, Sr(89). Decay chain was shown in Section (a.)

	Se	Br	Kr	Rb	Sr
$r_o(89)$	—	0.0303	0	0.0119	0.0192
$1-r_o$	—	0.9697	1	0.9881	0.9808

$N(89,406)$	—	—	84	267	56
ΣN	—	—	84	351	407
$N''=(1-r_o)N$	—	—	84		
$\Sigma N''$			84	84	84
p_j			∞	0	0
$\Sigma N'' \Sigma N$			1	0.2393	0.2064
$r_o(89)$	—	—	0	0.7488	0.7804

3. Gross Fractionation Number

The gross fractionation number, r_X , or r_Q , is defined by Equation (47). The two ionization rates, $i_{fp}(t)$ and $i_{fp}^*(t)$, in this formula are defined by Equations (45) and (46) respectively. The computations are straightforward, though tedious, once the values of the fractionation numbers, disintegration multipliers and activities are known. The variations in the ionization rates of normal fission products with time, or simply the decay of normal fission products, for U-235, U-238 and Pu-239 have been calculated and are tabulated in Table V. From this table, the normal ionization rate of U-238 at $H + 1$ hour can be interpolated and obtained as

$$i_{fp}(1) = 6.973 \times 10^{-13} \text{ (r/hr at 1 hr) / (fission/sq. ft.)} \quad (65)$$

For a 10 MT surface burst, the condensed ionization rates for four different fireball rising times have been computed and are listed with the values of gross fractionation numbers computed from them:

t	$i_{fp}^*(1)$	$r_X(t)$
53 sec	2.408×10^{-13}	0.388

60 sec	3.255×10^{-13}	0.467
1.47 min	3.873×10^{-13}	0.554
2.15 min	5.029×10^{-13}	0.721

Since the fireball rising time, t , is related to the particle size parameter, α , by Equation (12), $r_x(t)$ is also a function of α , sometimes denoted as $r_\alpha(t)$.

C. Activity-Concentration Intensity Ratio

With Equations (47) and (48), the activity concentration intensity ratio for any isotope at any downwind location can be readily computed. The values of the ratio for six biologically important isotopes in a 10 MT surface burst are calculated and shown in Table VI.

TABLE V

Decay of Normal Fission Products from U-235, U-238 and Pu-239
(r/hr at 3 ft above an infinite plane for 10^4 fissions per sq. ft.)

Age			U-235		U-238	Pu-239	
Years	Days	Hours	Thermal	Fission	(8 Mev)	Thermal	Fission
		0.763	(8)9977 ^(*)	(8)9960	(8)9329	(8)8907	(8)8750
		1.12	(8)6648	(8)6632	(8)6172	(8)5866	(8)5761
		1.64	(8)4149	(8)4153	(8)3827	(8)3592	(8)3537
		2.40	(8)2453	(8)2484	(8)2256	(8)2071	(8)2065
		3.52	(8)1410	(8)1450	(8)1303	(8)1166	(8)1196
		5.16	(9)8079	(9)8418	(9)7582	(9)6642	(9)7098
		7.56	(9)4786	(9)5014	(9)4587	(9)3986	(9)4398
		11.1	(9)2964	(9)3094	(9)2897	(9)2555	(9)2821
		16.2	(9)1804	(9)1869	(9)1792	(9)1626	(9)1761
		23.8	(10)9716	(9)1094	(9)1073	(9)1010	(9)1063
	1.45	34.8	(10)6305	(10)6428	(10)6393	(10)6235	(10)6360
	2.13	51.1	(10)3730	(10)3786	(10)3817	(10)3869	(10)3811
		3.12	(10)2276	(10)2319	(10)2365	(10)2470	(10)2362
		4.57	(10)1483	(10)1524	(10)1556	(10)1645	(10)1546
		6.70	(11)9986	(10)1031	(10)1039	(10)1099	(10)1021
		9.82	(11)6774	(11)6972	(11)6899	(11)7244	(11)6655
		14.4	(11)4490	(11)4587	(11)4462	(11)4650	(11)4226
		21.1	(11)2910	(11)2940	(11)2845	(11)2953	(11)2660
		30.9	(11)1813	(11)1807	(11)1762	(11)1837	(11)1645
		45.3	(11)1061	(11)1039	(11)1034	(11)1092	(12)9777
		66.4	(12)6055	(12)5807	(12)5910	(12)6360	(12)5728
		97.3	(12)3676	(12)3497	(12)3559	(12)3896	(12)3543
		143	(12)2170	(12)2090	(12)2079	(12)2320	(12)2200
		208	(12)1194	(12)1164	(12)1133	(12)1287	(12)1180
		301	(13)4874	(13)4790	(13)4733	(13)5707	(13)5170
1.2	438		(13)1399	(13)1373	(13)1525	(13)2135	(13)1864
1.78	650		(14)3884	(14)3758	(14)5517	(14)9083	(14)7690
2.60			(14)2031	(14)1975	(14)3160	(14)4964	(14)4352
3.80			(14)1444	(14)1432	(14)2213	(14)2692	(14)2594
5.58			(14)1154	(14)1158	(14)1603	(14)1442	(14)1611
8.18			(14)1026	(14)1021	(14)1291	(15)9971	(14)1225
12.0			(15)9432	(15)9293	(14)1094	(15)8452	(14)1057
17.6			(15)8310	(15)8211	(15)9164	(15)7377	(15)9160
25.7			(15)7183	(15)6987	(15)7431	(15)6219	(15)7668

(*) Numbers in parentheses indicate the number of zeros between the decimal point and the first significant figure.

TABLE VI. Atom Concentration Intensity Ratio $[N^*(A)/I(1)] \left(\frac{\text{atoms}}{\text{sq. ft.}} / \frac{I}{\text{hr}} \text{ at } H + 1 \text{ hour} \right)^*$

α_o	X Miles	$r_\alpha(1)$	89		90		106		131		137		140	
			Sol.	Insol.	Sol.	Insol.	Sol.	Insol.	Sol.	Insol.	Sol.	Insol.	Sol.	Insol.
0.90	13.0	0.40	0	0.371	0	3.09	0	0.474	0	0.317	0	0.145	0	13.73
1.00	14.5	0.48	0	0.318	1.89	2.65	0.765	0.406	0.49	0.271	0	0.124	0	11.77
1.50	21.7	0.61	0	0.243	7.2	2.03	5.74	0.310	2.59	0.207	0	0.095	6.57	9.00
2	29.0	0.70	4.65	0.214	10.5	1.78	5.02	0.273	2.83	0.182	6.21	0.084	11.5	7.90
3	43.5	0.76	5.80	0.200	10.9	1.66	4.63	0.255	5.23	0.170	8.79	0.078	11.9	7.39
4	58.0	0.77	6.34	0.198	11.0	1.65	4.57	0.253	9.99	0.169	9.8	0.077	11.9	7.33
6	87	0.78	6.77	0.197	11.2	1.64	4.52	0.251	10.1	0.168	10.8	0.077	11.8	7.27
8	116	0.78	7.23	0.195	11.3	1.63	4.52	0.249	10.2	0.166	11.5	0.076	11.8	7.21
10	145	0.785	7.63	0.195	11.4	1.63	4.49	0.249	10.1	0.166	11.7	0.076	11.7	7.21
20	290	0.79	7.68	0.193	11.4	1.61	4.46	0.247	10.1	0.165	11.8	0.076	11.6	7.15
40	580	0.80	7.69	0.192	11.3	1.60	4.41	0.245	10.0	0.164	11.8	0.075	11.5	7.10
60	870	0.805	7.74	0.189	11.2	1.57	4.38	0.241	9.89	0.161	11.9	0.074	11.4	6.98
80	1160	0.81	7.79	0.187	11.1	1.56	4.35	0.239	9.83	0.160	12.0	0.073	11.4	6.92
100	1450	0.82	7.79	0.187	11.0	1.56	4.30	0.239	9.71	0.160	12.1	0.073	11.2	6.92

* All values to be multiplied by 10^{10} .

D. Particle Size Distribution

There is almost no data available on particle size distribution, nor has any rigorous theoretical approach been made. However, using the scaling functions of the previously discussed simplified fallout model, estimates can be made of the particle size groups that fall at any downwind location.

Given the fall velocity and the initial altitude, the size of spherical particles falling through a standard atmosphere can be found in curves prepared by D. E. Clark.⁽¹¹⁾ At any downwind distance X the first information needed is the maximum and minimum α size for the particle groups arriving at that location. Because the formulae for α_{\max} and α_{\min} depend on whether the α group descends from the stem or the cloud, it was decided that the X-coordinate intersection of the logarithmic line connecting (X_3, I_3) to (X_4, I_4) (point 3 to point 4 in Figure 4) with the logarithmic line from (X_5, I_5) to (X_6, I_6) - extended if necessary - would be the division mark. For any downwind distance less than this intersection X coordinate, the source of the particle group is assumed to be the stem. Then α_{\max} and α_{\min} for the stem may be solved by graphical methods or by the following computer approach. Essentially a Newton-Raphson iterative procedure is performed on the following function to find separately

α_{\max} and α_{\min} .

$$f(\alpha) = \frac{k_a(\alpha Z_o - \frac{V_w P}{K_Z})}{2.303(\alpha + \frac{V_w q}{K_Z})} - \log [X - \frac{a(Z_o \alpha - \frac{V_w P}{K_Z})}{\alpha + \frac{V_w p}{K_Z}}] + \log a_o \quad (66)$$

where

k_a is the exponential constant for the fireball major axis expansion,

Z_o is a yield dependent multiplier,

k_z is an empirical inverse time constant, 0.011 sec^{-1} ,
 V_w is the wind velocity, usually assigned to be 10 mph,
 p is the constant in the empirical formula of V_z/V_f , 0.95 when
 $Z = 5,000$ to $50,000 \text{ ft.}$, $d = 200$ to $1,200 \text{ microns}$,
 q is the constant in the empirical formula of V_z/V_f , 1.02×10^{-5}
when $Z = 5,000$ to $50,000 \text{ ft.}$, $d = 200$ to $1,200 \text{ microns}$, and
 a_0 is the major semi-axis of the fireball at ground zero.

The iterative procedure is

$$\alpha_0 = \text{initial estimate} \quad (67)$$

$$\alpha_{k+1} = \alpha_k - \frac{f(\alpha_k)}{f'(\alpha_k)} \quad (68)$$

If the sequence of α 's approach a limit, then this α is such that $f(\alpha) \doteq 0$;
or α is approximately equal to α_{\max} or α_{\min} depending on the sign of the
number enclosed in the absolute value symbol of Equation (56).

When the downwind distance is greater than or equal to the X
intersection coordinate, it is assumed that the fallout originates from
the cloud. For particle groups falling within the cloud area at any (X, Y)
location, the maximum and minimum α values can be calculated by:

$$\alpha_m = \frac{hX \pm \sqrt{X^2 b^2 (1 - y^2/a^2) + (a^2 - y^2) h^2 - b^2 (1 - y^2/a^2)}}{h^2 - b^2 (1 - y^2/a^2)} \quad (69)$$

where Y is translated to y by Equation (57).

For any α value, the fall-rate is given by $V_f = \frac{V_w}{\alpha}$. The height of fall
for the stem fallout is

$$z = \frac{(z_0 \alpha k_z - V_w p)}{\alpha k_z + V_w q} \quad (70)$$

For the particle groups that originate from the cloud the maximum and minimum height of fall is given by

$$z = \frac{\alpha(X - \alpha h)b^2 \pm ab \sqrt{(a^2 + \alpha^2 b^2)(1 - y^2/a^2) - (X - \alpha h)^2}}{a^2 + \alpha^2 b^2} \quad (71)$$

Using this information calculated in the particle size parameter program, Figure 7, and a set of curves prepared by D. E. Clark, see Figure 8, the approximate particle size distribution at (X, Y) can be estimated.

For a 10 MT detonation, and for various downwind distances the maximum and minimum α ; the falling velocity, V_f ; the initial altitude Z and particle diameter μ are given in Table VII.

Recent work by Clark and Cobbin⁽¹²⁾ is closely related to the subject of this report. These authors used the same fallout model as described herein for the calculation of particle size and radiation intensity at varying distances from ground zero. The results obtained are in good agreement with those herewith reported for weapons of similar yield.

Figure 7. Computer Program for Particle Size Parameters

```

0200      RAC-220 STANDARD VERSION 2/1/62
0200      COMMENT PARTICLE SIZE BY R. E. JAMES FOR A = 633 .
0202      ZC = 35565.872 $ LAO = 7.9940580 $ KA = 5.1166706E-5
0206      W = 5000.0 $ XINT = 12.0
0210      KZ = 0.011 $ VW = 22 $ P = 0.95 $ C = 1.02E-5
0218      XINT = XINT(5280)
0221      A = (2.45**3)W*0.431
0227      B = (1.40**3)W*0.300
0233      ABSO = A.A / (B.B)
0243      XX=X $ H=16600W*0.164 $ EGG=0 $
0252      SUBROUTINE EM $ BEGIN INTEGER EMD
0254      EMA = AM + 0.02
0257      EMB = (ZC * AM - 1900) / EMA
0263      EMC = AM * EMB - XX
0267      EMD = SIGN(EMC)
0275      EME = (KA(C*0.02 ZC + 1900)/EMA + (ZC*AM(EMA + C*0.2) - 38.0)
0287      / (XX * EMA - (ZC*AM-1900)A.)) / EMB
0304      EMF = KA * EMB - LOG(ABS(EMC)) + LAO
0315      FMG = AM - EMF / EME
0320      AM = (FMG + ABS ( FMG ) ) / 2
0325      RETURN END EM
0327      FOR XX = (5,5,50),75,100,150,200,300,4000 /10
0360      BEGIN WRITE(55EIK) $ FORMAT EIK(X) $
0370      XX = 5280 XX
0373      EITHER IF XX LSS XINT $ BEGIN
0382      FOR AN = XX/30000.0 * EMD*EMD(0.5 + W/10000.0)
0395      BEGIN ENTER EM
0400      UNTIL ABS(EMF/EMC) LSS 0.0001 $ ENTER EM
0411      Z = (ZC*AM*KZ - VW*P)/(AM*KZ + VW*0)
0430      WRITE(55END,EMP) END END
0439      OTHERWISE $ BEGIN
0439      HB = H*B = B*B
0447      FOR EMD = 10-1 $ BEGIN
0468      AM = (H*XX + EMD.SORT(XX*XX*B*B + A.A*H-))/H
0479      Z = H + AM(XX-AM*B)2*B/1A.A + AM*AM*B*B)
0500      WRITE(55END,EMP) END END
0509      XX = XX / 5280 END
0514      OUTPUT EMD(FIX(XX/5280), 41544561 + 394 EMD , AM , 22/AM , Z )
0542      FORMAT EMP(110,B5,45,3X16.6,W2)
0549      FINISH
COMPILED PROGRAM ENDS AT 0550
PROGRAM VARIABLES BEGIN AT 4340

```

Table VII

Particle Size Distribution at Various Downwind Distances for 5 MT Weapon Yield

		$V_z(\text{ft/sec})$	$Z(\text{ft})$	$d(\mu)$
5	AMAX	1.278423	17.288596	33544.392000
5	AMIN	.430318	51.124897	20740.633000
10	AMAX	2.039098	10.789082	34291.025000
10	AMIN	1.100357	19.993500	33223.220000
15	AMAX	2.761904	7.985517	59832.324000
15	AMIN	-.252719	-87.853061	67059.168000
20	AMAX	3.208437	6.856921	58629.4982000
20	AMIN	.137143	160.416230	66373.673000
25	AMAX	3.862314	6.007129	57718.555000
25	AMIN	.519660	42.335312	60856.467000
30	AMAX	4.123050	5.335855	56897.646000
30	AMIN	.895320	24.572218	70490.752000
35	AMAX	4.596117	4.792905	56163.886000
35	AMIN	1.264848	17.396143	72063.810000
40	AMAX	5.062976	4.345270	55511.772000
40	AMIN	1.628164	13.511982	73166.617000
45	AMAX	5.541091	3.970336	54934.673000
45	AMIN	1.986464	11.074955	74103.028000
50	AMAX	6.023951	3.652037	54425.326000
50	AMIN	2.339999	9.401712	75143.714000
75	AMAX	8.493898	2.590094	52653.792000
75	AMIN	4.052027	5.429360	78804.392000
100	AMAX	11.026300	1.955229	51620.713000
100	AMIN	3.701601	3.858565	81064.375000
150	AMAX	13.185545	1.352237	50736.047000
150	AMIN	8.906307	2.470129	83367.650000
200	AMAX	21.404335	1.027829	50424.696000
200	AMIN	12.051468	1.825503	84386.186000
300	AMAX	31.911227	.689412	50135.602000
300	AMIN	18.272474	1.201996	85209.921000
400	AMAX	42.455397	.518190	50029.304000
400	AMIN	24.456210	.899567	85518.724000

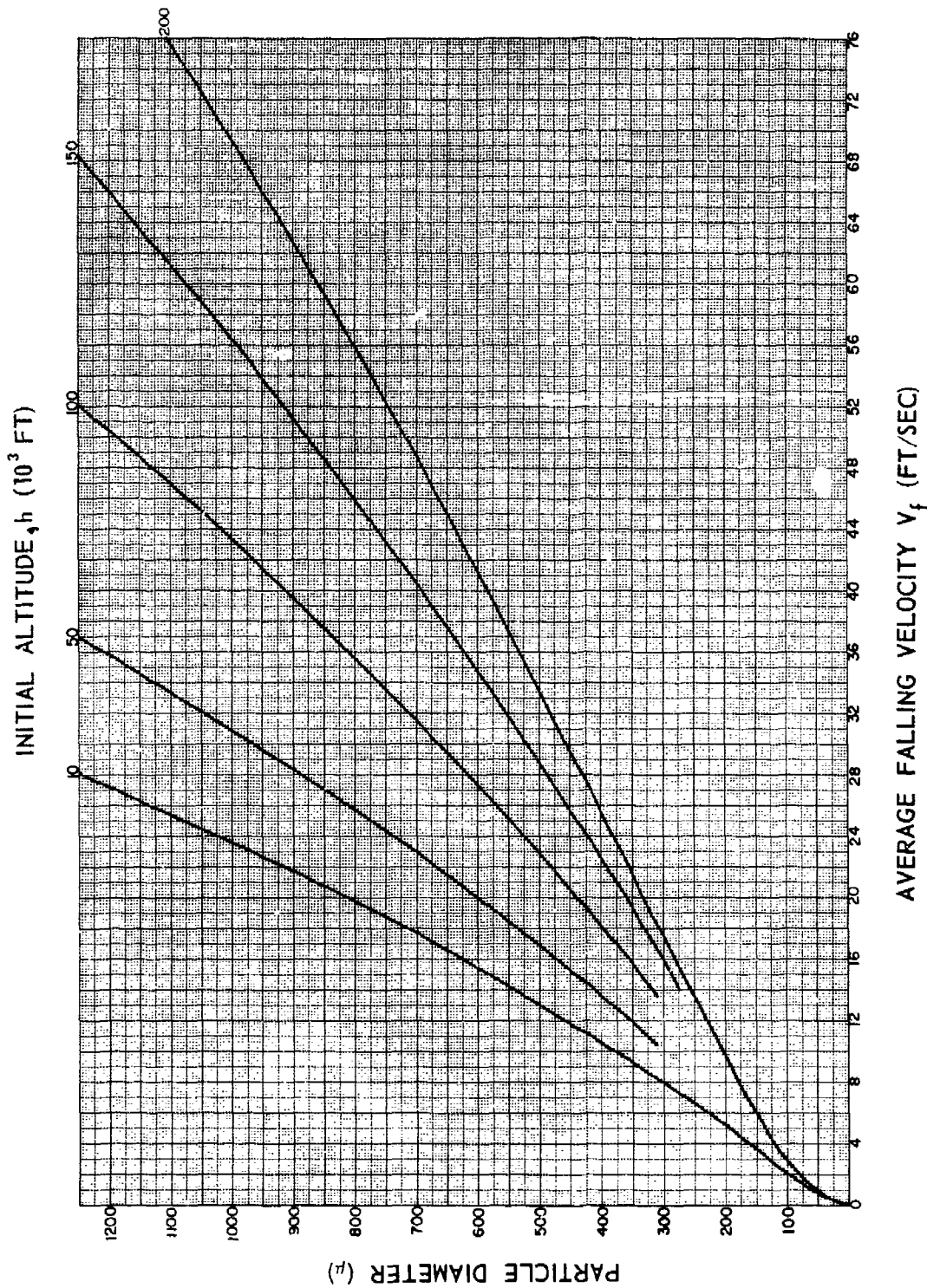


Figure 8. Falling Velocity for Spherical Particles Falling from Various Altitudes to Sea Level

IV. INDUCED RADIOACTIVITY IN SOILS

Elements can be made radioactive by the action of thermal neutrons which excite the stable atom making it unstable and radioactive. As thermal neutrons are liberated in a nuclear explosion, there will be some induced radioactivity in the soil around the detonation site. A small portion of this soil will be taken up into the fireball of the bomb (for a ground burst or near ground burst) and become part of the total fallout.

A..W. Klement⁽¹³⁾ in his report concerning the potential radionuclides produced in weapons detonations, lists the activities of the various nuclides that are induced in the soil. A total of 10^{26} neutrons per KT was assumed to be liberated, which agrees within a factor of 15 with that of 1.5×10^{27} neutrons per KT calculated from Glasstone⁽¹⁴⁾. The composition of the soil that was used for these calculations is given in Table VIII.

Figure 9 gives the decay of the induced radioactivity in soil. The data was obtained by taking the contributions of the various nuclides given in Table IX and summing them for the various times after detonation up to one year.

Figure 10 , "Integrated Neutron Flux as a Function of the Slant Range in Air of 0.9 Sea-Level Density for a 1-Kiloton Explosion" shows the neutron flux versus distance for a 1 KT bomb. These curves, as given by Glasstone⁽¹⁴⁾, were integrated over an area with a 2,500 yard radius and were used to correlate Klement's values.

Senftle and Champion⁽¹⁵⁾ give a detailed discussion concerning induced radioactivity. A method for calculating the induced radioactivity involving tables and formulas is also given. This method was used to prepare the data in Table X in order to correlate the data given by Klement⁽¹³⁾ and shown in Table IX.

TABLE VIII

Composition of the (NIS) Soil Assumed

<u>Element</u>	<u>% by weight</u>	<u>Element</u>	<u>% by weight</u>
H	1.00	Si	28.40
C	0.80	P	0.10
O	50.16	K	2.50
Na	1.60	Ca	5.70
Mg	0.80	Ti	0.20
Al	6.80	Mn	0.04
		Fe	1.90

Density: 1.18 gm/cu.cm.

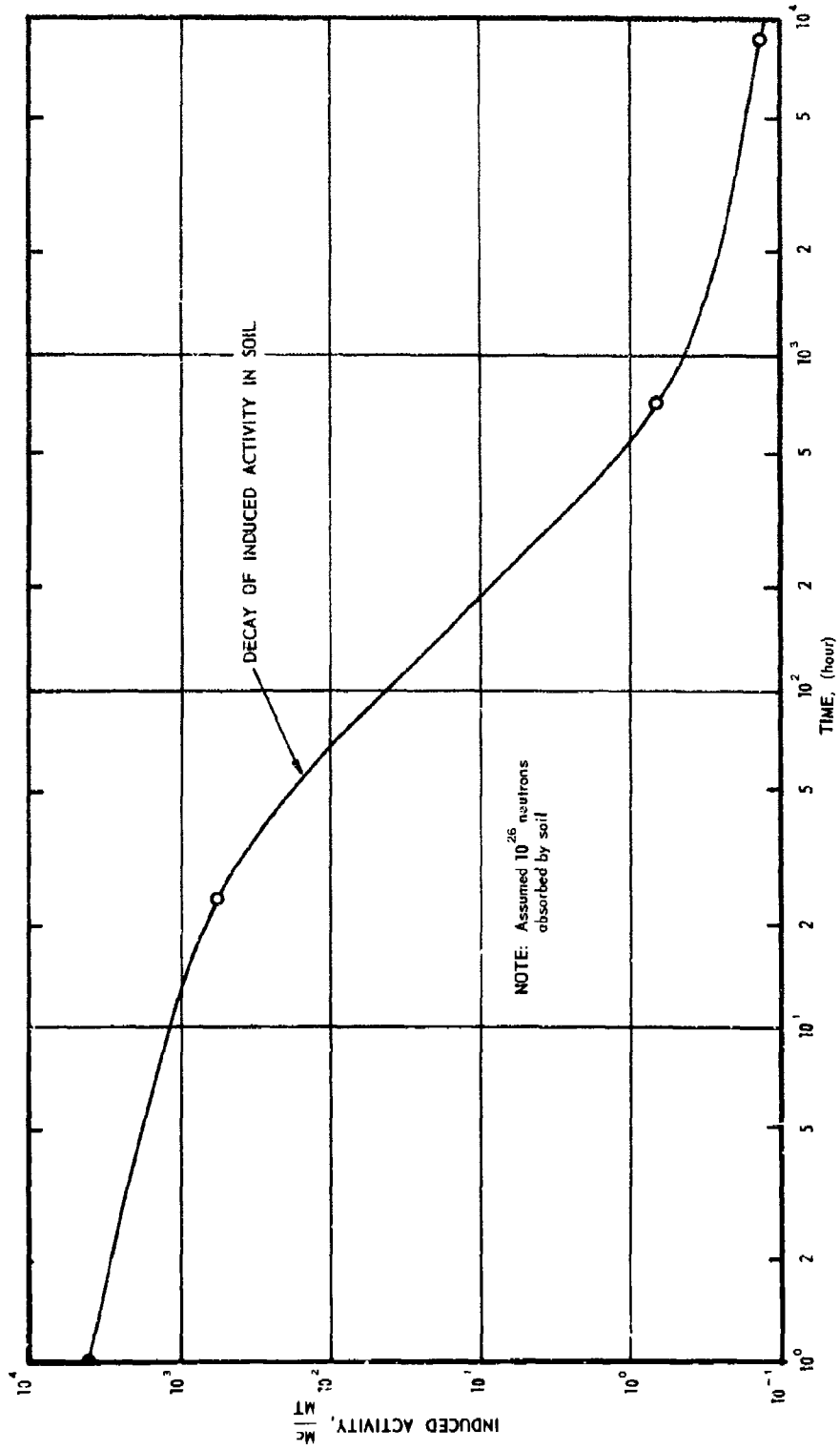


Figure 9. Total Activity of Soil

TABLE IX
Radioactivity in Soils (Mc/MT)

Nuclide	0	1 hr	1 day	1 month	1 year
Na ²⁴	1620	1430	542	a	a
Mg ²⁷	584	7.05	a		
Al ²⁸	83,870	15.9	a		
Si ³¹	991	773	1.78	a	
P ³²	1.21	1.21	1.15	0.276	a
K ⁴⁰	a				
K ⁴²	204.5	194	50.0	a	
Ca ⁴⁵	0.300	0.300	0.300	0.263	0.057
Ca ⁴⁹	1100	135	a		
Ti ⁵¹	156	0.0015	a		
Mn ⁵⁶	2122	1655	3.82	a	
Fe ⁵⁵	0.110	0.110	0.110	0.104	0.087
Fe ⁵⁹	0.014	0.014	0.014	0.0095	0.00006

a = less than one curie per megaton

The formula for the radioactivity induced in any element as given by Serfite and Champion⁽¹⁵⁾ is:

$$A_t = (\sigma f N k)(1 - e^{-0.693 t/T})(e^{-0.693 \theta/T}) \quad (72)$$

where

A_t = activity, in disintegrations per second, after the nuclide has been removed from the flux for a period θ

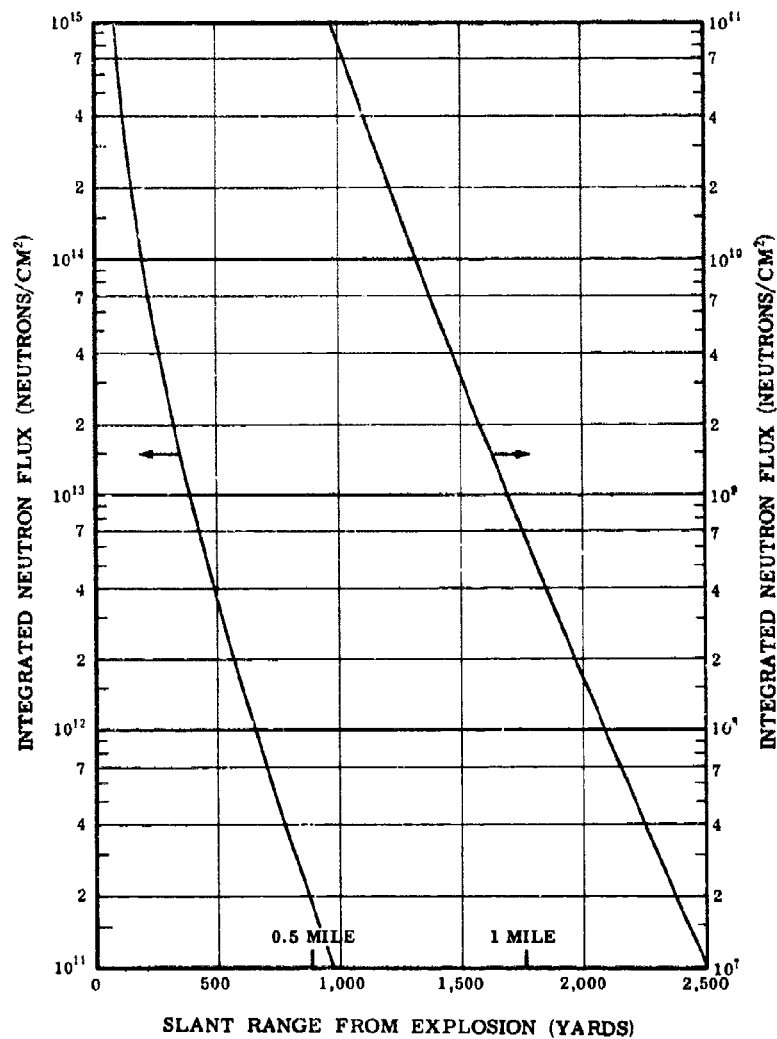


Figure 10. Integrated Neutron Flux as a Function of the Slant Range in Air of 0.9 Sea-Level Density for a 1-Kiloton Explosion

Table X

Calculated Activities of Various Nuclides in Soil^(a)

Nuclide	Induced Activity, $\frac{\text{Mc}}{\text{MT}}$ ^(b)
Na^{24}	24,800
Mg^{27}	11,100
Al^{28}	1,250,000
Si^{31}	12,300
P^{32}	18
K^{42}	3,350
Ca^{45}	4.67
Ca^{49}	16,400
Ti^{51}	4,730
Mn^{56}	36,200
Fe^{55}	0.580
Fe^{59}	0.665

(a) Assumes NTS soil

(b) At one minute after detonation; decay time equals zero

- σ = activation cross section in square centimeters for
2200 m/sec. neutrons;
- f = thermal flux in neutrons per square centimeter per
second;
- N = the total number of atoms of the element in the target;
- k = relative abundance of the isotope from which the
radionuclide is formed;
- t = time of irradiation;
- θ = time of decay;
- T = half-life of the radionuclide formed.

The product (σfNk) in Equation (72) has been calculated for a flux of 10^{12} neutrons/sq.cm-sec and for the number of atoms in 1 g of the target element. The values, designated A_s , are listed for each element by Senftle and Champion⁽¹⁵⁾. The values for A_s can be corrected to any neutron flux and weight of target element by multiplying by a suitable factor of proportionality. The corrected value of A_s is given by:

$$A'_s = \left[\frac{fW}{10^{12}} \right] A_s \quad (73)$$

where W is the weight of the element in the sample, and
 f is the neutron flux.

The formula used in the calculations was:

$$A_t = A'_s (1 - e^{-0.693 t/T}) (e^{-0.693 \theta/T}) \quad (74)$$

taking $t = 1 \text{ min}$ and $\theta = 0$.

As a special case, where t is known to be less than 15% of T , a further simplified formula was used.

$$A_t = A'_s \left(\frac{0.693}{T} \right) (e^{-0.693 t/T}) \quad (75)$$

Values used for A'_s obtained by Senftle and Champion⁽¹⁵⁾ are listed below:

Na ²⁴	-	1.39 x 10 ¹⁰	Ca ⁴⁴	-	1.78 x 10 ⁸
Mg ²⁷	-	1.3 x 10 ⁸	Ca ⁴⁹	-	2.54 x 10 ⁷
Al ²⁸	-	4.79 x 10 ⁹	Ti ⁵¹	-	9.01 x 10 ⁷
Si ³¹	-	6.74 x 10 ⁷	Mn ⁵⁶	-	1.39 x 10 ¹¹
P ³²	-	3.69 x 10 ⁹	Fe ⁵⁵	-	4.56 x 10 ⁸
K ⁴²	-	1.02 x 10 ⁹	Fe ⁵⁹	-	2.26 x 10 ⁷

In calculating the data of Table X, a neutron flux of 0.91×10^{16} neutrons/sq cm per megaton was assumed. The total weight of the soil involved was taken as 5.92×10^{11} grams. This value was calculated using a 2500 yd radius, a 1-ft depth, an average density of 1.18 gm/cu cm, and with a soil composition as that given in Table VIII. The irradiation time (t) was taken as one minute.

The data presented in Table X agree reasonably well with the data presented by Klement in Table IX. This agreement is within an expected factor of 15 as the neutron flux used was a factor of 15 higher than that assumed by Klement.

Mandeville⁽¹⁶⁾ states that the radioactivity of the fission products from a nuclear explosion overshadows the induced radioactivity by a factor of approximately 10^3 . Even though this tends to make the contribution of the induced radioactivity almost negligible there are conditions under which the

induced radioactivity might play a detectable part. The induced nuclides that form soluble salts will be readily dissolved in both surface and ground water and therefore will add to the contamination of the water supply.

It has been generally recognized that the activating neutrons will penetrate the soil before the blast wave arrives. Some of the activated soil will then be taken up into the cloud due to the cratering effect and thereby becomes part of the total fallout. According to Dr. C. F. Miller ⁽¹⁴⁾ the induced activity in the soil will be about 0.019 (1.9 per cent) of the ionization rate due to normal fission [$i_{fp}(t)$]. This fraction will be a small percentage of the total ionization rate. This estimate of the induced activity is applicable for a 100% fission yield, assuming 0.8 neutron capture per fission from U-238, regardless of weapon size.

It has also become established that the induced activity will predominate for a total fusion bomb. For a 50% fusion and 50% fission bomb the induced activity will be relatively small, except for a short period immediately after detonation. However, activated sodium and magnesium may contribute materially at a later time ⁽¹⁵⁾.

It is therefore concluded that the contribution of induced radioactivity to the contamination of water supplies will not be significant.

V. TRANSPORT OF FALLOUT PARTICLES BY SURFACE WATER

Transport of the insoluble portion of fallout may be divided into four general phases: transport in air, transport in overland flow, transport in stream flow and transport in reservoirs. Each of the four phases may be treated as a separate topic. Of the latter three, only transport by stream flow has been considered in any detail; overland transport and reservoir transport are mentioned only briefly. Transport in air is discussed in Section II of this report.

There are three major limitations on any stream-flow transport analysis. These are: (1) the complex nature of sediment behavior in streams; (2) the paucity of data concerning fallout, especially data concerning particle size distribution or the relation of radioactivity to particle size; and (3) the obvious impossibility of obtaining stream-flow data for every reach of stream. These limitations precluded an analysis of the quantity of sediment resulting from the fallout of a given burst, although work on the quantity of fallout is now being done. It could not be determined that a certain weight of sediment would fall on a water surface or what the particle size distribution would be.

Computations are available, however, from Glasstone⁽¹⁴⁾ and the OCD fallout model which gives certain relationships between particle sizes, downwind distance carried, and total activity.

Glasstone shows that 99 per cent of the total activity of fallout is carried by particles of 400 microns or less in diameter. This relation of particle size to total activity was derived from Figure 9.187 of Glasstone's book⁽¹⁴⁾ and is shown as Figure 11 of this report. The method contained in this section is based on this relationship.

Particles of 400 micron diameter are on the order of magnitude of normal stream sediment. This means that the particles carrying essentially all the activity will remain in suspension, or at least will not settle out immediately. It follows that most of the fallout particles which land on the water surface or find their way into the stream from overland transport will be carried by the stream and will present a hazard at some distance downstream.

A relationship of particle size versus downwind distance carried was computed in Section II of this report. (Table VII). Data from that table has been plotted in this section as Figure 12.

The following general assumptions were made:

- (1) Uptake by biological organisms is negligible.
- (2) The stream chemistry is not such as to dissolve ordinarily insoluble particles.
- (3) Effect of flocculation on settling rates is negligible.
- (4) Weapon size (5MT), wind speed (15mph), and fallout pattern are used to correspond with other sections of this report.
- (5) Radioactivity of particles over 500 microns may be ignored.

Further assumptions are made and discussed in the text. Some of these assumptions depend on the nature of a specific stream, some require further investigation, and some which are considered negligible in an approximate analysis may assume a proportionally greater importance in a more detailed computation.

An estimate must be made of stream width, volume, and surface area. This may be done by equating the cross-sectional area of the stream (at a gaging station) to a rectangle of equivalent area whose length

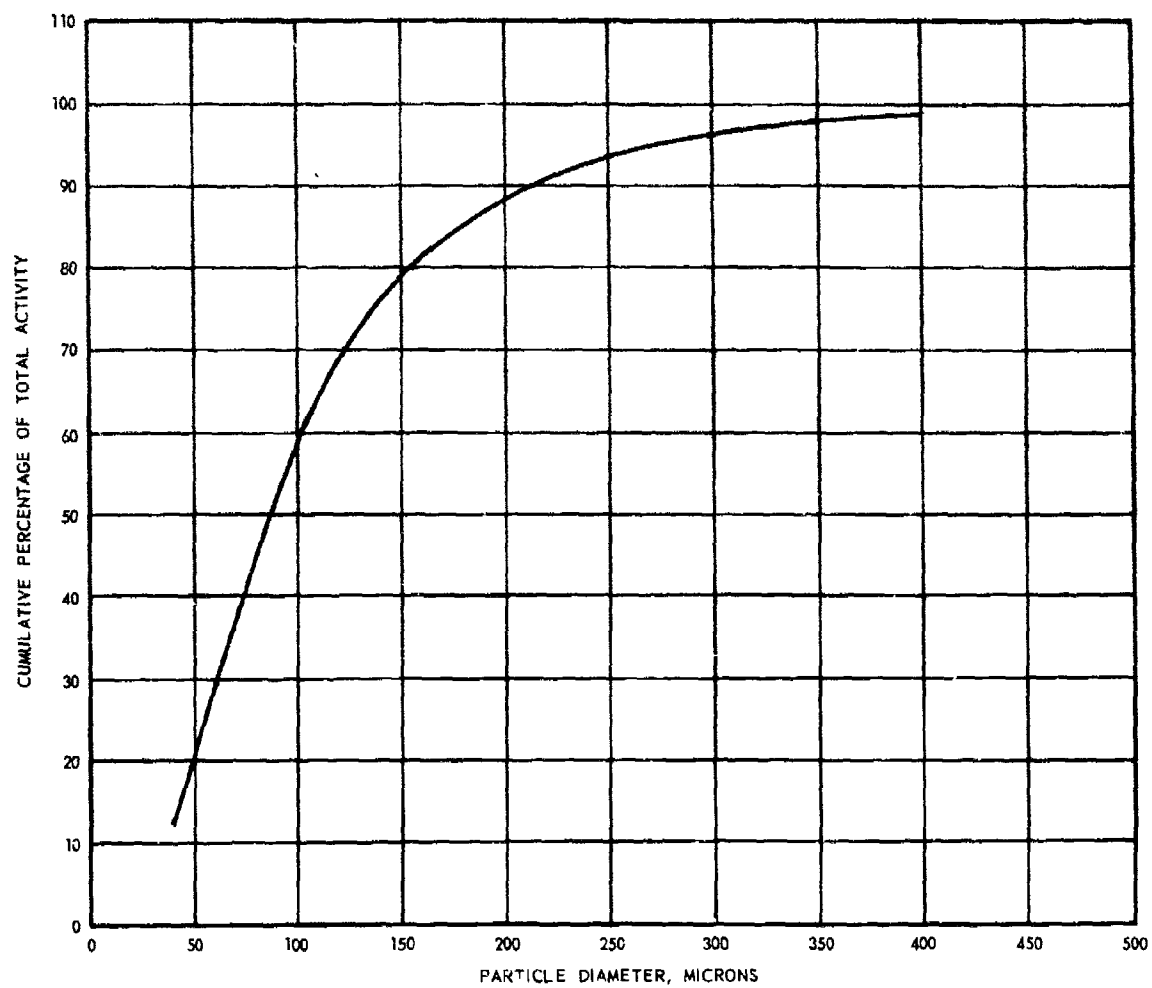


Figure 11. Total Activity Percentage in Relation to Particle Diameter

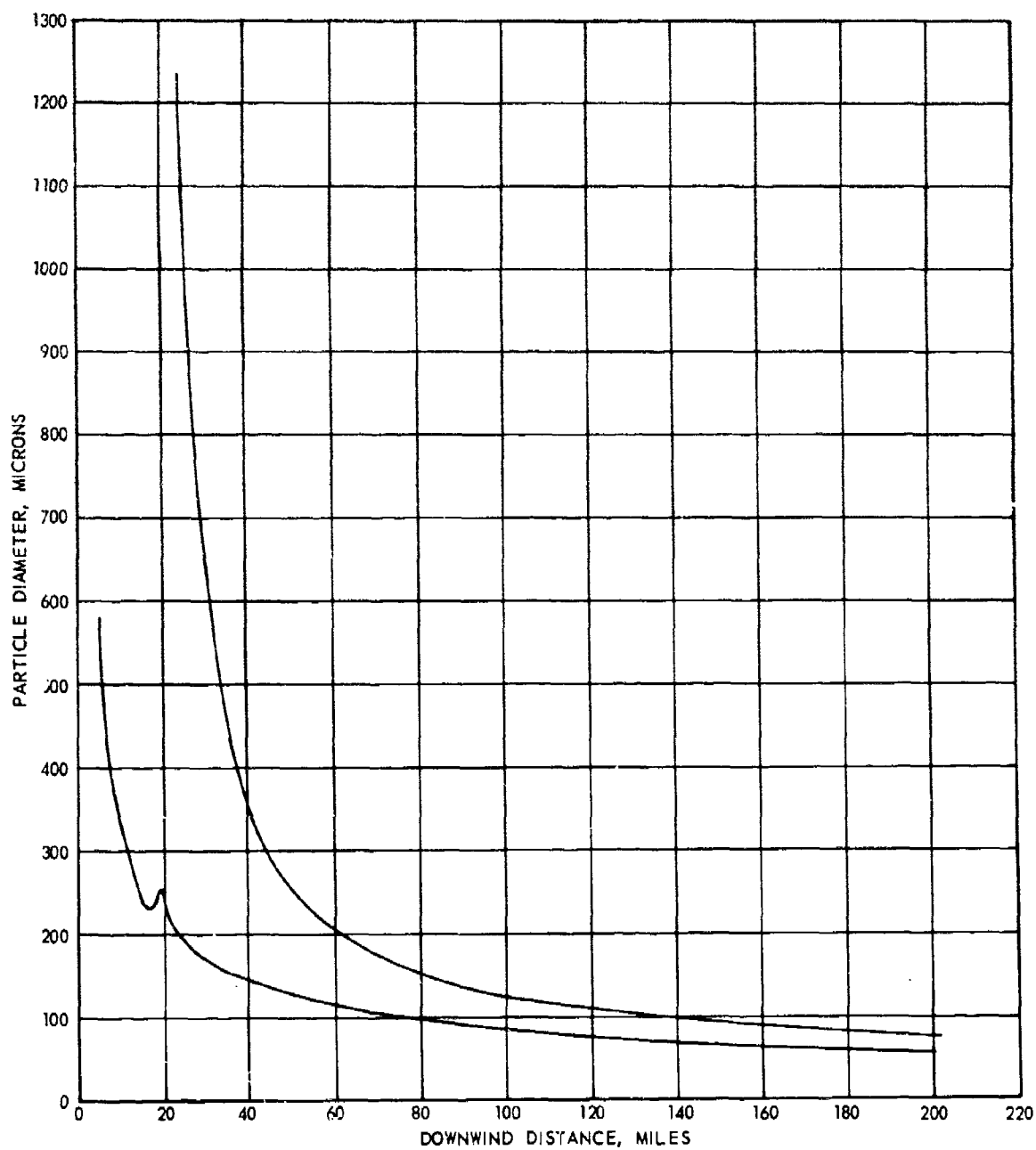


Figure 12. Particle Diameter versus Downwind Distance (Maximum and Minimum Curves)

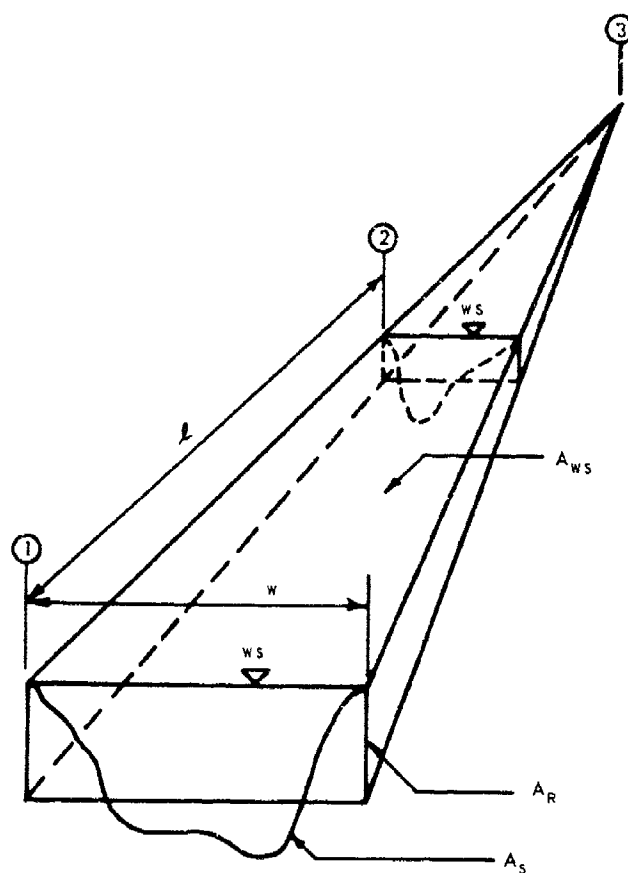
is equal to the stream width. This is shown in Figure 13. The length of the stream between any two sections is considered to be a straight line equal to the distance along the stream channel between the two sections. Each section of the stream may then be considered to be a truncated pyramid lying on its side with its bases the equivalent rectangles. (Or for the section containing the source, a complete pyramid, since the source is considered to be a point.) Concentrations may be found using the volume of the pyramids.⁽¹⁸⁾

Intensity (roentgen/hour) contours for a given burst are superimposed on the watershed. The intensities may then be converted to activities (atoms/sq. ft.) for insoluble (and soluble) portions of the various isotopes under consideration by use of Table VI. Details of this method are discussed on page 95 through page 98 of this report.

If fallout landing on the water surface is assumed to mix uniformly within the reach of channel enclosed by a given contour, an activity concentration may be computed using the idealized channel shape. This concentration will move downstream as a unit, and the time of arrival and time of lapse of this concentration may be found at a point downstream by considering the particles to move at mean stream velocity.

By plotting the various concentrations from units under given intensity contours as ordinate against time as abscissa, a series of horizontal bars is obtained. These may be averaged graphically to obtain a time-concentration curve for the stream. Note that concentration is expressed as activity rather than particle concentration.

By use of Figure 12 a maximum particle size at a given point downwind from the blast may be found. The maximum size particle landing



L = channel length between sections

W = stream width = length of equivalent rectangle

A_R = area of equivalent rectangle

A_S = area of stream cross-section (from gaging-station data)

A_{WS} = area of water surface between sections

$A_R = A_S$

$$A_{WS} = \left(\frac{W_1 + W_2}{2} \right) L$$

$$V = \left(\frac{A_1 + A_2}{2} \right) L$$

Figure 13. Idealized Stream Section

on the stream reach under consideration is compared to the maximum particle size which the stream will carry in suspension. If the maximum size particle is carried then it is to be assumed that smaller particles will also be carried, and the method remains valid.

If the stream will not carry the maximum size particle, then some percentage of the activity must be regarded as going into bed load, which travels at a much slower rate. The only way now available to find the proportion of activity which would go into bed load is by assuming that if particles of a given size are found to settle, that all particles of this size or larger will settle out, and all smaller particles remain in suspension. The relationship of particle size to activity given by Glasstone⁽¹⁴⁾ may then be used to find what percentage of the total activity would settle out with the larger particles.

The ability of a stream to carry particles of a given size or smaller is best defined by what may be termed the effective carrying velocity of the stream, i.e. that velocity below which settling of particles of a given size is most likely to occur. The effective carrying velocity is obviously not related to the idealized stream channel used to compute concentrations, but is rather a function of both channel characteristics (actual channel width and depth) and flow, as well as particle size and sediment distribution. Stream flow data, no matter how accurate or comprehensive, cannot cover every mile of channel. Conditions which will produce the greatest possibility of settling must therefore be generalizations of what is known of the nature of an individual stream.

Particle size distribution in air is, unfortunately, not known, except for maximum and minimum distance which a particle of given size will travel. There is no way at present to compute the number of particles

per unit area landing on the watershed. Sediment concentrations cannot, therefore, be computed. This is the reason for computing concentration in terms of activity. Additional fallout data, particularly on particle distribution, and additional study on sediment concentrations are needed to support the assumptions that the fallout particles mix uniformly, that particles will go out of suspension according to size, and that particles move downstream at mean stream velocity.

In order to approximate actual stream conditions, close scrutiny of maps and existing stream-flow records will be required. Large-scale topographical maps should yield much information on channel conditions and stream-bed slopes. The U. S. Geological Surveys and Corps of Engineers publish or have on file not only gaging-station records but much special measurement data.

No analysis has been made for transport resulting from overland flow. Fallout landing on the land portion of the watershed is considered less of an immediate problem than that landing on the water surface, and will probably present no immediate problem unless it is raining at time of fallout arrival. (In which case, incidentally, the fallout may be intensified.) Subsequent rain may produce a second activity peak at a water intake by washing particles into the stream. It is of interest to note that at Coweeta Hydrologic Laboratory it was found that much of the runoff which was formerly considered to flow overland actually goes under the surface, or alternates between sub-surface and above-surface flow. In work with radioactive tracers at Coweeta, great difficulty was experienced in finding a tracer which would follow the water at the same speed as the water. Most of the isotopes used at Coweeta tended to stay near the point where they were applied. These studies were carried out

on steep slopes on which there was a higher percentage of surface runoff than on the same soil at a lesser slope; however, the isotopes used were not absorbed within particles.⁽¹⁹⁾

Particles which go into bed load may present a long term hazard because of the slower and more irregular movement of bed load. A bed load analysis will be required if it is found that large particles, in spite of their possession of only a small percentage of the total activity, are found to actually carry a dangerous amount of activity. The smaller the particle size that is found to settle, the more significant becomes the bed load analysis. Note that such a bed-load analysis complements assumption 5 on page 86.

Transport in reservoirs is more likely to produce settling because reservoirs are more likely to approach quiescent conditions. Calculations will probably be simplified because the conditions of reservoir transport more closely approaches the condition of settling in a quiescent basin than do the other phases of the transport problem.

This method was presented not only because it is the one most likely at present to produce usable results, but because it provides an outline of the problem of stream transport. Assumptions, questions as to their validity, and areas requiring further study have been pointed out. Computations have not been included because it is wished to ascertain the validity of some of the assumptions, and because sufficient study has not been made on specific streams. This treatment therefore constitutes only a good start; however, further study in the same manner should produce results of known validity.

VI. EVALUATION OF MUNICIPAL WATER SUPPLY CONTAMINATION

A. Introduction

An approach to the problem of water contamination by radioactive fallout was taken which would give a more reliable set of concentration values than those calculated previously. The values presented in Quarterly Technical Report No. 3^{*} were maximized, in that they represented a case in which the highest concentration that could reasonably be expected at H + 1 hour from any kind of attack or environment, except for possibly a very high megatonnage attack. Following is presented a more detailed and realistic approach to the problem. The values herewith reported represent specific cases in which environmental and other factors have been considered, and it is believed they are at least of the same order of magnitude as would be expected following a nuclear attack.

Only the cities of Houston, Texas and New York were chosen for a full scale evaluation. Since the values calculated for these two watersheds were in good correlation, it was felt that the results could probably be applied without serious error to the other cities previously considered. Excellent watershed data was available on both cities, thus facilitating the calculations considerably.

A physical integration was performed over the considered watersheds and reservoirs to give realistic specific isotope concentrations at H + 1 hour for variously directed 15 mph winds. As before, the case of fallout contamination from that falling in the reservoir alone was considered as well as the case of runoff contamination from the entire watershed.

B. Calculations

Since large scale maps of both the Houston and New York watersheds were available, transparent overlays were superimposed over the watershed

* See Appendix A

areas and appropriate grids scaled in. These grids consisted of five mile squares for watershed areas, and two mile squares for the reservoir areas when large enough to apply. Figure 14 shows the grid on the watershed serving Houston. The ground zero of a 5 MT weapon detonation was located so as to give a fallout pattern which fell on the watershed for the 15 mph wind model. Various wind directions were also chosen so as to give some basis for comparison and to account for possible seasonal variation. It is obvious from the geography of New York and Houston that the wind directions from the east and north would give rise to a negligible amount of fallout over their respective watersheds, so that these wind directions were omitted.

The attacks that were evaluated were as follows:

- Case Ia Houston - Ground zero is downtown Houston and the wind direction is from the south.
- Case Ib Houston - Ground zero is downtown Houston and the wind direction is from the west.
- Case IIa New York - Ground zero is Central Park and the wind direction is from the south.
- Case IIb New York - Ground zero is Binghamton, New York, and the wind direction is from the west.

Separate evaluations were made for each of these cases with respect to contamination from the reservoir and that from runoff of the entire watershed. In the case of Houston, the concentration of activity was calculated for one of the feed streams from direct fallout contamination for comparison purposes.

For the reservoir study, the area of the respective reservoirs within each two mile grid was found by planimeter. In the Houston watershed

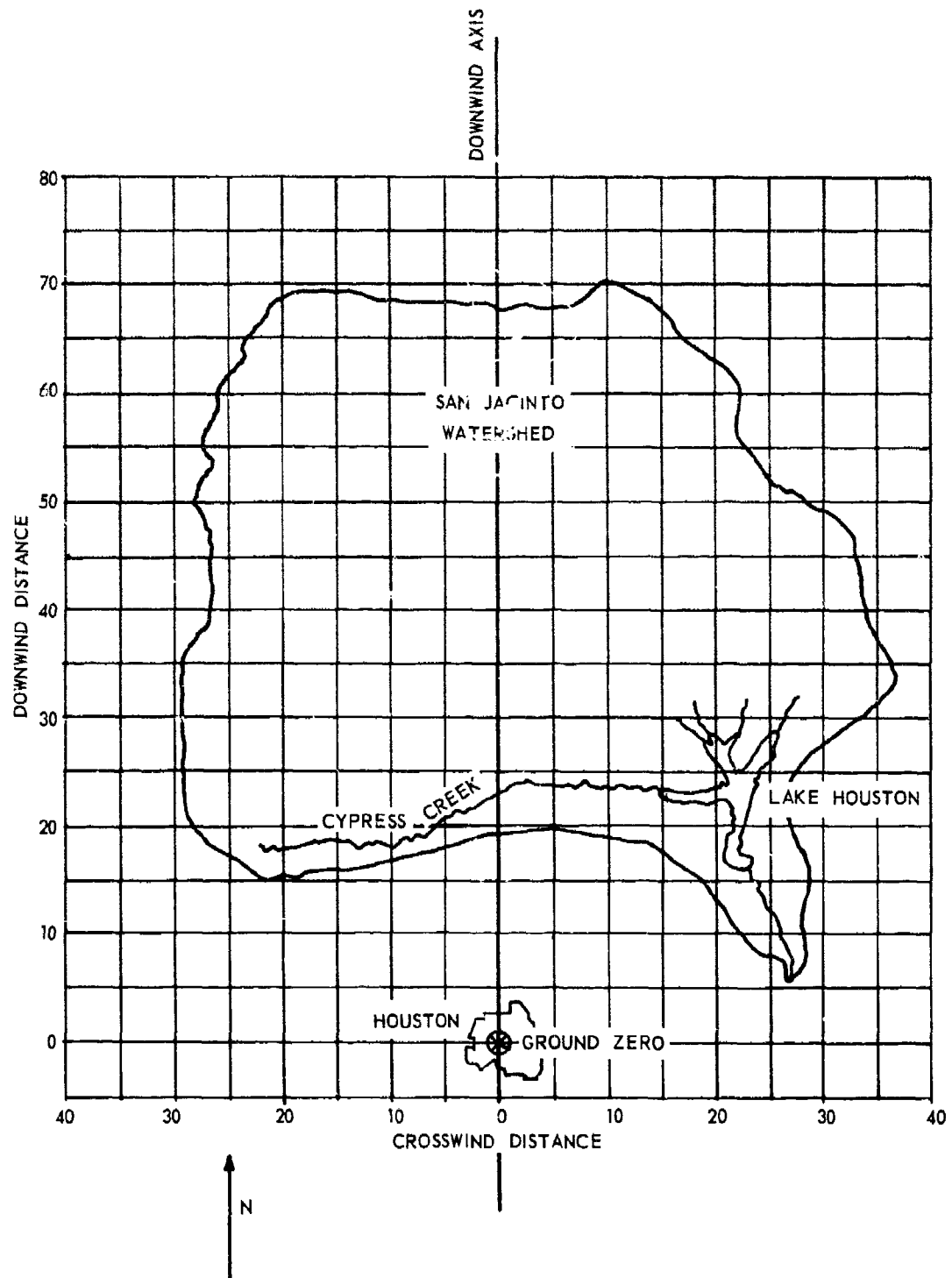


Figure 14. Method of Graphical Integration Used for the San Jacinto Watershed Serving Houston, Texas

there is only one reservoir and in the New York watershed all six reservoirs empty into one so that the problem is somewhat simplified if complete mixing is assumed. The centroid of each selected grid area was estimated, and its coordinates measured with respect to ground zero. An intensity was then assigned to each set of coordinates, and it was assumed to be constant over that specific area. The intensity values were chosen according to whether the specified area was either covered by the upwind or downwind cloud. Those values related to the upwind cloud were arrived at by interpolation between previously estimated intensity contours, and those of the downwind cloud were arrived at by interpolation of computer calculated contours.

To convert from the intensity over each area to activity in atoms/sq ft in each area, the value of $N^*(A)/I(1)$ from the fallout model, for each isotope considered, was taken as its value corresponding to the downwind distance X . By multiplying the appropriate $N^*(A)/I(1)$ value by the intensity over each square, the concentration in atoms/sq ft is found for each area. By then multiplying each atom concentration by its corresponding area, the total number of atoms in each square of the grid is found. The total number of atoms of each isotope at $H + 1$ hour in the reservoir was then found by adding up the contributions from each square over the reservoir. By assuming that complete mixing has occurred, the concentration of activity in the reservoir in atoms/liter may be obtained by dividing by the total volume of water in the reservoir. The concentration of each isotope considered at $H + 1$ hour, for the Houston and New York reservoirs is shown in Tables XI and XII along with the equivalent activity in $\mu\text{C}/\text{ml}$.

Table XI

Activity Concentrations for Direct Contamination
of the Houston Reservoir

Isotope	South Wind		West Wind	
	Atoms/liter	μc/ml	Atoms/liter	μc/ml
Sr-89	4.6×10^9	1.9×10^{-5}	4.6×10^9	1.9×10^{-5}
Sr-90	10.9×10^9	2.3×10^{-7}	10.9×10^9	2.3×10^{-7}
Ru-106	5.1×10^9	3.0×10^{-6}	5.1×10^9	3.0×10^{-6}
I-131	9.8×10^9	2.7×10^{-4}	9.8×10^9	2.7×10^{-4}
Cs-137	5.3×10^9	1.4×10^{-7}	5.3×10^9	1.4×10^{-7}
Ba-140	13.7×10^9	2.3×10^{-4}	13.7×10^9	2.3×10^{-4}

Table XII

Activity Concentrations for Direct Contamination
of the New York City Reservoirs

Isotope	South Wind		West Wind	
	Atoms/liter	μc/ml	Atoms/liter	μc/ml
Sr-89	2.9×10^{10}	1.2×10^{-4}	3.9×10^{10}	1.6×10^{-4}
Sr-90	5.6×10^{10}	1.2×10^{-6}	6.9×10^{10}	1.5×10^{-6}
Ru-106	2.5×10^{10}	1.5×10^{-5}	3.0×10^{10}	1.8×10^{-5}
I-131	5.6×10^{10}	1.5×10^{-3}	6.8×10^{10}	1.9×10^{-3}
Cs-137	3.7×10^{10}	7.3×10^{-7}	5.1×10^{10}	1.0×10^{-6}
Ba-140	7.0×10^{10}	1.2×10^{-3}	8.4×10^{10}	1.4×10^{-3}

The activity concentrations for the Houston reservoir (Table XI) are the same for south wind and west wind because the same intensity contour falls across the center of the reservoir in both cases. When the wind is from the south, the right hand portion of the contour crosses the reservoir. With wind from the west, the left hand portion of the contour is involved.

A separate evaluation of stream contamination was made using a randomly selected creek feeding the Houston reservoir for the purpose of comparison only. This selected feed stream (Cypress Creek) ran perpendicular to the downwind fallout axis and emptied into the Houston reservoir. The evaluation was carried out in the same manner as that done on the reservoir. The stream was assumed to approximate an isocles triangle with the base representing the width of the stream mouth. Two mile lengths were laid off and the trapezoidal areas calculated. Intensity values and activity conversion values were chosen as before to obtain the total activity falling directly on this stream. To present an estimation of the concentration of activity in the stream, complete mixing was assumed. However, it is evident that the activity will really move in a slug type of formation, completely mixing, if at all, only when the radioactivity reaches the reservoir. Although some mixing during stream flow will occur due to turbulence and diffusion, the presented case will never be actually attained, since countercurrent mixing is unlikely. From the presented values in Table XIII it may be seen that some build-up of activity may occur in areas immediately surrounding the stream feed-in points. However, this build-up will not represent a serious problem in the studied case because of its distance from the municipal intake, and the relative time elapsed from the time of detonation to the intake time.

The second case studied was that of the contamination to be expected assuming runoff from the entire watershed. This study was made for both the New York and Houston watersheds, the method being similar to that of the first

Table XIII

Activity Concentrations for Cypress Creek (South Wind)

Isotope	Atoms/liter	μc/ml
Sr-89	2.2×10^{12}	9.4×10^{-3}
Sr-90	5.4×10^{12}	1.1×10^{-4}
Ru-106	2.6×10^{12}	1.6×10^{-3}
I-131	4.4×10^{12}	1.2×10^{-1}
Cs-137	2.5×10^{12}	4.9×10^{-5}
Ba-140	6.8×10^{12}	1.2×10^{-1}

case. Five mile grids were used, however, instead of two mile grids. Wind conditions were selected identical to those of Case I. To calculate the actual amount of radioactivity (soluble fraction only) that reaches the reservoir, the runoff coefficients supplied by the respective municipal water works were assumed valid in that they represent a maximum value to be expected. The calculated activities are therefore considered to be maximum values. The actual radioactive runoff coefficient will actually be less than the aqueous runoff coefficient depending on (1) the instantaneous moisture content of the soil, (2) the duration of time from detonation to rainfall, (3) ion-exchange and absorption in and on the soil, and (4) plant uptake. The calculated values of activity concentrations of the selected isotopes at H + 1 hour, assuming complete dilution by the composite lakes and streams in the watershed for both Houston and New York is presented in Tables XIV and XV. The factors involved obviously vary widely from one environment to another, so that general assumptions made from any particular reservoir should be applied with caution to other situations.

Table XIV
Activity Concentrations for Contamination from Runoff
for the Houston Watershed

Isotope	South Wind		West Wind	
	Atoms/liter	μc/ml	Atoms/liter	μc/ml
Sr-89	4.5×10^{12}	1.9×10^{-2}	3.6×10^{10}	1.6×10^{-4}
Sr-90	8.8×10^{12}	1.9×10^{-4}	8.5×10^{10}	1.8×10^{-6}
Ru-106	4.1×10^{12}	2.5×10^{-3}	4.0×10^{10}	2.4×10^{-5}
I-131	9.2×10^{12}	2.5×10^{-1}	8.4×10^{10}	2.3×10^{-3}
Cs-137	5.3×10^{12}	1.0×10^{-4}	4.3×10^{10}	8.5×10^{-7}
Ba-140	11.3×10^{12}	1.9×10^{-1}	11.0×10^{10}	1.9×10^{-3}

Table XV
Activity Concentrations for Contamination from Runoff
for the New York City Watershed

Isotope	South Wind		West Wind	
	Atoms/liter	μc/ml	Atoms/liter	μc/ml
Sr-89	0.36×10^{12}	1.5×10^{-3}	1.6×10^{12}	6.8×10^{-3}
Sr-90	0.65×10^{12}	1.4×10^{-5}	2.8×10^{12}	5.9×10^{-5}
Ru-106	0.29×10^{12}	1.7×10^{-4}	1.2×10^{12}	7.1×10^{-4}
I-131	0.65×10^{12}	1.8×10^{-2}	2.8×10^{12}	7.6×10^{-2}
Cs-137	0.48×10^{12}	9.5×10^{-6}	2.2×10^{12}	4.4×10^{-5}
Ba-140	0.8×10^{12}	1.4×10^{-2}	3.4×10^{12}	5.8×10^{-2}

C. Conclusions:

It is not the purpose here to draw any conclusions in regard to the biological hazard resulting from the concentrations of activity presented in Tables XI - XV. This aspect is being considered elsewhere in this report and also by other investigators.

It may be prudent, however, to consider the relative value of the previous calculations. It must be remembered that only a 5 MT weapon was considered and that all concentrations are for H + 1 hour. Thus for any other size weapon, appropriate revisions in the fallout model will have to be made before it may be applied. As for a multi-bomb attack, one cannot but accept some method based on additivity. Complications arrive here, as far as forming a model is concerned, because of ground zero locations. Since H + 1 hour values of concentration are given, one may apply suitable decay curves to adapt them to any specific stream flow, reservoir flow-through, or intake time, etc. for a particular watershed system.

It is not to be implied here that the Houston and New York values are representative of all municipal reservoirs. However, they do present a reasonable value to be expected in a realistic case, and also demonstrate the ease with which an evaluation may be made. By making such an integrated evaluation for any specific watershed and applying local conditions, the relative radiological hazard may be estimated.

The Houston and New York values will be seen to vary from the potential values if unusual conditions prevailed such as would occur during a dry spell. However, the effects will be somewhat counterbalancing in that high reservoir concentration due to low volume will be somewhat

offset by the lack of runoff contamination. It is doubted that unnatural conditions, unless very severe, will change the concentration of activity by more than an order of magnitude.

VII. ANALYSIS OF RADIOACTIVITY IN WATER

A. Radiochemical Methods

1. Introduction

In most radiochemical analyses the steps are concentration, separation, purification, and counting. Evaporation and ion exchange are the two principal methods of concentration, but may not be necessary if the level of activity is sufficiently high. The individual radionuclides are usually separated by means of precipitation, solvent extraction, or ion exchange elution. Purification of the individual radionuclides usually follows standard chemical procedures which depend mainly on the solubility characteristics of compounds of the radionuclides. Coryell and Sugarman⁽²⁰⁾ have described purification of many of the more important radionuclides. Radioisotopes are counted using appropriate instruments, depending on the specific isotope and the desired accuracy.

"Carriers" are of prime importance in wet radiochemical procedures. The mechanisms and usage of radioisotopic carriers have been well defined by Overman and Clark⁽²¹⁾. A carrier, which is normally the stable isotope of the element being determined or a stable element with very similar properties, is added to increase the total concentration of the element, because the radioactivity will normally be present in micro quantities only. Hence, if the carrier is not added, part of the radioactive material will usually be lost, even though employing the most scrupulous analytical techniques. By weighing the final solid to be counted, and knowing the original amount of carrier added, the percentage chemical and physical loss may be calculated. By assuming complete interchange of carrier and radionuclide, the same percentage of each will be lost, and the original concentration of activity may readily be calculated. The carrier itself is

normally added as a solution of a soluble salt of the carrier element prior to any chemical procedure. Carrier addition is used extensively throughout the described analytical procedures, although some carrier-free determinations are now coming into use.

There are several compilations available which describe detailed procedures for the quantitative determination of many radionuclides (20,22,23,24) Most of these methods have been proven and are in general use.

2. Procedures for the Determination of Specific Radionuclides

a. Radiostrontium

Strontium-90 has been generally recognized as being a very biologically hazardous radionuclide as it accumulates in bone. Due to its relatively dangerous nature, wide interest has been aroused to find a simple and rapid method of analysis for strontium-90. Techniques that have been in use for several years are still finding widest use because of their accuracy, the time consideration being less important in peacetime.

Strontium-89, perhaps somewhat less of a hazard than strontium-90, because of its shorter half-life, will also be present in fallout contaminated water. Separate analyses of strontium-89 and strontium-90 are thus desirable. Strontium-89 activity is normally found by subtraction of strontium-90 from total radiostrontium concentration.

(1) Radiostrontium and Radiobarium by Nitrate Separation⁽²⁵⁾

Strontium and barium carriers are added and the Group II cations are precipitated as the carbonates. Partial separation from calcium is accomplished by nitrate precipitation in fuming nitric acid. The remaining calcium nitrate is then extracted with acetone. Rare earths and other trivalent cations are removed by two hydroxide scavengings. Barium is finally separated from strontium by precipitation as barium chromate. Strontium is then collected as the oxalate and counted. The barium is converted

from the chromate to the chloride for counting. The lowest level of detection for radiostrontium by this method is 4×10^{-8} $\mu\text{c/ml}$ and for radiobarium, 10^{-7} $\mu\text{c/ml}$. A precision of about 10% may be obtained.

The calculation of the total amount of radioactivity due to either radiostrontium or radiobarium, using an internal proportional counter, is made by use of the following equation:

$$\frac{\mu\text{c}}{l} = \frac{\text{net cpm}}{(A)(B)(C)(D)(2.22)},$$

where A = efficiency factor,
 B = chemical yield,
 C = self-absorption factor, and
 D = volume in liters.

This formula also holds true for determination of the other radionuclides

A variation of the preceding technique was introduced by Kooi⁽²⁶⁾
 After the separation of strontium by carbonate and nitrate precipitations, barium removal is effected by barium chloride precipitation in a hydrochloric acid-ether system. Any lanthanum-140 which may be present from barium-140 decay is removed by a ferric hydroxide scavenge. Sensitivity in the 10^{-10} $\mu\text{c/ml}$ range is obtainable by this procedure.

(2) Strontium-90 by Solvent Extraction of Yttrium-90⁽²⁷⁾

Strontium carrier is added and carbonate precipitation is performed. The carbonate precipitate is dissolved in hydrochloric acid and the solution scavenged with hydroxide. The strontium is again precipitated as the carbonate,

which is then allowed to stand, thus permitting yttrium-90 ingrowth. The yttrium is extracted with tributyl phosphate equilibrated with 1M nitric acid. Following extraction, the yttrium is washed from the organic phase with 0.1 N HNO_3 , dried in a planchet, and counted in an anti-coincidence beta counter.

A decontamination factor of approximately 10^4 is obtained. The chemical yield is greater than 70% for strontium; the recovery of yttrium by the solvent extraction is 85%.

Strontium-90 determinations, such as that shown above, are normally made by measuring the activity of its beta decay daughter, yttrium-90. After a suitable period has elapsed, the yttrium-90 ingrowth is separated from the bulk of the strontium by some suitable means. The yttrium-90 is then purified and counted. The strontium may then be determined by calculation using the following formula:⁽²⁸⁾

$$\text{Strontium-90, } \mu\text{c/l} = \frac{\text{net cpm}}{(A)(B)(C)(D)(E)(F)(2.22)},$$

where:

- A = efficiency factor,
- B = per cent extraction factor,
- C = per cent ingrowth factor,
- D = chemical yield,
- E = sample volume (liters), and
- F = decay factor; calculated from

$$A = A_0 e^{-\lambda t},$$

where:

A = activity remaining after a time interval t,

A₀ = activity of sample at some original time,

$\lambda = \frac{0.693}{\text{half-life of yttrium-90 (62.4 hrs)}}$, and

t = time (hours) from separation to counting.

By knowing the total strontium-90 activity and the total activity due to radiostrontium, the strontium-89 concentration may be obtained from the difference.

(3) Strontium-90 by Direct Precipitation of Yttrium-90⁽²⁹⁾

Strontium-90 activity may also be easily measured by a variation of the preceding method. After a suitable time has elapsed for yttrium-90 in-growth, yttrium carrier is added and subsequently precipitated as the hydroxide by the addition of sodium hydroxide. The radioyttrium is then purified by standard radiochemical techniques, which will depend on the concentration and species of the other rare earth radionuclides present. Resolution of the decay curve will be necessary if yttrium-91 is present.

(4) Radiostrontium by Ion-Exchange Methods

Kahn and Reynolds⁽³⁰⁾ utilized ion-exchange resins for the concentration of radiostrontium. Strontium carrier is added to a 10-liter water sample and the solution is passed upflow through a cation exchange resin in hydrogen form. The strontium is then eluted with 14N nitric acid. The radiostrontium is then separated from other alkaline earths and purified by previously mentioned methods,⁽²⁶⁾⁽²⁷⁾⁽²⁹⁾ depending on whether total radiostrontium concentration is desired or strontium-90 alone.

By means of concentration of activity with ion-exchange resins, great sensitivity can be obtained, possibly down to the 10^{-10} $\mu\text{c/ml}$ range.

A similar ion-exchange method was described by Kahn, Eastwood, and Lacy⁽³¹⁾. Using appropriate radiochemical techniques, other long-lived radio-nuclides could also be determined. In every case, the recovery of activity was greater than 99%.

Bryant, Sattizahn and Warren⁽³²⁾ utilized an ion-exchange procedure to separate yttrium from strontium after a ten day ingrowth period. The yttrium was then selectively eluted from a cation exchange resin, followed by a readsorption on another resin and finally counted. The radiochemical recovery was greater than 97%. Gravimetric measurement is not required when using this procedure.

(5) Radiostrontium by Evaporation Methods

According to Libby⁽³³⁾ strontium-90 may readily be determined in low concentrations by concentrating the activity by evaporation.

The sample (1 liter) is evaporated to dryness, and dry strontium nitrate carrier is added. Following addition of calcium chloride, to the dry residue, the sample is dissolved in phosphoric acid. Yttrium is then removed by the addition of lanthanum carrier, followed by hydroxide scavenging. The precipitate is redissolved and the milking repeated twice more. The third precipitate is saved, ignited and counted. The analysis itself takes two hours to perform. It is necessary to utilize decay curves to determine the yttrium-90 activity, due to the presence of yttrium-91 and other rare earths.

b. Radiocesium

Radiocesium is considered to be one of the more important of the biologically hazardous radionuclides. Cesium is chemically similar to the other alkali metals, such as sodium and potassium, which are commonly found in the internal organs. Thus ionic interchange within the body is easily accomplished. Cs-137 and Cs-134 with half-lives of 33 years and 2.2 years respectively constitute the greatest radiocesium danger.

Selective alkali precipitation and ion-exchange elution have proven to be the best methods of separation for the analysis of radiocesium. Determination of the various isotopes appears to be most feasible by gamma spectroscopy.

(1) Radiocesium by Phosphomolybdate Precipitation⁽³⁴⁾

After the addition of cesium carrier to the sample, phosphoric acid and ammonium molybdate are added and the cesium is precipitated as cesium ammonium phosphomolybdate. After dissolving the precipitate in sodium hydroxide, the cesium is reprecipitated as cesium cobaltinitrite. This precipitate is dried at 100°C on an aluminum planchet and counted in an internal proportional counter. A 93% removal of cesium activity was attained by the phosphomolybdate precipitation. Concentrations as high as 10^{-4} $\mu\text{c/ml}$ and as low as 10^{-10} $\mu\text{c/ml}$ were measured with good accuracy. The two principal cesium radioisotopes measured by this method were cesium-137 and cesium-134.

(2) Radiocesium by Cobaltinitrite Precipitation⁽³⁴⁾

After the addition of cesium carrier, the cesium and other Group I cations were precipitated as the cobaltinitrite after the addition of sodium nitrite and cobaltous chloride. After washing, the cobaltinitrite is dissolved in hydrochloric acid. Cesium silicotungstate is then precipitated by the addition of silicotungstic acid. The silicotungstate is then dissolved in dilute base and the solution scavenged with ferric hydroxide. The excess tungsten is removed as the insoluble trioxide. Cesium and sodium perchlorates are then precipitated by the addition of perchloric acid and absolute alcohol to the solution. The sodium perchlorate is then removed by washing the precipitate with absolute alcohol. The final cesium precipitate is then washed, dried and counted. This method has been proven to be quite accurate and is now in wide use.

Osmond, et al.⁽²⁹⁾ co-precipitated cesium cobaltinitrite on potassium cobaltinitrite and followed with a similar purification procedure. This method has found little popular use.

(3) Radiocesium by Silicotungstate Precipitation⁽³⁵⁾

This procedure is based on a method originally described by Yamagata and Yamagata⁽³⁶⁾. The cesium is first precipitated as the silicotungstate. Dissolution of the precipitate is then followed by a ferric hydroxide scavenging. The cesium is then reprecipitated as the dipicrylamine. This salt is dissolved in 4-methyl-2-pentanone and the cesium is extracted by means of 2M hydrochloric acid. The cesium is finally precipitated as the perchlorate, in which form it is dried, weighed, and counted. The chemical yield is 80%, and eight analyses may be performed in eight hours.

(4) Radiocesium by a Co-crystallization Procedure⁽²³⁾

A method has been described by which cesium is separated from the bulk of the alkali elements and the mixed fission products by co-crystallization with ammonium aluminum sulfate. The ammonium salts are decomposed by heating, and the cesium is precipitated for counting from a dilute hydrochloric acid solution as the chloroplatinate. This method has been in use as standard procedure in some laboratories.

(5) Radiocesium by Ion-Exchange Methods

Kahn, Eastwood, and Lacy⁽³¹⁾ have developed a separation scheme for the analysis of the more hazardous radionuclides by ion exchange. The specific radioelements studied were cesium, cerium, cobalt and strontium. The lower limit of detection was decreased a hundredfold by concentrating the radioactivity of a large sample with a cation exchange resin.

Cesium was selectively eluted by means of 6M hydrochloric acid from the cation exchange resins studied. Standard purification procedures were

then used to prepare the sample for counting. The cesium was separated from the other alkali cation contaminants by precipitating it as the silicotungstate, dissolving the precipitate in sodium hydroxide, and then reprecipitating it as the perchlorate for counting. The activity recovered for all radionuclides was greater than 99.2%.

Tsubota and Kitano⁽³⁷⁾ found that an ammonium formate - formic acid buffer of pH 3.2 selectively eluted the alkali metals from a cation exchange resin. This buffer was employed particularly for the determination of radiocesium, being somewhat superior to hydrochloric acid or citrate buffer as an eluant.

c. Radioiodine

Radioiodine may be either beta or gamma counted, although gamma scintillation is preferred for determination of the individual radioisotopes of iodine.

(1) Radioiodine by Chemical Methods

Glendenin and Metcalf⁽²⁸⁾ determined radioiodine activity by an extraction purification procedure. Carrier sodium iodide is added to the water sample, and interchange is accomplished by oxidation to the iodate with sodium hypochlorite in basic solution, followed by reduction to the iodide by sodium bisulfite in acid solution. Sodium nitrite is then added to oxidize the iodide to elemental iodine which is then extracted into carbon tetrachloride. The iodine is further purified and concentrated by back-extraction into sodium bisulfite solution which is finally gamma counted at the iodine-131 photopeak. The sensitivity of the method is approximately 10^{-8} c/ml for a liter sample.

The problem of incomplete carrier interchange is overcome by this procedure which employs oxidation-reduction.

The same authors ⁽³⁸⁾ also describe a procedure in which the iodate is reduced directly to the iodide by hydroxylamine hydrochloride. The iodide obtained after the sodium bisulfite back-extraction is precipitated with silver nitrate as silver iodide which is then dried, weighed, and beta counted.

A similar but faster method for radioiodine determination was developed by Lewis ⁽³⁹⁾. He developed a continuous extractor employing two centrifugal pumps, to promote mixing and extraction. The iodine was extracted into carbon tetrachloride and backextracted into bisulfite solution in one operation. The gamma emission of a pipetted sample was then measured. The time of analysis was cut from 2 hours to 30 minutes. An accuracy of $93.0 \pm 8.0\%$ was achieved.

d. Total Radio Rare Earths Determination

(1) Total Rare Earth Activity by Fluoride Precipitation

Hume and Martens ⁽⁴⁰⁾ have developed a rapid method for the determination of rare earth activity by which the beta and gamma activities are determined separately. The method is quite rapid, the gamma determination taking only a half-hour.

Two rare earth fluoride precipitations serve to remove zirconium and niobium, the principle gamma emitters of fission material. Barium and strontium, which are heavily coprecipitated, are removed by hydroxide precipitation after the addition of holdback carrier. The sample may then be gamma counted. To estimate the beta activity, the rare earths must be precipitated as the oxalates before counting.

(2) Total Rare Earth Activity by an Alternate Method

Boldridge and Hume ⁽⁴¹⁾ developed a method similar to that above

for the determination of total rare earth activity. It is somewhat lengthier, but more accurate, particularly for beta counting.

Stable cerium is added as a carrier for the entire group of rare earths. The rare earths are then precipitated as fluorides, redissolved in boric and nitric acids, and reprecipitated as the hydroxides. Zirconium is then removed by precipitation as the iodate after reduction of all the rare earths to the trivalent state. Following hydroxide scavenging for alkaline earth removal, the rare earths are precipitated as the oxalates and beta-counted in an internal proportional counter.

Alstad and Pappas⁽⁴²⁾ employed a similar technique, using lanthanum as a carrier for all the rare earths. Following separation and purification of the group of rare earths, individual separation was attained by elution from a cation exchange column with ammonium lactate. The ion-exchange separation step was performed without additional carrier, and the recovery of activity for each radionuclide was assumed to be the same as that for the lanthanum. The advantage of the non-carrier separation is that a "weightless" sample is obtained, thus eliminating self-absorption and self-scattering factors.

e. Miscellaneous Radionuclides

(1) Radiobarium

Determination of radiobarium may easily be made during the radio-strontium analysis. Both strontium and barium form insoluble carbonates, and subsequent separation may be made by precipitation of barium as the chromate. This method, by Hahn and Straub,⁽²⁵⁾ was described earlier under radiostrontium. Hunter and Perkins⁽⁴³⁾ followed the same procedure except that the precipitate is counted as the carbonate instead of the chloride.

Minkinen⁽²⁴⁾ has developed a procedure for the analysis of radio-barium in which barium chloride carrier is specifically precipitated as the monohydrate from a concentrated hydrochloric acid-ethyl ether mixture. This precipitate is dissolved in water to which ferric hydroxide is subsequently added as a scavenger. The barium is then isolated as the chromate. The chemical yield of barium chromate is about 70%. The barium chromate precipitate is then set aside for 134 hours to allow the barium-140 and its daughter lanthanum-140 to come to equilibrium.

(2) Radiocerium

Burgus and Engelkemeir⁽⁴⁴⁾ have developed a method of analysis for radiocerium (cerium-144), employing a series of precipitations. After the addition of cerium carrier and alkaline earth holdback carriers, cerium was separated along with the rare earths by fluoride precipitation. Alternate hydroxide and fluoride precipitations are then employed to remove zirconium and alkaline earths completely. The cerium is then oxidized to the tetravalent state with perchloric acid and precipitated as the iodate. Thorium activity is then removed as the iodate following the reduction of cerium with sulfur dioxide. After scavenging with thorium and further reprecipitation, the cerium is finally precipitated as cerous oxalate, which is subsequently ignited to the oxide. After weighing, the cerium activity is counted on an internal proportional counter.

The percentage of chemical recovery is only about 30%, but the radioactive purity of the final precipitate is very high.

It is likely that this process could be shortened because of the probable absence of thorium from fallout contaminated water.

Ames⁽⁴⁵⁾ employed a similar procedure for the analysis of total radiocerium. The concentration of cerium-144 is obtained by counting immediately, using a 217 mg/cm² aluminum absorber. This shields all the

cerium betas, counting only those from praseodymium-144, the daughter product of cerium-144. The difference between the total radiocerium concentration and cerium-144 concentration is assumed due to cerium-141, a neutron induction product.

Barnes⁽⁴⁶⁾ describes a method by which radiocerium is isolated by an extraction method and counted for cerium-144. Carrier interchange is accomplished by means of an oxidation-reduction cycle. Two dibutyl phosphate extractions are then carried out to remove the heavy elements. The cerium is then precipitated as the fluoride, oxidized to the tetravalent state, and extracted into hexone. Finally it is converted to the dioxide and counted for cerium-144 by means of a beta counter using a 217 mg/cm² aluminum absorber. The chemical yield varies from 50-60%.

Kahn and Reynolds⁽³⁰⁾ have developed another method for the determination of radiocerium activity employing the use of ion-exchange resins. Concentration of radiocerium and added carrier was attained by passing a one-liter water sample through either Dowex-50 on the hydrogen cycle or IR-220 on the sodium cycle. Cerium was selectively eluted from the resin with 25 ml of 3M nitric acid. Purification of the radiocerium is obtained by successive precipitations as the fluoride, the hydroxide and finally as the oxalate. The cerium oxalate is weighed to determine carrier loss and then counted. Sensitivity of detection was increased to approximately 10^{-8} $\mu\text{c/ml}$.

(3) Radioruthenium

Glendenin⁽⁴⁷⁾ has developed an analysis scheme for the determination of radioruthenium which has been utilized as a standard method of procedure. Separation of the radioruthenium with carrier ruthenium is accomplished by oxidation with perchloric acid to the volatile tetroxide which is subsequently distilled off. Sodium bismuthate is added prior to distillation to prevent

volatilization of the halides by oxidizing them to the oxyacids. The ruthenium is absorbed into a sodium hydroxide solution and precipitated in the form of its lower oxides by reduction with ethanol. The ruthenium oxides are then dissolved in hydrochloric acid, and ruthenium is precipitated in the metallic state by reduction with magnesium metal. The ruthenium metal is weighed for carrier loss and counted. The chemical yield is about 65%.

Melnick⁽⁴⁸⁾, using an almost identical chemical procedure, describes a process for the determination of ruthenium-106. By using a series of heavy aluminum absorbers with a beta proportional counter, a correction factor for the presence of ruthenium-103 (half-life = 42d) may be obtained by extrapolation. Extrapolation for the correction is necessary, in that while counting the betas from ruthenium-106 through a 210 mg/cm² aluminum absorber, the gamma rays from ruthenium-103 are also counted. If the activity due to ruthenium-103 alone is desired, gamma scintillation may be used with a 2,000 mg/cm² aluminum absorber.

Merritt⁽⁴⁹⁾ describes a method of radioruthenium analysis in which the ruthenium is determined in the presence of strontium, cesium and cerium by fusion and extraction. Following the addition of carrier ruthenium to the water sample, the sample is fused with potassium hydroxide, sodium nitrite, and sodium carbonate at 550°C for two hours. The melt is leached twice with water to dissolve the ruthenate and cesium, leaving strontium and cerium in the residue. Strontium, cerium and cesium are then analyzed by previously mentioned procedures. The ruthenium is extracted from the leach, after the addition of periodate, with carbon tetrachloride. The ruthenium is then stripped from the carbon tetrachloride with 6N hydrochloric acid. Magnesium is then used to reduce the ruthenium to its elemental metallic state in which form it is subsequently counted. This method has proven satisfactory for soil leaching analysis, etc., but could well be used on water samples.

(4) Radiozirconium-Radioniobium

Steinberg⁽⁵⁰⁾ has developed a method for the determination of zirconium-niobium activity which has been tested and proven. Following the addition of both zirconium and niobium carriers, the two elements are complexed by the addition of oxalic acid. Thorium oxalate scavenging is carried out by the addition of potassium chlorate to the acidified solution. The niobium oxide is redissolved and reprecipitated as the oxide hydrate. The water is then driven off by ignition and the niobium oxide is weighed and mounted for counting. The zirconium is precipitated from the original solution as the phenylarsonate by the addition of phenylarsonic acid. This precipitate is dissolved in oxalic acid, forming the soluble oxalate. The zirconium is reprecipitated as the phenylarsonate, which is subsequently ignited to zirconium dioxide. This precipitate is weighed and counted. Both precipitates (niobium and zirconium) are beta counted on an internal proportional counter.

Brady and Engelkemeir⁽⁵¹⁾ have developed a phosphate method for the determination of activity due to zirconium-niobium which is somewhat lengthier than the preceding method. Separation of zirconium is based upon the precipitation of zirconium phosphate. The phosphate is then redissolved as the fluoride and precipitated as the phenylarsonate which is subsequently ignited for counting. Niobium is precipitated in acid solution, dissolved as the fluoride complex and finally weighed and counted as the oxide. About 10 hours is required for the entire analysis. The chemical recovery of zirconium is about 75%, and that of niobium is about 80%.

A method is also described by Stanley⁽⁵²⁾ for determination of zirconium-95. Carrier interchange is effected by the formation of the fluoro-zirconate complex, ZrF_6^{-2} . Rare earth activities are removed by lanthanum

fluoride scavenging. The zirconium is then separated by means of three barium fluorozirconate precipitations. The zirconium is finally precipitated with mandelic acid from hydrochloric acid solution and ignited to the dioxide, in which form it is weighed and counted. A chemical yield of about 75% is obtained. It is essential to not begin the analysis until zirconium-97 ($t_{1/2} = 17$ hours) has had time to decay to a negligible amount. After the final precipitate has been obtained, counting should begin immediately so that no appreciable niobium-95 has time to grow in. A beta proportional counter should be employed for the counting.

3. Summary of Radionuclide Analyses

For the convenience of the reader, additional references, as well as those previously cited, are summarized in Table XVI.

Table XVI

Summary of References of Radionuclide Analyses

Element	References Cited	Additional References
1. Radiostrontium	25, 26, 27, 29, 30, 31, 32, 33	49, 53, 54, 55, 56, 57, 61, 62
2. Radiocesium	23, 31, 34, 35, 36, 37	29, 49, 54, 55, 58, 64, 65
3. Radioiodine	28, 38, 39	55, 59
4. Total Radio Rare Earths	40, 41, 42	55, 60
5. Radiobarium	24, 25, 43	29
6. Radiocerium	30, 44, 45, 46	29, 31, 49, 63
7. Radioruthenium	47, 48, 49	30
8. Radiozirconium - Radioniobium	50, 51, 52	30

B. Instrumentation

Quantitative analysis of radioactive elements in trace concentrations is done most conveniently by means of radiation-detecting instruments. Due to the very small amounts of radionuclides present, such instruments are usually superior in speed and sensitivity to conventional wet chemical analyses. However, when complete chemical analyses are required, extensive use is made of wet chemical procedures for the separation of various isotopes, as described on pages 105 - 121. Such separations are not required when only gross fission product activity is to be measured or when only one radioisotope is present.

If the activity of a sample is sufficiently high, this activity may be determined directly using a simple detector and ratemeter. At very low concentrations in aqueous samples or for beta emitters, for which self-absorption in the sample is a major factor, preconcentration of the sample and specially designed instruments such as a flow counter may be required.

A survey of commercially available portable radiation instruments has been carried out and the information obtained is summarized in Tables XVIII and XIX. These are all instruments of the ratemeter type capable of recording count rates down to a few counts per minute. To establish their usefulness for the determination of fallout product concentrations in water it is necessary to correlate the sensitivity of the equipment with different types of detectors and reasonable sample volumes with the level of contamination concentration expected in emergencies.

For raw, untreated aqueous solutions, Figure 15 shows the relation of nuclide concentration to measured dose rate for various isotopes of

interest for a representative commercial instrument. It has been shown in Tables XLV and XLVI that fallout product concentrations of the order of 10^{-3} - 10^{-4} $\mu\text{C}/\text{ml}$ may be expected in the water supplies of typical watersheds during the early post-attack period. Table XLVII taken from Lacy and Kahn⁽⁶⁶⁾ shows the relative detectability of selected radioisotopes with survey meters with a lowest-scale sensitivity down to 0.01 mr/hr assuming ideal counter geometry.

If it is merely desired to determine the presence or absence of these high-level fallout concentrations, it is evident that available survey instruments should be capable of supplying this information, provided that they are fitted with a detector head suitable either for immersion into the liquid sample or for flow-through measurements.

However, in most cases the concentrations measured are well above the ICRP maximum permissible levels of concentration in water⁽⁶⁷⁾ or close to the limits of detectability of the instruments listed in Table XLVIII. For this reason it seems necessary to develop and make available procedures and facilities for the more accurate measurement of low-level fission product concentrations to ensure the safety of available sources of drinking water.

This development can follow two paths:

1. Preconcentration of the sample to increase the number of radioactive atoms to a level that is readily detected by conventional survey instruments; or
2. Increasing the sensitivity of the detectors by an increase in sample volume, background reduction by added shielding and coincidence circuit arrangements, or more intimate contact between sample and detector volumes, as in proportional flow counters or in liquid scintillation counting.

Table XVII

Approximate Minimum Detectable Concentrations in Water ($\mu\text{c/ml}$)*

For Survey Meters with Full Scale Sensitivity

Radioisotope	0.01 mr/hr	0.1 mr/hr	1.0 mr/hr	10 mr/hr
Ru ¹⁰⁶	5×10^{-6}	5×10^{-5}	5×10^{-4}	5×10^{-3}
Pd ¹⁴⁰	1×10^{-5}	1×10^{-4}	5×10^{-4}	5×10^{-3}
I ³²	5×10^{-6}	1×10^{-4}	1×10^{-3}	1×10^{-5}
Tl ²⁰⁴	5×10^{-4}	1×10^{-3}	1×10^{-2}	5×10^{-2}
Zr ⁹⁵	1×10^{-4}	1×10^{-3}	5×10^{-3}	5×10^{-2}
T ¹³¹	5×10^{-4}	1×10^{-3}	1×10^{-2}	5×10^{-2}
Na ²⁴	1×10^{-5}	1×10^{-4}	1×10^{-3}	1×10^{-2}
K ⁴²	5×10^{-6}	5×10^{-5}	5×10^{-4}	5×10^{-3}
Sc ⁴⁶	1×10^{-3}	5×10^{-3}	5×10^{-2}	1×10^{-1}
Cr ⁵¹	5×10^{-4}	1×10^{-3}	1×10^{-2}	5×10^{-2}
Co ⁶⁰	1×10^{-3}	5×10^{-3}	5×10^{-2}	1×10^{-1}
Sr ⁹⁰	1×10^{-5}	1×10^{-4}	5×10^{-4}	5×10^{-3}
Au ¹⁹⁸	1×10^{-5}	1×10^{-4}	5×10^{-4}	5×10^{-3}
Cs ¹³⁷	1×10^{-3}	5×10^{-3}	5×10^{-2}	1×10^{-1}

* Values extrapolated from Lacy, W. D. and Kahn, B., "Survey Meters and Electroscopes for Monitoring Radioactivity in Water," J.A.W.W.A., 46, 59 (1954)

Preconcentration Methods

Many methods of preconcentration have disadvantages which limit their use in an emergency. Concentration by evaporation, for example, requires a great deal of care and skill to obtain reasonably accurate results. The use of ion exchange resins to remove the activity from the sample can give very good reproducibility and in some applications can be almost completely automated. Emmons and Lauderdale⁽⁶⁸⁾ have developed a continuous water monitor which employs a long G.M. tube at the center of a column of cation exchange resin. By employing two columns, one may be used while the other is being regenerated with strong acid. With this system sensitivities of around 10^{-7} $\mu\text{c/ml}$ have been obtained.

The mixed resin bed is potentially capable of sensitivities in the 10^{-7} - 10^{-8} $\mu\text{c/ml}$ range when used with low background counters. Although the measurement of radioactivity on resin presents problems of self absorption in the sample, reasonable efficiencies and reproducibilities can be obtained if sufficient care is taken in sample preparation.

One method which may be employed to overcome self-absorption in the resin is to detect the beta particles with a scintillation resin. Little work has been done on scintillation resins, but when techniques are developed this should become a very valuable tool in contamination evaluation work.

A highly accurate way in which the radioisotope content of water can be determined is by radiochemical analysis. By chemically separating the various elements of interest and then measuring the activity of each constituent, the activity concentration as well as the identity of the radio contaminants may be obtained. This type of analysis requires a

skilled radiochemist and such an individual may be difficult to find in emergencies. Solvent extraction methods have also been used, but at present a method involving a mixed-bed ion-exchange resin seems to offer the simplest practical approach⁽⁶⁹⁾.

Detector Development

Improvement in detector sensitivity can be achieved by a suitable choice of detector characteristics, detector geometry, and electronic circuit parameters. In order to measure the contamination level of water supplies the radiation emitted from the water sample must be determined as efficiently and as accurately as possible. Because of the statistical nature of the radiation emission, higher accuracies can be obtained only by increasing the total number of counts registered by the detector, while at the same time keeping background counts to a minimum. For this reason, at low levels of activity individual counting circuits or scalers are superior to integrating counting circuits such as ratemeters.

If the radioactivity is composed largely of beta particles, a major problem in measuring beta activity in water is the short distance which a beta particle can travel in this dense medium. It is, therefore, desirable to bring as large a volume of water as possible into the immediate proximity of the detector.

One of the most convenient monitors for this purpose is the flow-through type which allows the water to come in contact with the detector for a brief period and then be flushed out. The most common detector used in flow-through monitors is the G.M. tube⁽⁷⁰⁾. Various configurations of the G.M. monitor type have been used to check cooling water effluent at many of the water-cooled reactors in the country.

Lately, the geometrical flexibility of plastic scintillators has increased the volume of water which can be brought close to the active volume of the detector. There are presently on the market, water monitors which use large, spherical scintillators capable of measuring activities in the range of 10^{-7} $\mu\text{c/ml}$ ⁽⁷⁵⁾. Another method which displays much of the geometrical advantage of liquid scintillation but has none of the chemical problems is the use of scintillation fibers⁽⁷⁶⁾. Although this method has been used for the most part to measure C^{14} and tritium in water, it should yield good results with fission products and extend direct monitoring capabilities below the 10^{-8} $\mu\text{c/ml}$ range.

Liquid scintillation techniques have yielded very accurate results, high efficiencies and good sensitivity in the determination of radioactivity in water. This method may prove quite valuable in the hands of an experienced radiochemist.

The limiting factor in the sensitivity of a detection device is the background or "zero activity" response of the device. Both electrical and physical approaches have been pursued in the reduction of this background. Physical methods include the shielding of detectors and the reduction of detector sensitivity to the gamma radiation which can penetrate the shielding. Since the cross section of plastic scintillators is quite high for beta radiation while being fairly low for gamma radiation, very thin scintillation discs have been used to produce good beta detection efficiencies with a background of less than one half count per minute for a one inch diameter sample

The electrical method of reducing background involves a shielding detector and anti-coincidence circuits. The detection device is thus made

insensitive to most of the background radiation which enters the detector. Most of the anti-coincidence detectors presently on the market reduce the apparent background to a range of 0.5 to 2 counts per minute.

The only reliable method presently applicable to civil defense use for measuring the amount of specific isotopes in water is gamma-energy analysis. Most gamma analyzers are large and quite complicated to operate, although some that are portable and easy to use are now appearing on the market.⁽⁷⁴⁾ With a small amount of training civil defense personnel should be able to make good use of these instruments.

Summary

Preparation for the post attack monitoring of drinking water supplies for radioactive contaminants, may now be divided into four areas of required action. These include the installation of continuous monitoring equipment at treatment plants, dissemination of information on the use of available instruments for water activity, insuring the availability of battery-powered equipment designed for water or general liquid radioactivity assay, and continuing the research on equipment capable of meeting emergency requirements.

A large number of water treatment plants would probably still be operational after a nuclear attack. The danger of contamination from fallout would require that the water be continuously monitored for contamination even at levels well below the maximum permissible levels. In this way alternative water sources could be located or decontamination procedures could be brought into operation as soon as the possibility arises that existing water supplies become unfit for consumption. It would be desirable for this permanent equipment to be able to determine the relative concentrations of the various radiocontaminants.

Many commercial instruments which detect nuclear radiations can be set up to measure the amount of radioactivity in water to a degree of accuracy suitable for emergency use. This measurement would require a given procedure and a set of conversion tables for each type of instrument or class of instruments.

Of the widely available instruments, the most common type, the G.M. survey meter, can be adapted for emergency use by either dipping the probe into the water or holding the probe close to the water surface, to measure radio-contamination levels down to 10^{-5} $\mu\text{c/ml}$ of some of the isotopes. Some scintillation meters can reduce this lower limit below 10^{-6} $\mu\text{c/ml}$ with the absolute limit depending on background radiation. Most ion chamber survey meters are not as sensitive as the G.M. or scintillation types, although some of the more sensitive ones might be used when no other equipment is available.

Companies marketing nuclear detection equipment were asked to supply detailed specifications on their survey-type instruments. A summary of information received by January 30, 1963 is given in Table XVII. The instruments are listed in order of decreasing sensitivity (minimum full scale readings).

Pertinent specifications in the table include the maximum full scale range, battery life, type of radiation detected, type of detector used, weight, the manufacturer's model number, and unit cost of the instrument. The ability of an instrument to discriminate between various types of radiation is also included, as well as the type of radiation to which a given instrument is sensitive, is indicated by an "X" in the appropriate column. If an "O" appears under the indicated type of radiation

TABLE XXII Capabilities of Portable Survey Instruments

Full Scale Dose Rate (m/hr)		No. of Ranges	No. of Decades if Log Scale	Max. Integrated Dose (r)	Bat- tery Life (hrs)	No. Bat. "D"	Type of Radia- tion α β γ	Type of Detec- tor	Weather- proof	Instrument Wt. (lbs)	Mfgs. Model No.	Commer- cial Source	Price
High	Low												
5	5x10 ⁻⁴	5	-	.5	40	-	x x	Sc		33	15-2	12	\$1960
2.5	.01	5	-	-	-	-	x	Sc		10	FS-11	9	450
100	.02	4	-	-	40	2	0 x	GM	x	5	E-510	3	395
17.5	.07	3	-	-	500	-	x x x	Ion		8	D6	8	395
17.5	.07	3	-	-	300	-	x x x	Ion		8	ASM-94	1	395
10	.1	3	-	-	300	3	0 x	GM		5	CS-30	13	285
100	.1	7	-	-	300	4	x x	GM		5	2651	11	295
100	.1	7	-	-	300	4	0 0 x	GM		5	2652	11	345
20	.2	3	-	-	100	4	0 0 x	GM, Sc	x	4	489	4	175
20	.2	3	-	-	400	4	0 x	GM	x	7	H-575	8	375
2x10 ³	.2	5	-	-	100	5	0 x	GM	x	7	E-500B	3	550
25	.25	6	-	-	-	-	0 x	GM			RM2B	6	200
25	.25	3	-	-	150	-	0 x	GM		6	SU14	10	275
25	.25	3	-	-	150	-	0 0 x	GM		6	SU-14TW	10	335
50	.5	3	-	-	100	5	0 x	GM		5	CDV-700	1	100
50	.5	3	-	-	100	5	0 x	GM	x	5	H-572	8	139
50	.5	3	-	-	100	5	0 0 x	GM	x	5	H-752T	8	240
50	.5	3	-	-	150	5	0 x	GM	x	5	20813	7	60
50	.5	3	-	-	100	5	x x	GM	x	5	701	5	225
500	.5	4	-	-	40	2	0 x	GM	x	5	EP-271	4	535
100	1	3	-	-	250	5	0 x	GM		6	BA-420S	1	230
100	1	3	-	-	250	5	0 0 x	GM		6	BA-420E	1	280
100	1	3	-	-	250	5	0 x	GM		5	SM-131-A	1	280
1x10 ⁶	1	7	-	-	50	2	x	GM	x	7	IS-145	8	460
300	3	5	-	-	100	4	0 0 x	Ion		5	440	4	595
5x10 ⁴	5	5	-	-	-	-	x	Ion		5	CS-40A	8	350
5x10 ⁴	5	5	-	-	500	-	0 0 x	Ion		5	CP-1	6	350
5x10 ⁴	5	5	-	-	500	-	x x x	Ion		5	20815	7	450
1x10 ³	10	3	-	-	500	-	x	Ion	x	5	529B	4	325
1x10 ⁵	10	4	-	-	40	-	x x	GM	x	1	MUTE	8	50
1x10 ⁵	10	4	-	-	40	-	x x	GM	x	1	RM-100	13	53
10x10 ⁷	10	3	3	-	350	-	x x	Ion		5	AGB-10KG-SR	4	445
15x10 ²	15	3	-	.15	800	-	0 x	Ion		5	SU-1H	10	370
25x10 ²	25	3	-	-	800	-	0 0 x	Ion		5	CP-3A	9	295
25x10 ²	25	3	-	-	800	-	0 0 x	Ion		4	74CB	4	295
25x10 ⁴	25	6	-	25	200	5	0 x x	Ion		5	2514	11	695
5x10 ³	50	3	-	-	800	-	0 0 x	Ion		5	CP-3	9	295
5x10 ³	50	3	-	-	800	-	0 0 x	Ion		7	SRJ-7	9	325
5x10 ³	50	3	-	-	150	-	0 x	Ion		3	D-1A	13	275
5x10 ³	50	3	-	-	200	-	0 0 x	Ion		4	740-A	4	295
5x10 ⁴	50	2	3	-	-	-	0 x	Ion		4	AGB-500GB-SR	4	295
1x10 ⁴	100	3	-	-	200	-	0 0 x	Ion		4	740	4	295
25x10 ³	250	3	-	-	800	-	0 0 x	Ion		7	HRJ-7	9	325
5x10 ⁴	500	5	-	-	300	-	0 x x	Ion		10	BA-415	1	435
5x10 ⁴	500	3	-	-	800	-	0 x	Ion		6	CP-TP-1A	9	450
5x10 ⁵	500	4	-	-	100	1	x	Ion	x	5	CDV-715	1	100
5x10 ⁵	500	2	3	-	-	-	0 x	Ion		4	AGB-500GB-SR	4	295
1x10 ⁶	1x10 ³	4	-	-	30	5	x	Sc	x	6	GADORA-1	3	400
3x10 ³	3x10 ³	1	3	-	-	-	0 x x	Ion		9	414	2	475
5x10 ⁴	5x10 ⁴	1	4	-	100	-	x	Ion		1	M50	4	130
5x10 ⁶	5x10 ⁴	3	-	-	800	-	x	Ion		6	CP-TP-1B	9	450
2x10 ⁵	2x10 ⁵	1	4	-	100	-	x	Ion		1	M20C	4	130

it simply means that it can be shielded out by a movable absorber. In the event an instrument may be powered by standard "D" cells, the number of batteries required is indicated. Instruments which are specified to be moisture proof or immersion proof are indicated to be "weather proof" by an "X" in the appropriate column. It is believed that the above cited characteristics are the most important to be considered in selecting an instrument for surveying and measuring water supplies and for other general uses. The manufacturer of each instrument may be determined by referring to the "Commercial Source" column in the table and then to the company number listed in Table XIX.

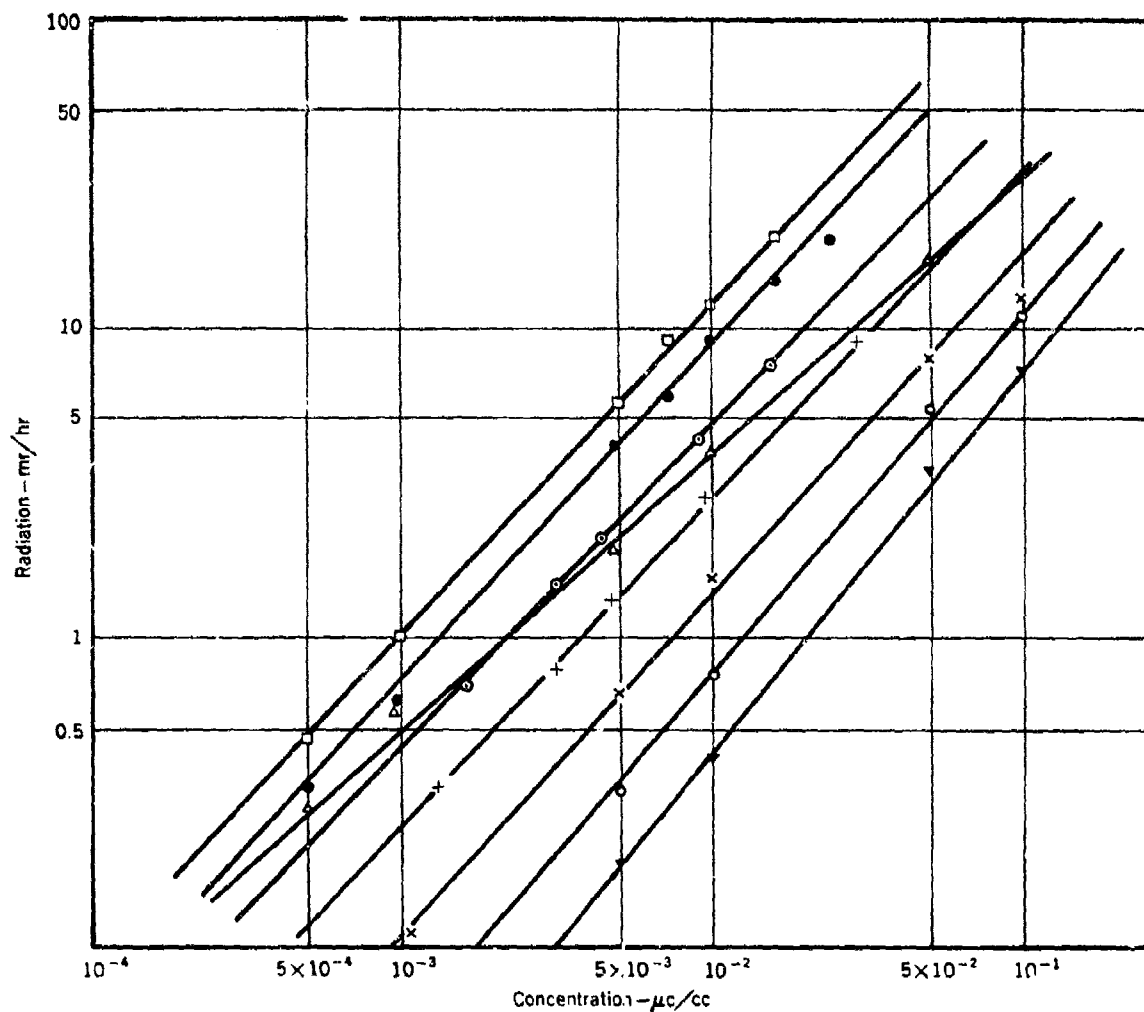
Table XIX

Equipment Manufacturers

- | | |
|--|---|
| 1. Atomic Accessories, Inc.
811 W. Merrick Road
Valley Stream, New York | 8. Radiation Equipment and
Accessories Corp.
665 Merrick Road
Lynbrook, New York |
| 2. Baird Atomic, Inc.
33 University Road
Cambridge 38, Mass. | 9. Technical Associates
140 W. Providencia Avenue
Burbank, California |
| 3. Eberline Instrument Corp.
P. O. Box 279
Santa Fe, New Mexico | 10. Tracerlab
1601 Trapelo Road
Waltham 54, Massachusetts |
| 4. Victoreen Instrument Co.
5806 Hough Avenue
Cleveland, Ohio | 11. Nuclear-Chicago Corporation
333 East Howard Avenue
Des Plaines, Illinois |
| 5. Lionel/Anton Electronic Laboratories
1226 Flushing Avenue
Brooklyn 37, New York | 12. Franklin Systems
2734 Hillsboro Road
West Palm Beach, Florida |
| 6. Nucleonic Corporation of America
196 Degraw Street
Brooklyn 31, New York | 13. Nuclear Corporation of America
Instrument and Control Division
2 Richwood Place
Denville, New Jersey |
| 7. Radiation Counter Laboratories, Inc.
5121 W. Grove Street
Skokie, Illinois | |

Using the information in Figure 15 to convert the instrument sensitivities in Table XVIII into equivalent concentration values, Table XVII has been compiled to show the concentrations of typical isotopes which can just be detected with instruments of the sensitivities stated⁽⁶⁶⁾. It must be borne in mind that the dose calibration in mr/hr for most instruments is done with a cobalt or radium ground source, and that the dose extrapolation to other isotopes and energy ranges will not be the same for different detectors.

It is evident from the foregoing discussion that there appear to be adequate commercial instruments on the market which can be adapted to give a reliable indication of high-level contamination of water supplies. The assay of isotopic contamination and the accurate determination of safe concentrations of radioisotopes in water by field instruments under emergency conditions, however, does require some further research and development work. Such equipment will have to be made available in sufficient quantity for extensive water analyses as soon after an attack as possible.



All values are for submerged readings with Nuclear Corp. meter. Key:

\square Ru ¹⁰⁶ -Rh ¹⁰⁶	\triangle P ³²	\circ Zr ⁹⁵ -Nb ⁹⁵
\bullet Ba ¹⁴⁰ -La ¹⁴⁰	\times I ¹³¹	\blacktriangledown Ti ²⁰⁴
\odot Mixed fission products (3 years)	+ Mixed fission products (10 days)	

Figure 15. Relation of Dose Rate to Nuclide Concentration

VIII. DECONTAMINATION OF WATER SUPPLIES

As discussed in Quarterly Technical Report #3 (see Appendix A) radiologically contaminated waters have been subjected to decontamination procedures of both conventional and non-conventional nature. Of the six radioisotopes of biological importance, all have been found to be amenable to removal to some degree. The degree of treatment required has been predicted in previous reports, predicated by the Maximum Permissible Concentration for peacetime consumption of water or exposure over a considerable period of time. These requirements are very unrealistic when considered in the light of the occurrence of a nuclear incident. The removal efficiencies for the most part have been derived from laboratory data on small volumes of water treated under rigidly controlled conditions. Of practical importance, only those data obtained by actual treatment plant operation are to be considered reliable on a major scale. Even in this respect, it must be pointed out that these data were derived from analysis of water supplies which had been contaminated by long-range weapon debris. It has been discussed elsewhere in this report that the long-range fallout is more soluble than short-range or early fallout. It is for this reason that we may expect full-scale operations to be more efficient in radioisotope removal of early fallout, than the presently reported efficiencies.

It appears that water decontamination in the early phases of a nuclear incident aftermath are not beyond the realm of practical application of the basic sanitary engineering principles of water treatment. The major problem involved in water decontamination will be the long-term exposure of the surviving population to concentrations of the long-halflived isotopes

of biological importance. The reduction of these contaminants to desirable levels will constitute the primary long-term problem to the water treatment field, but is by no means an insurmountable task.

IX. BODY BURDEN FROM CONTAMINATED WATER

In the analysis of body burden from continued ingestion of water contaminated with radioactivity resulting from nuclear attack, it has been found that the development of a rational formula is desirable. A formula has been developed in this report which gives values of body burden comparing closely with those obtained by empirical means.

Many of the empirical values used in this analysis were derived from animal studies, and may or may not be applicable to man per se; however, the values obtained by formulas developed in this report are in good general agreement with data collected from experiments with man. Data from man has been used wherever possible; unfortunately experiments with man are not sufficiently comprehensive to serve as the entire basis of an analysis.

The relation of body burden to many of the radioisotopes found in fallout is not easily understood for short periods of time, that is, when the study period is a very small fraction of the physical half-life of the radioisotope. In this report, in addition to study of the immediate effects, several cases are analyzed for periods of time in excess of fifty years. (Figures 18 and 20)

Numerous studies have been made on the affinity of certain types of tissue for particular radioisotopes. These selectivity studies are of special interest to anyone who wishes to set up theoretical values which may not be exceeded without permanent damage, that is, such values as "Maximum Permissible Concentration," "emergency limits," etc. Although it is not within the scope of this report to determine such values, it is of interest to note that allowable body burden is the total concentration of a given isotope allowed in the most critical organ. The most critical

organ is that organ which receives its damaging dose first during the chain of biological processes.

The phenomenon involved in the rate of turnover of various isotopes by a particular organ is of interest since this rate may be equal to, greater than, or less than the rate for the entire body.⁽⁷⁵⁾ A sample plot of the critical organ A_n versus physical half-life is shown in Figure 16.

Both biological and physical decay rates are considered in this report. In order to demonstrate the difference in body burden levels obtained by (1) considering only physical decay and (2) considering both physical and biological decay, i.e. effective decay, A_n values for both cases are plotted in Figures 16 through 21 as curves B and A respectively.

A_n values plotted as curve A are parameters of the rate at which the radioactivity level in the body is reduced by a combination of bodily processes and physical decay. These A_n values are therefore parameters of the effective decay rates of the various radioisotopes. The amount of any radioisotope which passes through the body must further be related to the amount retained by the critical organ. This relation is represented by an f_w value which gives the amount of a radioisotope taken up by the organ critical for that isotope.

In the interest of generality we have developed a method of computation (using A_n values) rather than a list of specific figures for a limited number of cases.

No attempt has been made to evaluate cell damage resulting from various levels of body burdens. It is obvious that the greater the body burden the more extensive is the radiation damage. Examples are cited in this report of some of the biological blocking processes which may be applied to effectively reduce the body burden. These A_n values will give

the highest burden resulting only from drinking contaminated water while eating a normal uncontaminated diet and breathing uncontaminated air. With an easily derived scaling factor, however, these same graphs may be applied to ingested solids. A_n values may be obtained either from formulas to be derived later in this section or from the graphs in Figures 16 through 21. The graphs are easier to use and are included as an aid to computation.

No limitations of physical death or early genetic death of the individual under study have been placed on the data shown here, since both these limitations require an analysis of damage. We cannot overlook the possibility that at certain levels of contamination or consumption physical or genetic death will limit the continuity of our data, as will any departure from the size and age of a standard man.

Establishment of a Criteria

- (a) The data to be presented should be in the most useful and general form applicable to the subject matter.
- (b) Analysis of damage that may occur at the various levels of body burden is not to be attempted; however, comment regarding damage in general will be incorporated to give depth to the conclusions.
- (c) The development of a rational method for evaluating the body burden is to be outlined and explained. The correlation of the values obtained by the use of this method and those obtained by empirical means will be discussed.
- (d) Assumptions should be as few and as reasonable as possible in order to maintain the integrity of the data to be presented.
- (e) All values used for the various calculations shall be those derived from the most authoritative information available.

Assumptions

(a) The biological decay rate used is that of a standard man. Since the age and overall metabolism of the individual will affect the turnover and replacement rate of radioactive materials in the body, and therefore the biological decay rate, it is necessary to standardize these parameters for the present study.

(b) The contamination of an individual's water supply takes place all at one time, and no further contamination occurs. The analysis of a fluctuating contamination level would require that we assume rates of fallout, wind direction and numerous other meteorological conditions. In order to retain the generality of our investigation we have taken a case in which weather and attack data were not applicable. A_n curves may be added to each other if new contamination occurs (possibly from fallout from a different burst or fallout return from wind reversal).

(c) The radioactive contamination of the water supply is reduced only by physical decay. This assumption is conservative in nature, since it disregards entirely the amount of activity which might settle out or be consumed by life forms found in the water supply, e.g. plankton, algae, fish.

(d) Effective decay rates, even if extrapolated from animal data, are applicable to man. In the absence of experimental data on man, the animal data used was the best available. It may be of interest to note that many contemporary investigators are not satisfied with many of the extrapolations of animal body burden data that have heretofore been accepted as correct, or at least useable, for the case of humans.

(e) The daily intake of water is constant and takes place instantaneously. Virtually all of an individual's water intake occurs

in sixteen hours, and over half occurs in eight hours; however, the errors associated with this simplification tend to be compensating if the individual's drinking habits are consistent. For reasons of generality we are forced to consider that the man under study is a creature of habit. By drawing a smooth curve through the daily A_n points we have essentially integrated over the time periods between the daily values and have described a continuous function as if the individual had spread his intake over the entire day. The combination of the two effects results in a close approximation of the actual build-up of body burden.

Development of a Rational Method of Analysis of Body Burden for Continuous Consumption of Water Contaminated with Radioactive Elements

Based on the Geiger-Nutall Law of radioactive decay we may say that the amount of activity present at any time is equal to

$$A = A_0 e^{-\lambda_p t}$$

when only physical decay is considered. λ_p is the physical decay constant for a particular radioactive element, and A_0 is the amount of activity initially present.

Furthermore, if only biological decay is considered we may say that

$$A' = A_0 e^{-\lambda_b t}$$

where λ_b is the biological rate of elimination constant.

If we define "Effective Half Life" as the time required for a radioactive element fixed in the tissues of an animal body to be diminished by fifty per cent as a result of the combined action of radioactive decay

and biological elimination, then we may say that the effective half-life is⁽⁷⁶⁾

$$\frac{\text{Biological half-life} \times \text{Radioactive half-life}}{\text{Biological half-life} + \text{Radioactive half-life}} = T_{\text{eff}}$$

An effective decay constant (λ_{eff}) may be defined:⁽⁷⁶⁾

$$\lambda_{\text{eff}} = \frac{0.693}{T_{\text{eff}}}$$

Let us assume initially that for any activity taken into the body the entire amount will be fixed in tissue. It is then apparent that immediately before initiation of consumption of contaminated water, the body burden is equal to whatever radioactivity is present as a result of previous activity. For the development of our argument we shall take this initial body burden to be zero and correct it in later developments for the case of initial body burden not equal zero.

The following reasoning may then be applied:

(1) Just before initiation of consumption activity in the body equals zero.

(2) Immediately following the start of consumption the activity in the body equals A_0 , that is, the activity per unit volume of the water ($\mu\text{c/ml}$, atoms/gal, etc.) times the volume of water consumed. Since we have assumed that the amount of liquid is constant we may drop the volume term and reincorporate it later in the development. Furthermore, by considering A_0 equal to unity we will develop an equation which when multiplied by the actual initial activity will give activity present at any given day n . We wish to develop a plot which is independent of both amount consumed and initial activity, and is dependent only on the radioisotope in question.

(3) Immediately prior to consumption on the second day the body burden would be

$$A_1 = A_0 e^{-\lambda_{\text{eff}} l}$$

and just after consumption the body burden is

$$A'_1 = A_0 e^{-\lambda_{\text{eff}}(1)} + A_0 e^{-\lambda_p(1)}$$

(4) Just before consumption on the third day the body burden would be

$$A_2 = A'_1 e^{-\lambda_{\text{eff}} l} = (A_0 e^{-\lambda_{\text{eff}} l} + A_0 e^{-\lambda_p l}) (e^{-\lambda_{\text{eff}} l})$$

and immediately following ingestion, the expression for body burden may be written

$$A'_2 = (A_0 e^{-\lambda_p l}) e^{-\lambda_p l} + (A_0 e^{-\lambda_{\text{eff}} l} + A_0 e^{-\lambda_p l}) e^{-\lambda_{\text{eff}} l}$$

(5) Continuing this reasoning, a recursion formula is developed of the form

$$A_n = A_0 [e^{-n\lambda_{\text{eff}} l} + e^{-[(n-1)\lambda_{\text{eff}} + \lambda_p] l} + \dots \\ \dots + e^{-[\lambda_{\text{eff}} + (n+1)\lambda_p] l} + e^{-n\lambda_p l}] - A_0 e^{-n\lambda_p l}$$

However, rather than deal with the $(n + 1)$ terms necessary to evaluate this equation at n days we simplify the equation as follows

$$A_n = A_0 b \left(\frac{b^n - p^n}{b - p} \right)$$

where $b = A_0 e^{-\lambda_{\text{eff}}(1)}$ and $p = A_0 e^{-\lambda_p(1)}$

(5) This general expression for A_n is the value plotted as curve A in Figures 16 through 21.

(7) We may now incorporate into our formula the portions of total body burden which have thus far been neglected.

(a) Since we have considered A_o to be unity, we may find the total body burden by multiplying A_n by the true original activity, $A_o \text{ true}$, and the volume consumed daily, D.

$$\text{Therefore Body Burden}_I \left(\frac{\text{atoms}}{\text{body}} \right) = A_o \text{ true} \left(\frac{\text{atoms}}{\text{liter}} \right) \times D \left(\frac{\text{liters}}{\text{day}} \right) \times$$

$$A_n \left(\frac{\text{days of consumption}}{\text{body}} \right)$$

(b) The assumption that all the activity taken into the body is immediately incorporated into the intestine is highly improbable. We may however, consider the amount incorporated into tissue as a fraction of the ingested activity reaching an organ (f_w) and multiply the body burden of (a) above by f_w to obtain a more reasonable value.

$$\text{Thus Body Burden}_{II} = f_w \times A_o \text{ true} \times D \times A_n$$

Some values of f_w for isotopes under consideration are given in Table

(c) While reducing the body burden by the factor f_w we have neglected the activity, A_{GI} , which is present in the intestinal tract on day n. This activity is an addition to the body burden, therefore:

$$\text{Body Burden}_{III} = f_w \times A_o \text{ true} \times D \times A_n + A_{GI}$$

where by the reasoning and definitions previously expressed

$$A_{GI} = (1 - f_w)(A_o \text{ true}) e^{-\lambda_p(n-0.25)} (e^{-1.25\lambda_b})$$

Since the time required for ingested material to pass through the body is 31 hours or about 1.25 days, the A_{GI} term is strictly transitory. It may or may not be negligible depending on the period in which it takes place. On the first day, for example, it would be the largest portion of the total, but by the time the fractional half life ($n/T_{1/2}$) is equal to one, the A_{GI} term may in some cases be considered negligible. (n equals time in days since beginning of consumption and $T_{1/2}$ equals radioactive physical half-life in days.)

(d) The only term still missing from the mathematical expression is that for the activity present in the body at the time drinking of contaminated water started (A_I). That which was already present in the tissue at time of initial ingestion will, after n days of effective decay, equal

$$A_T = A_I e^{-\lambda_{eff} n}$$

That present in the gastro-intestinal tract at the time of initial ingestion will give an additional activity equal to

$$A_X = f_w \times A_G e^{-\lambda_{eff} n}$$

where A_G is the pre-ingestion activity in the intestinal tract.

(8) After combining the various components, the expression for body burden from any particular radioisotope at day n may be written:

$$\begin{aligned} \text{Body Burden} &= (f_w)(A_{O \text{ true}})(D)(A_n) + (1-f_w)(A_{O \text{ true}} e^{-\lambda_p(n-1.25)}) (e^{-1.25\lambda_b}) + \\ & (A_I + f_w A_G) e^{-\lambda_{eff} n} = (f_w)(A_{O \text{ true}})(D)(A_n) + A_{GI} + A_T + A_X \end{aligned}$$

The full explanation of this development has been presented in order to allow the user of the equations to decide which, if any, terms may be neglected for any specific analysis. Should the individual in question be an average U. S. citizen who has sought shelter during an attack, the term

$$A_I + f_w A_G e^{-\lambda_{eff} n} \text{ or } A_T + A_X$$

will for practical purposes equal zero. As previously noted, the value of A_{GI} will generally be negligible after a relatively short period of consumption. If the $(A_T + A_X)$ and A_{GI} terms are dropped, the practical expression for body burden is $(f_w)(A_o \text{ true})(D)(A_n)$. The A_{GI} term, however, may be of major importance when the physical half-life is much greater than the effective half-life.

It must also be stressed that to evaluate the effect of A_{GI} , A_T and A_X on any individual that individual's history of exposure to radiation must be known. It is only by thorough knowledge of the development of this rational method that one may make a reasonable calculation of body burden.

Reduction of Body Burden by Blocking

It has been found that in certain cases uptake of radioisotopes may be reduced by biological blocking. For example, by administering a soluble, non-toxic, inert compound of iodine one can prevent uptake of radioactive iodine by the thyroid. Ten to one hundred milligrams of potassium iodide taken at one time will prevent the uptake of any more iodine, radioactive or otherwise, by the thyroid for about one week. To continue this effect, it is believed that an additional 200 milligrams every two days would be required.⁽⁷⁷⁾ Blocking lowers the value of f_w in body

burden calculations.

In the case of Strontium 89 and Strontium 90, which behave like calcium, it is believed that blocking may be completely or partially accomplished by consuming a calcium compound far in excess of normal requirements. This is, however, a conclusion made on the basis of extrapolated data; the only case in which it has definitely been proved that blocking is effective is that of iodine.

Should the body be initially deficient in a given stable isotope (possibly from deficiency of a common mineral in the pre-ingestion diet) the value of f_w for the radioactive isotope of that mineral or a chemically similar mineral may be increased because of the increased affinity of the body for that mineral.

Blocking should not be considered a panacea to the problem of body burden, since it may result in the cure being worse than the disease. In the iodine example, for instance, the prescribed amounts of potassium iodide constitute a daily input of iodine into the body one thousand times normal. Although it is believed that for the majority of the U. S. population this treatment would not be harmful for two or three weeks, the secretion rate of the thyroid is decreased. Extended treatment will produce other still more harmful side effects which have not yet been fully evaluated. Blocking, however, may play an important role in computing body burden values and should not be overlooked when selecting f_w values.

Discussion

(1) In Figures 16 through 21, curve A gives the value resulting from the effective decay rate. Curve B, included for purposes of comparison, represents the rate at which physical decay alone takes place. It seems to

point out that because of the body's tendency to eliminate certain radioisotopes, or not to incorporate them into tissue at all, body burdens are significantly lowered.

(2) Table XXIV gives a few selected values of f_w for six radioisotopes and various organs. These are values which result from a normal uncontaminated diet. Values of f_w may vary from this table according to the excess or deficiency of certain minerals in the body. Note that the concentration of specific isotopes must be known before body burdens can be computed.

Table XX
Selected Values of f_w for Various Organs

Isotope	Organ	f_w
Sr ⁸⁹	Bone	2.5×10^{-1}
Sr ⁹⁰	Bone	2.5×10^{-1}
Ru ¹⁰⁶	Kidney	2.0×10^{-5}
I ¹³¹	Thyroid	2.0×10^{-1}
Cs ¹³⁷	Whole Body	1.0×10^0
Cs ¹³⁷	Liver	4.8×10^{-1}
Ba ¹⁴⁰	Bone	7.0×10^{-2}

Notes:

(1) The f_w values shown are for critical organs. The critical organ will determine the A_n since it is the one used in computing λ_{eff} .

(2) The f_w value for the entire body is the summation of f_w values for all the individual organs concerned.

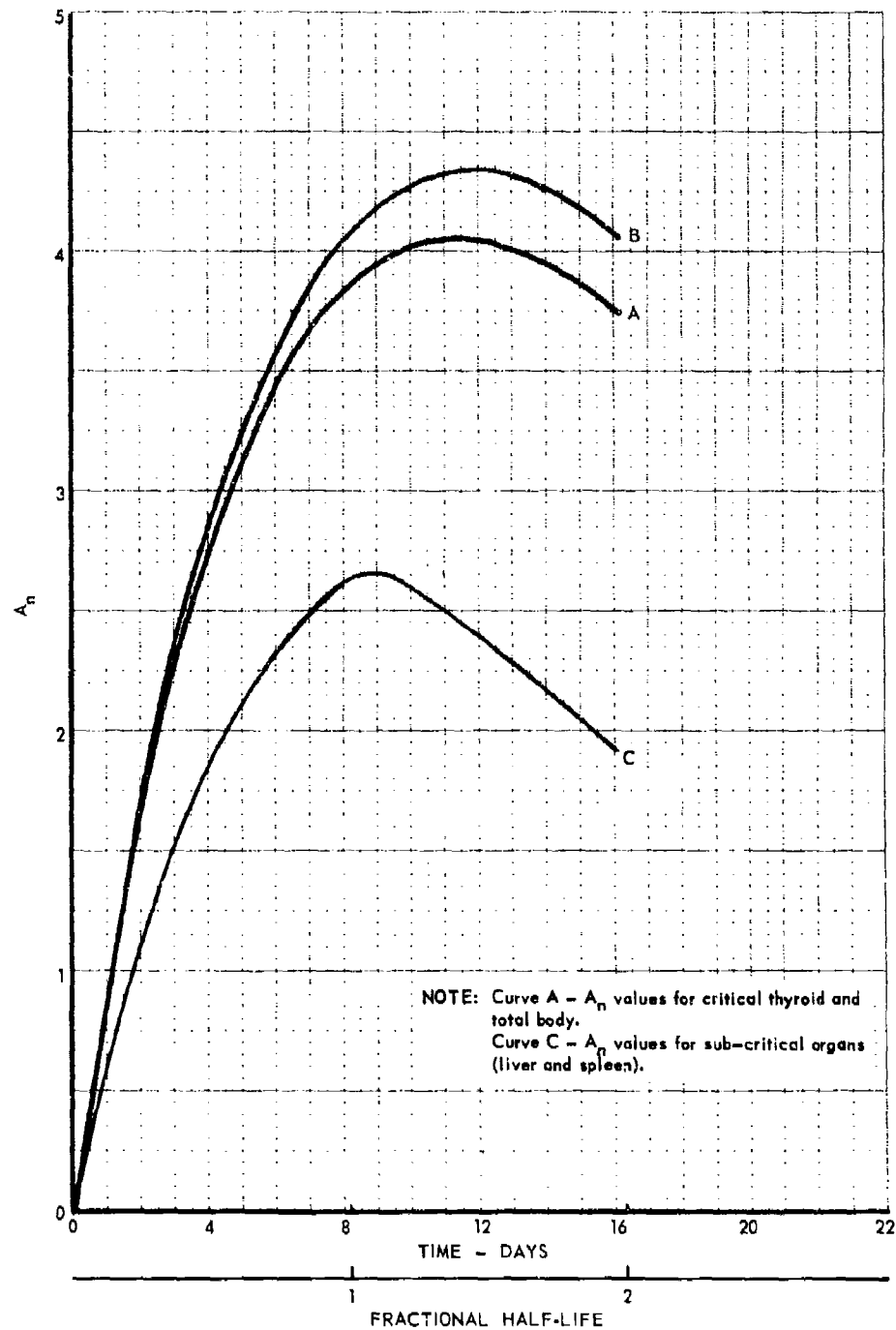


Figure 16. A_n versus Time for Iodine 131

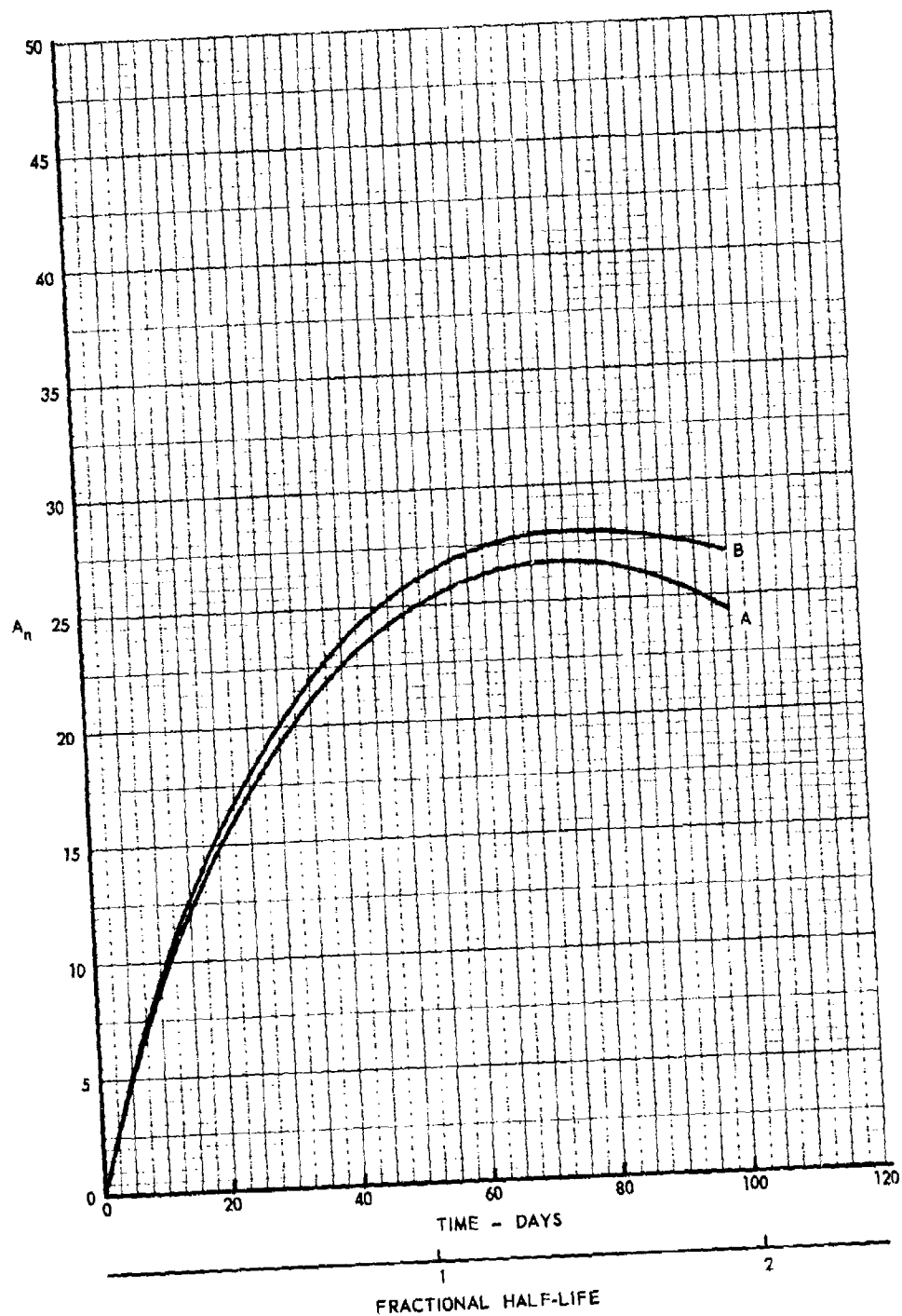


Figure 17. A_n versus Time for Strontium 89

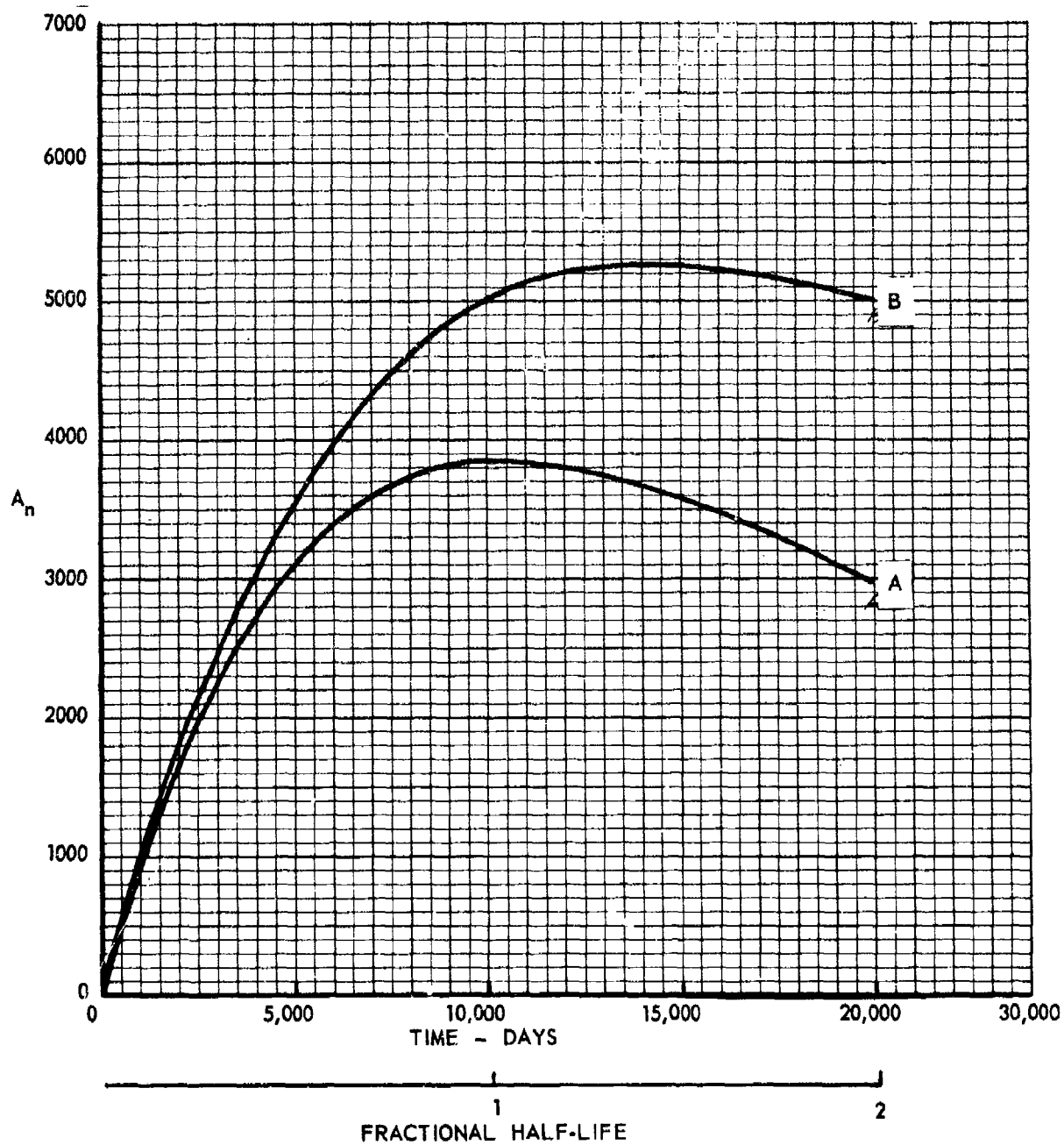


Figure 18. A_n versus Time for Strontium 90

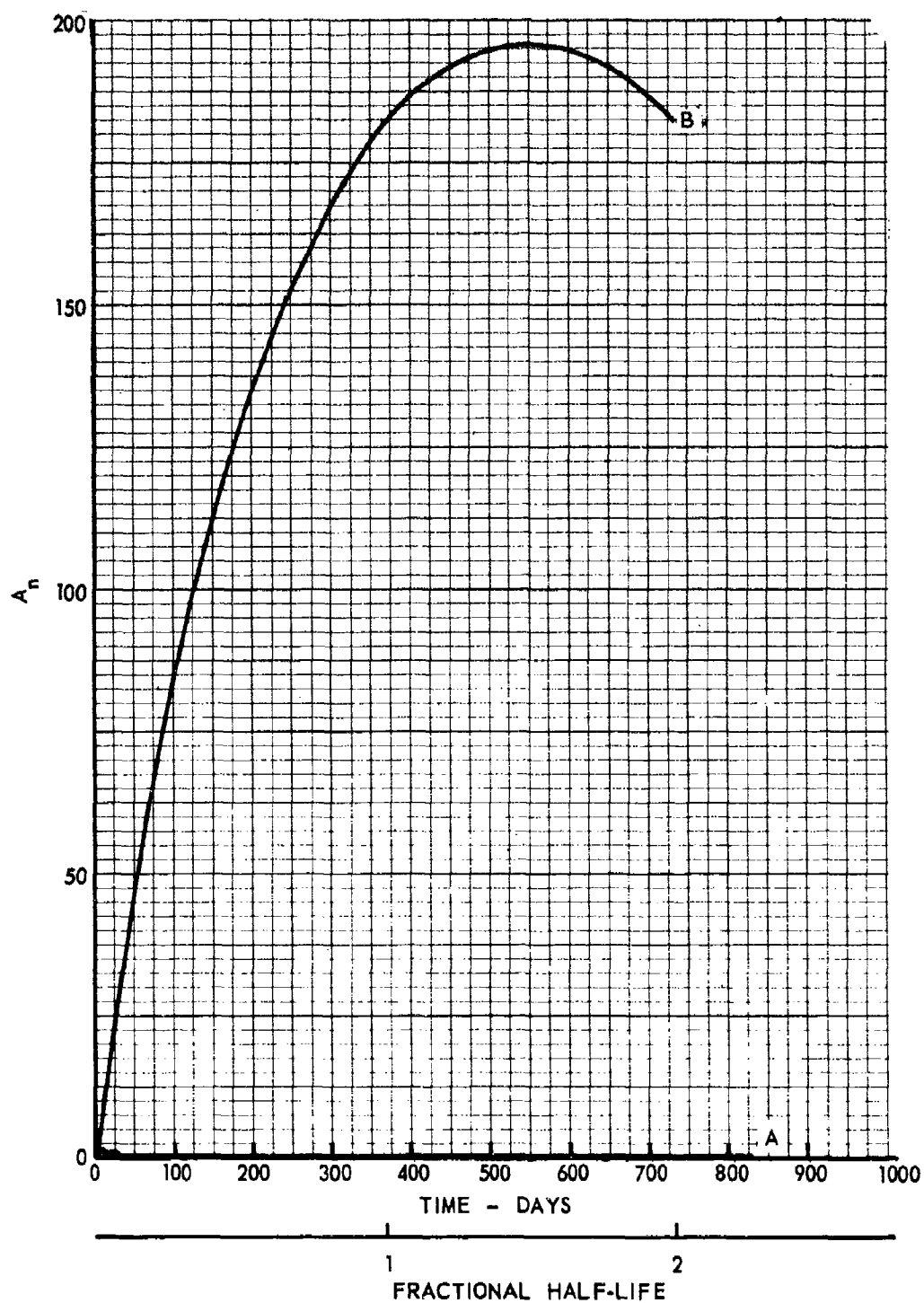


Figure 19. A_n versus Time for Ruthenium 106

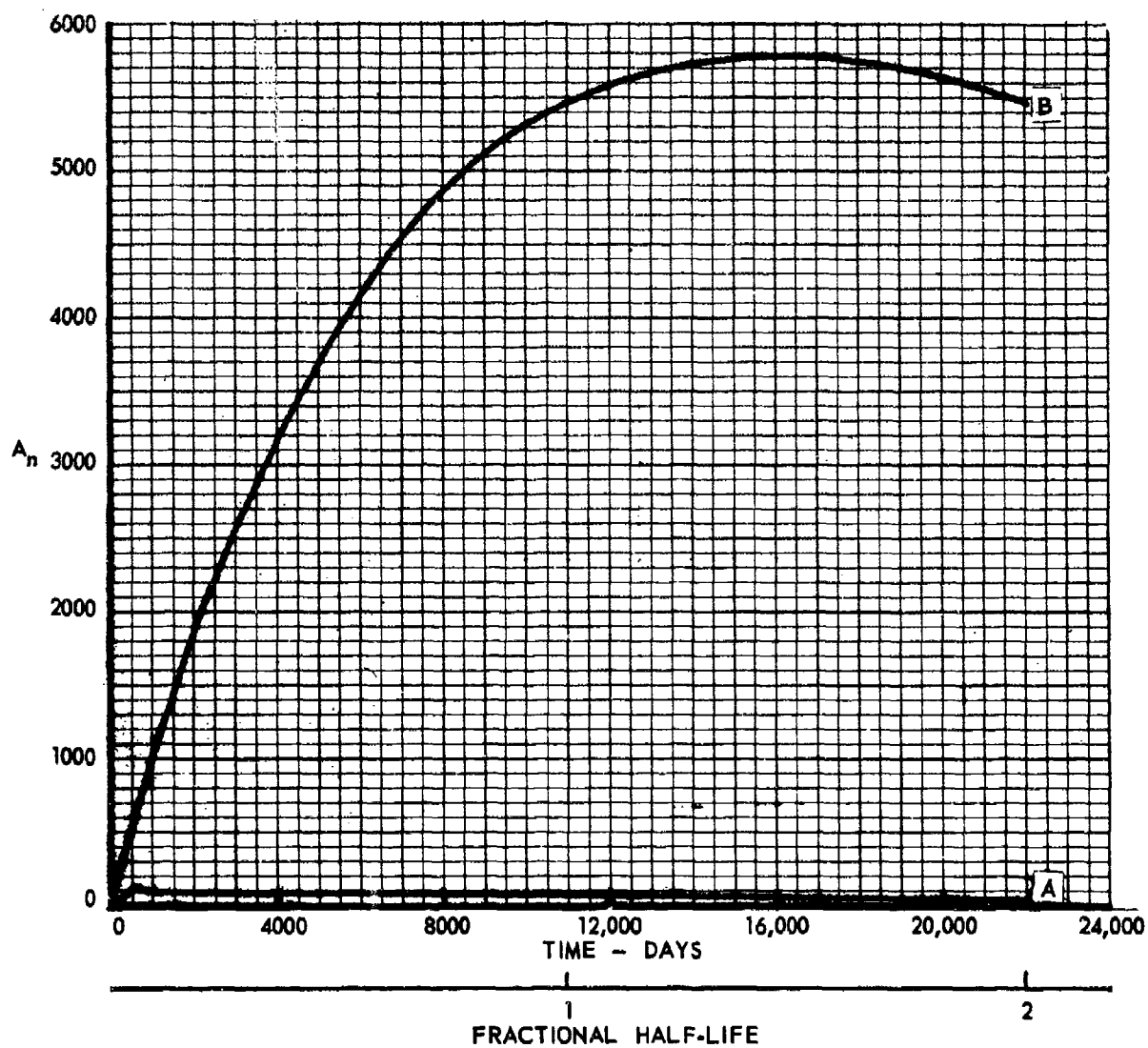


Figure 20. A_n versus Time for Cesium 137

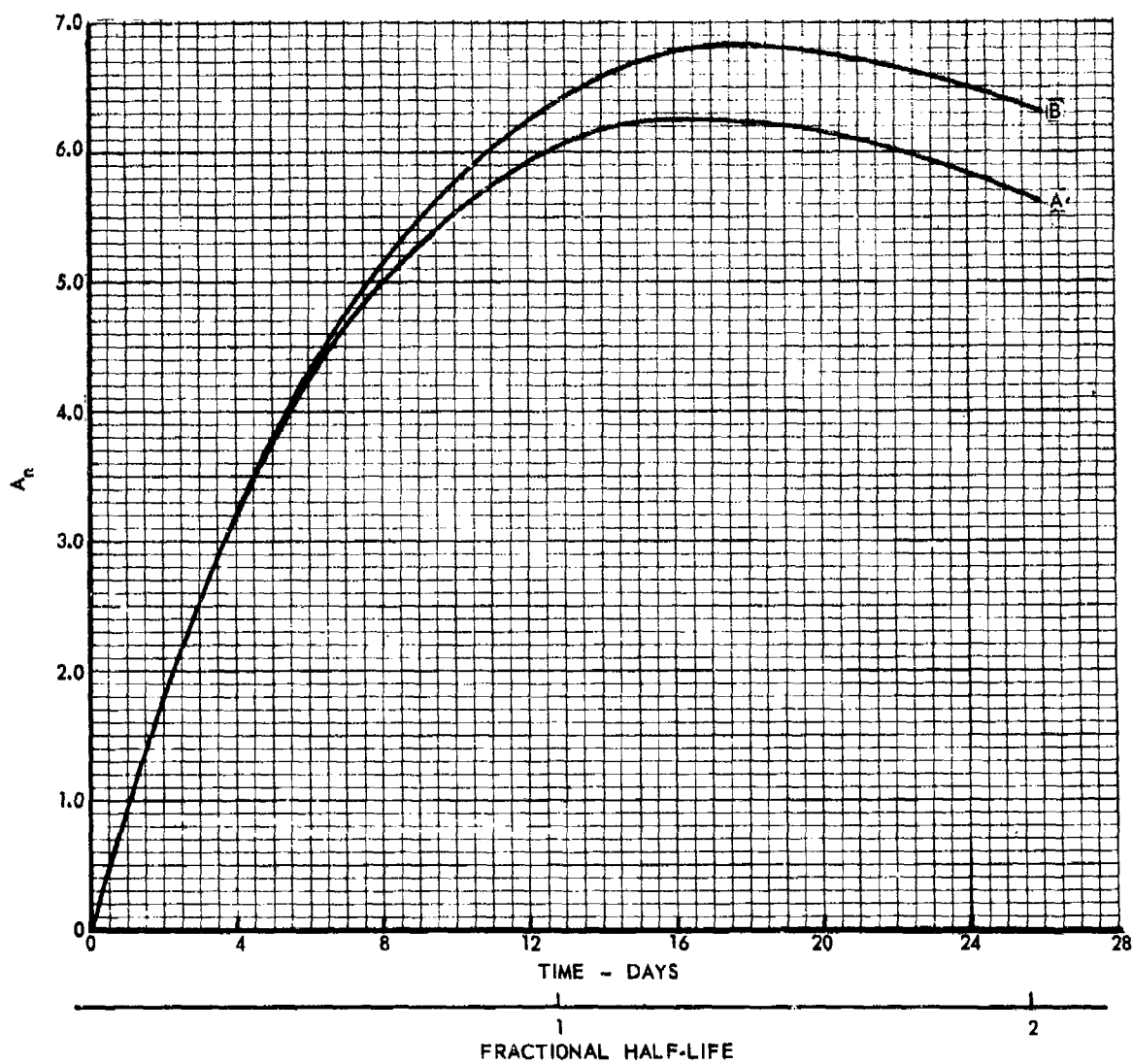


Figure 21. A_n versus Time for Barium 140

X. REFERENCES

- (1) "Biological and Environmental Effects of Nuclear War - Summary - Analysis and Hearings, June 22-26, 1959", Joint Committee on Atomic Energy, 86th Congress of the United States, First Session, 1959, United States Government Printing Office (August 1959)
- (2) "Nuclear Attack and Industrial Survival", McGraw-Hill Special Report, Nucleonics, 20, 1 (January 1962)
- (3) Callahan, E. D., Rosenblum, L. Kaplan, J. D., and Batten, D. R., "The Probable Fallout Threat over the Continental United States" Report No. TO-B 60-13, Technical Operations Inc., Burlington, Massachusetts (December 1, 1960)
- (4) Miller, C. F., "Fallout and Radiological Countermeasures", to be published by Interscience Publishers Inc., New York, N. Y.
- (5) Grune, W. N, Craft, T. F., Jr., and Hill, D. F., "Evaluation of Water Contamination from Fallout", Quarterly Technical Report No. 3 to the Office of Civil Defense, Contract No. OCD-OS-62-189 (February 9, 1963)
- (6) "The Adequacy of Government Research Programs in Non-Military Defense", Report by the Advisory Committee on Civil Defense, NAS-NRC, Washington, D. C. (1958) p. 12
- (7) Bolles, R. and Ballou, N., "Calculated Activities and Abundances of U-235 Fission Products, USNRDL-456 (1956)
- (8) Katcoff, S., "Fission-Product Yields from U, Th and Pu", Nucleonics 4, 78-85 (1958)
- (9) Miller, C. F. and Loeb, P., "Ionization Rate and Photon Pulse Decay of Fission Products from the Slow-Neutron Fission of U-235", USNRDL-TR-247 (1958)
- (10) Miller, C. F., Private Communication, February 18, 1963
- (11) Clark, D. E. and Anderson, A. D, USNRDL, Private Communication with C. F. Miller, July 1960
- (12) Clark, D. E., Jr. and Cobbin, W. C., "Some Relationships among Particle Size, Mass Level and Radiation Intensity of Fallout from a Lead Surface Nuclear Detonation", USNRDL-TR-639 (1963)
- (13) Klement, A. W., Jr., "A Review of Potential Radionuclides Produced in Weapons Detonations", AEC WASH-1024, Div. of Biol. and Med., USAEC, Washington, D. C. (July 30, 1959)
- (14) Glasstone, S., "Effects of Nuclear Weapons", 2nd Ed. United States Atomic Energy Commission (April 1962)

REFERENCES
(Continued)

- (15) Senftle, F. E. and Champion, W. R., "Tables for Simplifying Calculations of Activities Produced by Thermal Neutrons", Nuovo Cimento, 12, Suppl. No. 3, 549-71 (1959)
- (16) Mandeville, C. E., "The Slow Neutron-Induced Radioactivities of Nuclear Explosions", J. Franklin Inst., 252, 297-308 (October, 1951)
- (17) Miller, C. F., Private Communication, December 4, 1962
- (18) Wade, W. O. and Hawkins, M. B., "Procedures for the Estimation of the Concentration of Nuclear Weapon Fallout in River Water", University of California Institute of Engineering Research Technical Memorandum, Civil Defense Research Project, Series No. 2, Issue No. 37, Berkeley, Calif., October 2, 1961
- (19) Hewlett, John D., Private Communication, April 1963
- (20) Coryell, C. D. and Sugarman, N. (Eds.), "Radiochemical Studies: The Fission Products", McGraw-Hill Book Co., New York (1951) Book 3
- (21) Overman, R. T. and Clark, H. M., "Radioisotope Techniques", McGraw-Hill Co., New York (1960)
- (22) Kleinburg, J., "Collected Radiochemical Procedures", Radiochemistry Group J-11, Los Alamos, N. M., LA-1721 (1962) 2nd Ed.
- (23) HASL Manual of Standard Procedures, NYO-4700 (August 1959) p. E-55-01-01
- (24) Kleinburg, J., "Collected Radiochemical Procedures", Radiochemistry Group J-11, Los Alamos, N. M., LA-1721 (1962) 2nd Ed., Minkinen, C.O., p. Ba-1
- (25) Hahn, R. B. and Straub, C. P., "Determination of Radioactive Strontium and Barium in Water", J.A.W.W.A., 47, 335-40 (April 1955)
- (26) Kooi, J., "Quantitative Determination of Strontium-89 and Strontium-90 in Water", Anal. Chem., 30, 532-5 (April 1958)
- (27) Goldin, A. S., Velten, R. J. and Frishkorn, G. W., "Determination of Radioactive Strontium", Anal. Chem., 31, 1490-2 (1959)
- (28) "Radionuclide Analysis of Environmental Samples, A Laboratory Manual of Methodology", Technical Report R59-6, R. A. Taft Sanitary Engineering Center, USPHS, Cincinnati 26, Ohio (1959)
- (29) Osmond, R. G. D., and Evett, T. W., Arden, J. W., Lovett, M. B. and Sweeney, B., "The Determination of Radioactivity Due to Cesium, Strontium, Barium and Cerium in Waters", AERE-AM-84 (1961)
- (30) Kahn, E. and Reynolds, S. A., "Determination of Radionuclides of Low Concentrations in Water", J.A.W.W.A., 50, 613-20 (May 1958)

REFERENCES
(Continued)

- (31) Kahn, B., Eastwood, E. R. and Lacy, W. J., "Use of Ion Exchange Resins to Concentrate Radionuclides for Subsequent Analysis", ORNL-2321 (1956)
- (32) Bryant, E. A., Sattizahn, J. E. and Warren, B., "Strontium-90 by an Ion-Exchange Method", Anal. Chem., 31, 335-6 (March 1959)
- (33) Libby, W. F., Personal communication with T. R. Ostrom for thesis presented to Faculty of Arts and Sciences of Harvard University, Doctor of Sanitary Engineering, May 7, 1955
- (34) Kahn, B., Smith D. K., and Straub, C. P., "Determination of Low Concentrations of Radioactive Cesium in Water", Anal. Chem., 29, 1210-13 (August 1957)
- (35) Kleinberg, J., "Collected Radiochemical Procedures", Radiochemistry Group J-11, Los Alamos, N. M., LA-1721 (1962) 2nd Ed. P. Cs II-1, by Cushing, B. E.
- (36) Yamagata, N. and Yamagata, T., "The Rapid Radiochemical Determination of Cesium-137", The Analyst, 85, 282 (April 1960)
- (37) Tsubota, H. and Kitano, Y., "A Rapid Method for Determining Fission Products Contained in Waters Using an Ion Exchanger", Bull. Chem. Soc. Japan, 33, 765-69 (1960)
- (38) Coryell, C. D. and Sugarman, N. (Eds.) "Radiochemical Studies: The Fission Products", McGraw-Hill Book Co., New York (1951) Book 3, Glendenin, L. E. and Metcalf, R. P., p. 1625
- (39) Lewis, M., "A Rapid Method for the Determination of Radioiodine", HW-18151 (1950)
- (40) Coryell, C. D. and Sugarman, N., (Eds.), "Radiochemical Studies: The Fission Products", McGraw-Hill Book Co. Inc., New York 1951, by Hume, D. N. and Martens, R. I., p. 1732
- (41) Coryell, C. D. and Sugarman, N., (Eds.), "Radiochemical Studies: The Fission Products", McGraw-Hill Book Co. Inc., New York, 1951, by Boldridge, W. F. and Hume, D. N., p. 1693
- (42) Alstad, J. and Pappas, A. C., "Radiochemical Studies of Fission Products Lanthanum and Lanthanides-I", J. Inorg. Nucl. Chem., 15, 222-36 (1960)
- (43) Hunter, C. J. and Perkins, M., "The Determination of Radiobarium", AERE-AM-65 (1960)
- (44) Coryell, C. D., and Sugarman, N. (Eds.) "Radiochemical Studies - The Fission Products", McGraw-Hill Book Co., New York 1951) Book 3, Burgus, W. H. and Engelkemeir, D. W., p. 1668

REFERENCES
(Continued)

- (45) Kleinburg, J., "Collected Radiochemical Procedures", Radiochemistry Group J-11, Los Alamos, N. M., LA-1721 (1962) 2nd Ed., Ames, D. C., p. Ce-1
- (46) Kleinburg, J., "Collected Radiochemical Procedures", Radiochemistry Group J-11, Los Alamos, N. M., LA-1721 (1962) 2nd Ed., Barnes, J. W. p. Ce 144-1
- (47) Coryell, C. D., and Sugarman, N. (Eds.) "Radiochemical Studies: The Fission Products", McGraw-Hill Book Co., New York (1951) Book 3, Glendenin, L. E., p. 1549
- (48) Kleinberg, J., "Collected Radiochemical Procedures", Radiochemistry Group J-11, Los Alamos, N. M., LA-1721 (1962) 2nd Ed. Melnick, M. A., p. Ru-1
- (49) Merritt, W. F., "Radiochemical Analysis for Long-Lived Fission Products in Environmental Materials", Can. J. Chem., 36, 425-8 (March 1958)
- (50) Coryell, C. P. and Sugarman, N. (Eds.) "Radiochemical Studies: The Fission Products", McGraw-Hill Book Co., New York (1951) Book 3, Steinberg, E. P. p. 1495
- (51) Coryell, C. D., and Sugarman, N., (Eds.), "Radiochemical Studies: The Fission Products", McGraw-Hill Book Co., New York (1951) Book 3 Brady, E. L. and Engelkemeir, D. W., p. 1491
- (52) Kleinberg, J., "Collected Radiochemical Procedures", Radiochemistry Group J-11, Los Alamos, N. M., LA-1721 (1962) 2nd Ed., Stanley, C. W. p. Zr-95 - Zr-97 - 1
- (53) Lindner, M., "Radiochemical Procedures in Use at the University of California Radiation Laboratory (Livermore)", UCRL-4377 (1954) p. 29, Nethaway, D. R. and Hicks, H. G.
- (54) Wish, L., "Quantitative Radiochemical Analysis by Ion Exchange", Anal. Chem., 33, p. 1002 (July 1961)
- (55) Boni, A. L., "Quantitative Analysis of Radionuclides in Process and Environmental Samples", Anal. Chem., 32, p. 599-604 (May 1960)
- (56) Misumi, S. and Taketatsu, T., "Separation of Yttrium-90 from Strontium-90 and Lanthanum-140 from Barium-140 with an Anion Exchange Resin of Carbanate Form", J. Inorg. and Nuc. Chem., 20, 127-130 (1961)
- (57) Stanley, C. W., and Kruger, F., "Determination of Strontium-90 Activity in Water by Ion-Exchange Concentration", Nucleonics, 14, 11, 114 (1956)

REFERENCES
(Continued)

- (58) Gray, P. R., "Separation of Cesium from Fission Product Waste Solutions", J. Inorg. and Nuc. Chem., 12, 304-314 (1960)
- (59) Technical Manager (Chemistry) Technical Branch, Windscale Works, "The Determination of Iodine-131 in Vegetation, Milk, Thyroid Glands and Natural Water", PG-Report-204 (1961)
- (60) Freiling, E. C. and Bunney, L. R., "Ion Exchange as a Separation Method. VII. Near Optimum Conditions for the Separation of Fission Products Rare Earths with Lactic Acid Eluant at 87°C", Jour. Am. Chem. Soc., 76, 1021-2 (1954)
- (61) Cohen, P., Pardo, G., and Wormser, G., "Determination of Strontium-90 in Waters Rich in Calcium", Energie Nucleaire, 6, 1957, No. 1, 89-90 (1957)
- (62) Turk, E., "A Modified Radiochemical Strontium Procedure", ANL-5184, (1953)
- (63) Marsh, S. F., Maeck, W. J., Booman, Glenn, L., and Rein, J. E. "Solvent Extraction Method for Radiocerium", Analytical Chemistry, 34, 1406 (October 1962)
- (64) Owers, M. J., "The Concentration by Electrodialysis of Caesium and Strontium Radioactivities in Water", AERE-R-3010
- (65) Evans, H. B., "Bismuth Iodide Method for the Determination of Cesium Activity in Fission", Paper 284, Nat. Nuclear Energy Series, Div. IV. 2, Book 3, 1646-8 (1951)
- (66) Lacy, W. J. and Kaly, B., "Survey Meters and Electroscopes for Monitoring Radioactivity in Water", J.A.W.W.A., 46, 55 (1954)
- (67) Report of ICRP Committee II on Permissible Dose for Internal Radiation (1959), Health Physics 3, 1-234, 1960
- (68) Emmons, A. H., Lauderdale, R. A., "Low Level Radioactive Contaminants in Water", Nucleonics, 11, 22 (June 1952)
- (69) Grune, W. N., Hughes, R. B., and Nagel, A. E., "Development of a Rapid Assay Method for Gross Low-Level Radioactivity in Water", Report to AFEB contract DA-49-193-MD-2243, Georgia Institute of Technology (1963)
- (70) Hurst, W. M., "Monitoring of Liquids for Radioactivity", Nucleonics, 11, 34 (August 1953)
- (71) Franklin Systems, Inc., West Palm Beach, Florida, Specifications Sheet #1075 - 2 Model 30 Gamma-Beta Scintillation Water Monitor, Sept. 1960
- (72) Stone, C. A., Preston, C., "Fiber Beta Counters", Nucleonics, 20, 82, (January 1962)

REFERENCES
(Continued)

- (73) G. G. Eichholz, Nuclear Instruments and Methods, 8, 320, 1960
- (74) Tracerlab Division of Laboratory for Electronics, Inc., 1601 Trapelo Road, Waltham 54, Mass., "PS-1 Portable Radiological Spectrometer"
- (75) "Report of Committee II on Permissible Dose for Internal Radiation 1959", Health Physics Journal, 3 (1959)
- (76) Kinsman, S., "Radiological Health Handbook", U. S. Dept. of Health, Education and Welfare, Public Health Service, Cincinnati, Ohio (1957)
- (77) Clarke, E. T., Kaplan, A. L. and Callahan, E. D., The Potential Radiation Hazard from Water Supplies and Milk After a Nuclear Attack, (Revised), Technical Operations, Inc., Burlington, Mass. (1961)
- (78) Grune, W. N., Craft, T. F. Jr., and Hill, D. F., "Evaluation of Water Contamination from Fallout", Quarterly Technical Report No. 3 to the Office of Civil Defense, Contract No. OCE-CS-62-189 (February 9, 1963)
- (79) Fair, G. M. and Geyer, J. C., "Elements of Water Supply and Waste Water Disposal", P. 294, John Wiley and Sons, Inc., New York, N. Y., 1959
- (80) "Water Decontamination", Report of the Joint Program of Studies on the Decontamination of Radioactive Water, ORNL-2557 (1959)
- (81) Straub, C. P., Morton, R. I. and Placak, O. R., "Studies on the Removal of Radioactive Contaminants from Water", J.A.W.W.A., 43, 773 (October 1951)
- (82) Eliassen R., Kaufman, W. J., Nesbitt, J. B. and Goldman, M. I., "Studies on Radioisotope Removal by Water Treatment Processes", J.A.W.W.A., 43, 615 (1951)
- (83) Lacy, W. J., "Removing Radioactive Material from Water by Coagulation", Water and Sewage Works, 100, 410 (1953)
- (84) Matsumura, T., et al., "Treatment of Radioactive Waste Water by Flocculation", Annual Report Radiation Center Osaka Prefect 2, 33-42 (1962), Chem. Abst., 57, 7047a (1962)
- (85) Hannah, S. A. and Printz, A. C., Jr., "An Evaluation of the Effectiveness of Polyelectrolyte Coagulant Aids for the Removal of Radioactive Isotopes by Water Treatment Process", A report to the Office of Civil Defense and Mobilization under provisions of contract CDM-SR-60-56 with the University of Florida, NP11105 (1961)
- (86) Hoyt, W. A., "The Effects of the Lime-Soda Water Softening Process on the Removal of Radioactive Strontium-90 - Yttrium-90", Master of Science thesis, North Carolina State College, Raleigh, (1952)

REFERENCES
(Continued)

- (87) McCauley, R. F., Lauderdale, R. A. and Eliassen, R., "A Study of the Lime-Soda Softening Process as a Method for Decontaminating Radioactive Waters", NYO-4439 (September 1, 1953)
- (88) Health Physics Division Quarterly Progress Report for the period ending January 20, 1953, ORNL-1488 (1953)
- (89) Downing, A. L., Wheatland, A. B. and Eden, G. E., "Observations on the Removal of Radioisotopes During the Treatment of Domestic Water Supplies: II. Radio-Strontium", Jour. of the Inst. of Water Eng., 7, 7 (November 1953)
- (90) Eden, G. E., Elkins, G. H. and Truesdale, G. A., "Removal of Radioactive Substances from Water by Biological Treatment Process", Atomics, 5, 3 (May 1954)
- (91) Amphlett, C. B. and Sammon, D. C., "Survey of Treatments Considered for Low-Activity Wastes", "Atomic Energy Waste, its Nature, Use and Disposal", edited by E. Glueckauf, Interscience Publishers, Inc., New York, N. Y. (1961)
- (92) "News Quarterly", p. 8, Sanitary Engineering Research Laboratory, University of California, Berkeley, California (July 1961)
- (93) "Radioactivity in Water Supplies", Public Works, 91, 176 (June 1960)
- (94) Lauderdale, R. A., "Treatment of Radioactive Water by Phosphate Precipitation", Ind. Eng. Chem., 43, 1538 (1951)
- (95) Nesbitt, J. B., Kaufman, W. T., McCauley, R. F. and Eliassen, R., "The Removal of Radioactive Strontium from Water by Phosphate Coagulation", NYO-4435 (1952)
- (96) Tamura, T. and Struxness, E. G., "Removal of Strontium from Wastes", ORNL-60-10-43 (November 1960)
- (97) Cowser, K. E. et al., "Radioactive Waste Disposal - Low Level Waste Water Treatment", Health Physics Division, Annual Progress Report for period ending July 31, ORNL-2994 (1960)
- (98) Eden, G. E., Downing, A. L. and Wheatland, A. B., "Observations on the Removal of Radioisotopes During Purification of Domestic Water Supplies: I. Radioiodine", J. Inst. Water Engr., 6, 511 (1952)
- (99) Lacy, W. J. and Delaguna, W., "Decontaminating Radioactive Water", Ind. Eng. Chem., 50, 1193 (1958)
- (100) Lacy, W. J., "Removal of Radioactive Material from Water by Slurrying with Powdered Metal", J.A.W.W.A., 44, 824 (1952)

REFERENCES
(Continued)

- (101) Silker, W. B., "Removal of Radioactive Ions from Waters", U. S. Patent 3,029,200 (April 10, 1962)
- (102) Lacy W. J., "Decontamination of Radioactivity Contaminated Water by Slurrying with Clay", Ind. Eng. Chem., 46, 1061, (1954)
- (103) Brockett, T. W., Jr. and Placak, O. R., "Removal of Radioisotopes from Waste Solutions by Soils - Soil Studies with Conasauga Shale", p. 393, Proceedings, 8th Industrial Waste Conference, May 4-6, 1953, Purdue University, Extension Series No. 83 (1954)
- (104) Straub, C. P. and Krieger, H. L., "Removal of Radioisotopes from Waste Solutions - Soil Suspension Studies", p. 415, Proceedings, 8th Industrial Waste Conference, May 4-6, 1953, Purdue University, Extension Series No. 83 (1954)
- (105) Tamura, T., "Treatment of High-Level Wastes by Sintering", Hearings before the Special Subcommittee on Radiation of the Joint Committee on Atomic Energy, Congress of the United States, 86th Congress, First Session on Industrial Radioactive Waste Disposal, January 28 to February 3, 1959, Vol. 3, p. 1938
- (106) Eliassen, R. and Goldman, M. I., "Disposal of High-Level Wastes by Fixation of Fused Ceramics", Hearings before the Special Subcommittee on Radiation of the Joint Committee on Atomic Energy, Congress of the United States, 86th Congress, First Session on Industrial Radioactive Waste Disposal, January 28 to February 3, 1959, Vol. 3, p. 1966
- (107) Ed., "Foam Separation Set to Go", Chem. Engrg., 68, 100 (April 3, 1961)
- (108) Schoen, H. M. and Mazzella, G., "Foam Separation", Industrial Water and Wastes, 6, 71 (May 1961)
- (109) Lacy, W. J., "Flotation Method for Treatment of Low and Intermediate Level Wastes", ORNL CF-57-9-31 (1957)
- (110) Woodward, R. L. and Robeck, G. G., "Removal of Radiological, Biological and Chemical Contaminants from Water", R. A. Taft Sanitary Engineering Center, Technical Report W59-2 (1959)
- (111) Pressman, M., Lindsten, D. C. and Schmitt, R. P., "Removal of Nuclear Bomb Debris, Strontium-90, Yttrium-90 and Cesium-137 - Barium-137 from Water with Corps of Engineers Mobile Water-Treating Equipment", ERDL-1673-RR (May 1961)
- (112) Lindsten, D. C., Schmitt, R. P. and Lacy, W. J., "Removal of Radioactive Contaminants from Water", Military Engineering, 53, 368-9 (Sept. - Oct. 1961)
- (113) Lindsten, D. C., unpublished material, ORNL 1952

REFERENCES
(Continued)

- (114) Lauderdale, R. A. and Emmons, A. H., "A Method for Decontaminating Small Volumes of Radioactive Water", J.A.W.W.A., 43, 327-30 (1951)
- (115) Nease, F. R. unpublished material based on data gathered by TVA under AEC sponsorship, ORNL (1951)
- (116) Lacy, W. J., Donahew, A. L., Lown, H. N. and Lindsten, D. N., Decontamination of Radioactively Contaminated Water with Water Purification Unit, Hand Operated 1/4-gpm and by a Field Expediant, Salty Dog III", ERDL-1404 (May 1955)
- (117) Lauderdale, R. A. and Eliassen, R., "The Removal of Radioactive Fallout from Water by Municipal and Industrial Water Treatment Plants", NYO-4441 (1956)
- (118) Setter, L. R. and Russell, H. H., "Chemical Coagulation Studies on Removal of Radioactivity in Water", J.A.W.W.A., 50, 590 (1958)
- (119) Hawkins, M. B., "The Influence of Reservoir Characteristics on the Internal Radiation Dose Resulting from the Consumption of Fallout-Contaminated Water", U. of California CDRP Series 2 Issue 32, December 1, 1960
- (120) Hawkins, M. B., "Procedures for the Assessment and Control of the Shorter Term Hazards of Nuclear Warfare Fallout in Water Supply Systems", U. of California CDRP Series 2 Issue 34, March 1, 1961

XI. GLOSSARY

A	empirical constant for sublimation or vaporization reaction
A	radioactivity after some period of decay
A_G	radioactivity already present in the intestinal tract at time of ingestion of contaminated water
A_{GI}	radioactivity present in the intestinal tract at some time after ingestion of contaminated water
A_I	radioactivity already incorporated into body tissue at time of ingestion of contaminated water
A_n	a parameter of the effective decay rate in the body of a given isotope
A_o	initial radioactivity per unit volume of contaminated water taken into the body
A_s	($\sigma f N_k$)
A'_s	$[\frac{f_w}{10^{12}}] A_s$
A_T	radioactivity present in body tissue resulting from decay of that activity initially present in tissue (A_I) after some time of effective decay
A_t	activity at time t
A_t	activity, in disintegrations per second, of the radionuclide in a target, after the nuclide has been removed from the flux for a period θ ;
A_X	radioactivity incorporated into tissue from that activity originally present in the intestinal tract (A_G)
a	cloud horizontal semi-axis
a_o	fireball horizontal semi-axis at ground zero
a_Z	fireball horizontal semi-axis at Z
B	empirical constant for sublimation or vaporization reaction
B	ratio of fission to total yield
Body Burden	radioactivity incorporated into body tissues as a result of ingestion of radioactivity
b	cloud vertical semi-axis

GLOSSARY
(Continued)

b_o	fireball vertical semi-axis at ground zero
b_Z	fireball vertical semi-axis at Z
C	empirical constant for sublimation or vaporization reaction
D	instrument response factor
D	daily water intake, volume
D_X	exposure dose
$d(t, 1)$	decay correct ion factor for H + 1 hour
$FD_r(t)$	fraction of device contour ratio
$FP_r(t)$	fission-product contour ratio
f	thermal flux in neutrons per square centimeter per second;
f_j	fugacity of the element in the liquid phase
f_w	a coefficient relating ingested radioactivity to Body Burden
g	acceleration due to gravity
h	cloud center height
$I_X(t)$	fallout intensity at time t
$i_{fp}(t)$	air ionization rate per fission at 3 ft above an infinite, ideal plane for a uniform distribution of the normal fission product mixture
$i_{fp}^*(t)$	air ionization rate per fission at 3 ft above an infinite, ideal plane for a uniform distribution of the condensed fission product mixture
$i_1(t)$	air ionization rate per fission at 3 ft above an infinite, ideal plane for a uniform distribution of the neutron induced activities
k	relative abundance of the isotope from which the radionuclide is formed
k	arbitrary constant
k_a	fireball horizontal semi-axis expansion constant
k_b	fireball vertical semi-axis expansion constant
k_j	Henry's Law constant

GLOSSARY
(Continued)

k_j^o	$k_j/[n(\ell)/V]RT$
k_z	inverse time constant
$M_r(t)$	mass contour ratio
M_x	mass of fallout per unit area at any downwind distance, X
m	mass
m	disintegration multiplier
N	the total number of atoms of the element in the target;
N_{fp}	number of atoms, or moles, of fission products per unit area
N_j	mole fraction of element j in the liquid phase
N_j^o	mole fraction of element j in the vapor phase
$N_{\alpha}^*(A)$	number of atoms (of the end member of mass chain and condensed on the outside of the particle) which land per square foot of ground
n	number of moles of vapor
$n(\ell)$	total moles of liquid carrier
n_j	abbreviation of $n_{jA}(t)$
n_j'	amount of element j condensed on the surface of the solid particles
n_j''	amount of element j in the vapor phase
n_j^o	abbreviation of $n_{jA}^o(t)$
$n_{jA}(t)$	number of moles of element j with mass number A dissolved in the $n(\ell)$ moles of liquid carrier, which is the particle in the liquid phase, prior to solidification
$n_{jA}^o(t)$	number of moles of element j with mass number A, which is mixed with moles from other mass chains to form n moles of vapor and not condensed in the liquid carrier
p	empirical constant in particle falling velocities relation
p_j	sublimation or vaporization pressure
p_j^*	partial pressure of the liquid

P_j^s	sublimation pressure
P_{jA}^s	$(y_{jA}''/Y_j'') P_j^s$
q	empirical constant in particle falling velocities relation
q_X	terrain shielding factor
R	molar gas constant
R_s	initial fireball spherical radius
$r_o(A, t)$	fractionation number of the first period of condensation
$r_o'(A, t)$	fractionation number of the second period of condensation
$r_X(t)$	gross fission product fractionation number
T	absolute temperature
T	half-life of the radionuclide formed
T_{eff}	time required for a radioactive element fixed in the tissue of an animal body to be diminished 50 per cent as a result of combined action of physical decay and biological elimination
$T_{\frac{1}{2}}$	radioactive (physical) half-life
t	time of irradiation
t	time
t_a	time of arrival for particle falling out of the cloud
t_c	time of cessation for particle falling out of the cloud
t_f	particle falling time in the fireball
t_r	particle rising time in the fireball
V	molar volume
V_f	average particle falling velocity
V_w	wind velocity
V_Z	instantaneous particle falling velocity
W	weapon yield in kiloton TNT units
X	longitude axis in ground coordinates system
x	longitude axis in cloud coordinates system

GLOSSARY
(Continued)

Y	latitude axis in ground coordinate system
Y_A	total amount of radionuclides for the entire chain yield of mass number A
$Y_j(t)$	total amount of radionuclides of element j present at time t
Y_j^0	total number of atoms of element j of all mass numbers
Y_m	maximum half-width of the crosswind distance on a 1 r/hr contour
y	latitude axis in cloud coordinate system
$y_{jA}(t)$	amount of radionuclides of element j and mass number A present at time t after fission
y_{jA}^0	number of atoms of element j of mass number A not condensed in the liquid carrier
Z	altitude axis of ground coordinate system
Z_0	yield dependent multiplier in fireball altitude equation
z	altitude axis in cloud coordinate system
z_a	smallest intercept of particle falling slope with cloud
z_t	largest intercept of particle falling slope with cloud
α	particle size parameter
α_m	maximum or minimum
α_0	X/h
λ_b	a constant expressing the biological rate of elimination of radioactivity
λ_{eff}	a constant expressing the rate of attenuation of radioactivity in the body as a result of both physical decay and biological elimination
λ_p	disintegration constant; the fraction of the number of atoms of a radioactive nuclide which decay in unit time
σ	activation cross section in square centimeters for 2200 m/sec neutrons
θ	time of decay

XII. STAFF

The following professional personnel have contributed to the preparation of this report:

F. Bellinger	Chief, Chemical Sciences and Materials Division, Engineering Experiment Station
G. G. Eichholz	Professor of Nuclear Engineering
W. N. Grune	Professor of Civil Engineering
R. H. Fetner	Associate Professor of Applied Biology
P. G. Mayer	Associate Professor of Civil Engineering
D. S. Harmer	Research Associate Professor, Physics
T. F. Craft, Jr.	Assistant Research Chemist
T. L. Erb	Research Assistant (Physics)
C. H. Kaplan	Research Assistant (Sanitary Engineering)
J. H. Mehaffey, Jr.	Research Assistant (Electrical Engineering)
W. M. Sloan	Research Assistant (Sanitary Engineering)
N. C. Aaron	Graduate Research Assistant (Mathematics)
C. F. Chueh	Graduate Research Assistant (Chemical Engr.)
S. K. Yu	Graduate Research Assistant (Physics)
J. M. Gutermuth	Technical Assistant (Chemical Engineering)
D. F. Hill	Technical Assistant (Chemistry)
C. T. Hill	Graduate Student (Sanitary Engineering)
R. M. Shaw	Graduate Student (Sanitary Engineering)

APPENDIX A

Excerpts from Quarterly Technical Report #3

F. Preliminary Evaluation of Water Supply Contamination for Selected Cities

1. Introduction

In order to have some basis for evaluating the relative hazard of nuclear fallout to the water supplies of different cities, attacks have been assumed on each city that would result in the same intensity over each watershed involved.

From this, the contamination of the water due to the soluble portion of the fallout has been calculated for $H + 1$ hour. Simplifying assumptions were made in regard to an average intensity over the specific watersheds and as to the time factors involved. These assumptions were made to provide a basis for the calculations of the activity concentrations shown in Table IV. These values are shown principally to demonstrate the approach being taken and to give an idea of the maximum contamination that could be expected immediately following a nuclear emergency.

The approach to be taken in future study will be more specific. Factors that will be taken into account to give somewhat more reasonable values, will be: (1) a realistic superimposition of intensity contours upon the specific watersheds with regard to seasonal wind directions and target sites, (2) consideration of decay factors to give expected activity at times later than $H + 1$ hour, (3) consideration of watershed characteristics such as runoff coefficient, feed-stream velocities, reservoir draft, transport phenomena, and reservoir mixing properties, (4) integration of intensity contours to give a more precise value for specific isotopic activities on the watershed and (5) a conversion of intensity to activity for sites off the downwind axis employing a known relationship to the predetermined values directly downwind.

Table IV

Activity Concentrations in Water of Selected Isotopes
Following 5 MT Nuclear Attacks

Radionuclide Concentration in Water ($\mu\text{c}/\text{ml}$)

City	Case (a)	Sr-89	Sr-90	Ru-106	I-131	Cs-137	Ba-140
Denver Colo.	I	2.7×10^{-3}	2.4×10^{-5}	3.0×10^{-3}	3.0×10^{-1}	1.9×10^{-4}	2.2×10^{-1}
	II	5.1×10^{-1}	4.6×10^{-3}	5.6×10^{-2}	5.7	3.5×10^{-3}	4.1
Duluth Minn.	I	7.3×10^{-4}	7.2×10^{-6}	8.2×10^{-5}	8.0×10^{-3}	4.9×10^{-6}	8.7×10^{-3}
	II	Not applicable					
Houston Texas	I	4.5×10^{-3}	4.1×10^{-5}	5.0×10^{-4}	5.0×10^{-2}	3.1×10^{-5}	3.6×10^{-2}
	II	4.5×10^{-1}	4.1×10^{-3}	5.0×10^{-2}	5.0	3.1×10^{-3}	3.6
New York N. Y.	I	10.1×10^{-4}	9.3×10^{-6}	1.1×10^{-4}	1.2×10^{-2}	7.2×10^{-6}	8.3×10^{-3}
	II	3.2×10^{-2}	2.9×10^{-4}	3.5×10^{-3}	3.5×10^{-1}	2.2×10^{-4}	2.6×10^{-2}
Springfield Mass.	I	1.2×10^{-3}	1.5×10^{-5}	1.4×10^{-4}	1.4×10^{-2}	8.5×10^{-6}	9.9×10^{-3}
	II	9.5×10^{-2}	8.5×10^{-4}	1.1×10^{-2}	1.1	6.5×10^{-4}	7.6×10^{-1}

(a) Case I applies to water surface only

Case II applies to total area of watershed

By employing the aforementioned characteristics and variables, it is believed that activity concentrations will be reached that would approach a realistic case.

2. Calculation of Activity Concentration

The calculation of concentration of activity used in the preliminary study is based upon a consideration of the area of the water surface, the volume of water, and the total watershed area. In the case of Duluth, Minnesota, where the entire municipal water supply is obtained from Lake Superior, only the depth of the lake at the intake point was considered.

Current information on the characteristics of the watersheds was obtained in each case from officials of the municipal water supply system involved or their engineering consultants. Data used in this report is tabulated in Table VI.

TABLE VI

Characteristics of Watersheds Serving Selected Cities

<u>City</u>	<u>Total Watershed Area (ft.²)</u>	<u>Total Water Surface (ft.²)</u>	<u>Total Water Volume (liters)</u>
Denver, Colo.	8.29×10^{10}	4.36×10^8	2.34×10^{11}
Houston, Tex.	7.84×10^{10}	7.85×10^8	2.50×10^{11}
New York, N. Y.	4.24×10^{10}	1.37×10^9	1.90×10^{12}
Springfield, Mass.	1.30×10^9	1.68×10^7	1.97×10^{10}

As an example of the procedure used, the derivations of the concentrations in the Denver, Colorado water supply prior to any municipal treatment are presented here in detail. The other cities listed in Table IV were analyzed in the same manner as Denver, except for Duluth which is presented separately.

Denver Case I

In case I, only that radioactive fallout deposited directly on water surfaces was considered as the source of the water contamination. The following assumptions were made prior to the calculation.

1. 5 MT bomb attack.
2. Wind speed of 15 mph.
3. An intensity of 5,500 r/hr over the entire watershed.
4. Complete homogeneous solution of the soluble portion of the fallout in the water within one hour.
5. A ratio of soluble radioactive atoms per square foot to intensity was chosen as that value for each isotope at 51.5 miles directly downwind.
6. That there will be no change in concentration of radioactivity either due to reservoir draft or feed-in.
7. That only Sr-89, Sr-90, Ru-106, I-131, Cs-137, and Ba-140 would be considered.
8. That the volume and area of feed streams will not affect the final concentration appreciably.

The soluble activity density, for each of the six isotopes being considered, in atoms/ft² was calculated as follows:

Given:

$$I(1) = 5,500 \text{ r/hr,}$$

$$\frac{N_4^*(89)}{I(1)} = 6.17 \times 10^{10} \text{ atoms/ft}^2/\text{r/hr,}$$

$$\frac{N_4^*(90)}{I(1)} = 11.1 \times 10^{10} \text{ atoms/ft}^2/\text{r/hr,}$$

$$\frac{N_4^*(106)}{I(1)} = 4.87 \times 10^{10} \text{ atoms/ft}^2/\text{r/hr,}$$

$$\frac{N_4^*(137)}{I(1)} = 10.7 \times 10^{10} \text{ atoms/ft}^2/\text{r/hr,}$$

$$\frac{N_4^*(137)}{I(1)} = 9.19 \times 10^{10} \text{ atoms/ft}^2/\text{r/hr, and}$$

$$\frac{N_4^*(140)}{I(1)} = 12.4 \times 10^{10} \text{ atoms/ft}^2/\text{r/hr,}$$

where the subscript 4 is the value of the particle size parameter, α , corresponding

to the downward distance.

By multiplying 5,500 r/hr by $N_4^*(A)/I(1)$ for each isotope, the total number of soluble atoms of each isotope per square foot, $N_4^*(A)$, will be obtained. This value for each isotope was found to be as follows:

$$N_4^*(A) = \frac{N_4^*(A)}{I(1)} I(1)$$

$$N_4^*(89) = 3.40 \times 10^{14} \text{ atoms/ft}^2$$

$$N_4^*(90) = 6.10 \times 10^{14} \text{ atoms/ft}^2$$

$$N_4^*(106) = 2.68 \times 10^{14} \text{ atoms/ft}^2$$

$$N_4^*(131) = 5.89 \times 10^{14} \text{ atoms/ft}^2$$

$$N_4^*(137) = 5.05 \times 10^{14} \text{ atoms/ft}^2$$

$$N_4^*(140) = 6.82 \times 10^{14} \text{ atoms/ft}^2$$

Multiplying the $N_4^*(A)$ value for each of the isotopes by the total area of water surface will give the total number of atoms, $N(A)$, of each isotope in soluble form, deposited in the water.

$$N_4^*(A) \times \text{Area} = N(A) \text{ atoms}$$

$$N(89) = 3.40 \times 10^{14} \times 4.36 \times 10^8 = 14.8 \times 10^{22} \text{ atoms}$$

$$N(90) = 6.10 \times 10^{14} \times 4.36 \times 10^8 = 26.6 \times 10^{22} \text{ atoms}$$

$$N(106) = 2.68 \times 10^{14} \times 4.36 \times 10^8 = 11.7 \times 10^{22} \text{ atoms}$$

$$N(131) = 5.89 \times 10^{14} \times 4.36 \times 10^8 = 25.7 \times 10^{22} \text{ atoms}$$

$$N(137) = 5.05 \times 10^{14} \times 4.36 \times 10^8 = 22.0 \times 10^{22} \text{ atoms}$$

$$N(140) = 6.82 \times 10^{14} \times 4.36 \times 10^8 = 29.7 \times 10^{22} \text{ atoms}$$

Thus knowing the total number of soluble atoms of each isotope; division by

the total water volume, V, in liters will give the concentration of each isotope in atoms per liter.

$$C_A^* = \frac{N(A)}{V} \frac{\text{atoms}}{\text{liter}} \quad (21)$$

$$C_{89}^* = \frac{14.8 \times 10^{22}}{2.34 \times 10^{11}} = 6.33 \times 10^{11} \text{ atoms/liter}$$

$$C_{90}^* = \frac{26.6 \times 10^{22}}{2.34 \times 10^{11}} = 11.4 \times 10^{11} \text{ atoms/liter}$$

$$C_{106}^* = \frac{11.7 \times 10^{22}}{2.34 \times 10^{11}} = 4.99 \times 10^{11} \text{ atoms/liter}$$

$$C_{131}^* = \frac{25.7 \times 10^{22}}{2.34 \times 10^{11}} = 11.0 \times 10^{11} \text{ atoms/liter}$$

$$C_{137}^* = \frac{22.0 \times 10^{22}}{2.34 \times 10^{11}} = 9.40 \times 10^{11} \text{ atoms/liter}$$

$$C_{140}^* = \frac{29.7 \times 10^{22}}{2.34 \times 10^{11}} = 12.7 \times 10^{11} \text{ atoms/liter}$$

We may now convert the activity in atoms/liter to microcuries/milliliter ($\mu\text{c}/\text{ml}$) by using an appropriate conversion factor for each isotope.

First, to change from atoms/liter to disintegrations per minute per liter, $\frac{\text{dpm}}{\ell}$, the following relationship is used.

$$C_n = C_A^* \lambda \quad (22)$$

Where: C_n = Concentration of activity in dpm/ℓ .

C_A^* = Concentration of activity in atoms/ ℓ , and

λ = Characteristic time constant defined by the equation

$$\lambda = \frac{.693}{T_{1/2}}$$

Where: $T_{1/2}$ = physical half-life of the specific isotope in minutes.

Since there are 2.22×10^{12} dpm/curie, a constant for all isotopes, division of C_n by this value will give the concentration in curies/liter.

$$C_c = \frac{C_n}{2.22 \times 10^{12}} = \frac{C_A \lambda}{2.22 \times 10^{12}}$$

where C_c is the concentration of radioactivity in curies per liter.

Multiplication of C_c by 10^3 will convert curies/liter to microcuries/milliliter. The entire conversion factor for each isotope is then

$$K_A = \frac{\lambda}{2.22 \times 10^9}$$

The conversion factor, K_A , for each of the six isotopes being studied are:

$$K_{89} = 4.25 \times 10^{-15}$$

$$K_{90} = 2.12 \times 10^{-17}$$

$$K_{106} = 5.95 \times 10^{-16}$$

$$K_{131} = 2.72 \times 10^{-14}$$

$$K_{137} = 1.93 \times 10^{-17}$$

$$K_{140} = 1.70 \times 10^{-14}$$

By multiplying each conversion factor by the respective concentration of each isotope in atoms per liter, the following values were obtained.

$$C(89) = 2.7 \times 10^{-3} \mu\text{c/ml}$$

$$C(90) = 2.4 \times 10^{-5} \mu\text{c/ml}$$

$$C(106) = 3.0 \times 10^{-4} \mu\text{c/ml}$$

$$C(131) = 3.0 \times 10^{-2} \mu\text{c/ml}$$

$$C(137) = 1.9 \times 10^{-5} \mu\text{c/ml}$$

$$C(140) = 2.2 \times 10^{-2} \mu\text{c/ml}$$

Case II

In this case the soluble fraction of the fallout particles deposited over the entire watershed was assumed to have been transported to and homogeneously dispersed in the streams and reservoirs. Other assumptions were the same as for Case I. To continue the Denver example, in Case II, the watershed area of $8.29 \times 10^{10} \text{ ft}^2$ was multiplied by the N_4^* value for each isotope to give the total number of atoms of each isotope. The remaining calculations were carried out in the same fashion as for Case I.

Duluth, Minn.

The entire water supply for the city of Duluth is obtained from Lake Superior, and hence, this situation is different from that at the other cities studied. The Duluth intake line extends out 1156 feet into the lake and terminates at a lake depth of 72 feet. The fallout deposited over this intake was considered to be evenly dispersed throughout this depth of water, and from this assumption the number of atoms per unit volume and subsequently the activity in $\mu\text{c/ml}$ was calculated.

3. Conclusions

In all of the cases thus far studied, the time factor has not been considered. Even at an assumed wind velocity of 15 miles per hour, a number of hours would have to elapse before the arrival of particulate matter at the far reaches of a distant watershed. Even if the material landed directly in the water, much more time would be involved in transportation in streams and through reservoirs to the

intake of the water works. There would be further delay in getting into streams those particles deposited initially on dry surfaces. Another delay would be in the occurrence of rainfall of sufficient intensity to dissolve and/or wash this material into streams. All of this time will allow radioactive decay to proceed thus ameliorating the hazardous effects of the fallout.

I. Decontamination of Water Supplies*

1. Removal by Conventional Water Treatment Processes

Conventional municipal water purification processes generally include aeration, chemical coagulation with sedimentation, rapid sand filtration and chlorination⁽⁷⁹⁾. To a lesser extent, lime-soda ash softening and slow sand filtration are used. Except for aeration, the processes are capable of removing radioactive contamination to some degree, either singularly or in combination. The decontamination capability of each type of process is discussed separately below, with particular reference to the six elements, barium, cesium, iodine, lanthanum, ruthenium and strontium.

a. Chemical Coagulation

The most common coagulants in water treatment, aluminum and iron salts, form aluminum or ferric hydroxides which precipitate as floc. The chemical floc acts as an efficient scavenger by adsorbing, entrapping or otherwise bringing together suspended matter, particularly that which is colloidal in nature. The artificial increase of the alkalinity in water may also form the hydroxides of heavy metals, which co-precipitate with the aluminum or ferric hydroxide.

Coagulation, followed by sedimentation, has been extensively studied by ORNL⁽⁸⁰⁾ with reported removals of only 36% and 51% for Cs and Sr, respectively. It appears that the method is effective for the removal of suspended or colloidal material and for most cations of valence 3, 4 or 5, including the rare-earths group. Removals in excess of 98% have been reported for P-32 as the orthophosphate⁽⁸¹⁾⁽⁸²⁾.

Removal of Ba, I and La by coagulation was investigated by Lacy⁽⁸³⁾, with a maximum of 70.7% found for both Ba and La, but only 45% for I.

* References begin on page 155.

Matsumura⁽⁸⁴⁾ states that Ru can be removed up to 92% by chemical coagulation.

b. Rapid Sand Filtration

The amount of radioactivity removed by filtration will vary depending on the nature of the material. Y and Zr, probably present in the colloidal state, were removed from up to 93% by sand filtration alone as reported in a comprehensive ORNL report⁽⁸⁰⁾, whereas materials such as Sr (4%) and Cs (50%) present in true solution, were not greatly reduced by passage through sand filters. They further reported that Ba and La could be removed up to 95% and 74%, respectively.

No data were reported on the removal of I or Ru by rapid sand filtration.

c. Chlorination

Hannah, et al⁽⁸⁵⁾ studied various methods for the removal of I-131 from water, and found that small dosages of chlorine in the presence of 100 ppm activated carbon produced up to 80% removal. The authors⁽⁸⁵⁾ concluded that the only effective method found for removing I-131 with materials normally available in water treatment plants involves chlorination followed by adsorption of liberated iodine on activated carbon. The optimum chlorine dosages were quite small, i.e., 0.05 to 0.1 ppm. The removal of I-131 decreases to less than 20% when the dosage of chlorine increases to 1ppm. Therefore, normal pre-chlorination employed by the water treatment plant could not be used for iodine removal because the chlorine residuals would generally exceed the required dosage for activity removal. Stable iodine, in dosages greater than 0.01 ppm, inhibited removal of I-131 with chlorine and Aqua Nuchar A (activated charcoal). Variation of pH, achieved by adding sulfuric acid and sodium hydroxide, was found to have little effect on the removal of iodine by chlorine and activated charcoal.

d. Lime-Soda Ash Softening

Softening plants remove excessive amounts of scale-forming, soap-consuming compounds, chiefly comprised of the cations of calcium and magnesium, by the addition of lime and soda ash which precipitates calcium as a carbonate and magnesium as a hydrate. Because of the similarity in the chemical properties between strontium and calcium, the former ion is co-precipitated. For most satisfactory removals of strontium, Hoyt ⁽⁸⁶⁾ found that excess dosages of both lime and soda ash were required. Removal efficiencies of 99.7% ⁽⁸⁰⁾ are possible under favorable conditions. Other isotopes which can be effectively removed by the lime-soda ash are: Ba, Cd, Y, Sc, Zr and Nb. The removal of Ba (99%) and La (90%) was reported by McCauley, et al ⁽⁸⁷⁾. ORNL ⁽⁸⁸⁾ reported that Cs could be removed by lime-soda softening, but not efficiently (25%).

e. Slow Sand Filtration

Downing, et al ⁽⁸⁹⁾ reported that the slow sand filter was very effective in the removal of radiostrontium in the first few days of operation, but that the efficiency decreased rapidly and essentially drops to zero at 14 days. In another paper, presented by Eden, et al ⁽⁹⁰⁾, on experiments carried out in the same Water Pollution Research Laboratory in Britain, the slow sand filter appeared to be effective for only a few hours. The activity of the effluent rose steadily and reached 30% of the initial (unfiltered) water in one day, 70% in 2 days, and 95% after 7 days. Eden, et al ⁽⁹⁰⁾ also reported that iodine was not efficiently (50%) removed by the slow sand filter.

2. Removal by Non-Conventional Treatment Methods

Below are listed several methods of decontamination of water not commonly employed in municipal treatment plants. Economic considerations may limit the use of many of these methods, except in emergency cases.

a. Ion Exchange

A few water treatment plants use ion exchange as a softening measure. Resins have been found to provide one of the most effective methods of

decontamination. Over 99.9% removal of Ba, Cd, Ce, Cs, I, La and over 99% removal of P and Zr was quoted by ORNL ⁽⁸⁰⁾, and Amphlett and Sammon ⁽⁹¹⁾ reported work using mixed beds. A decontamination factor of 10^4 to 10^5 may be achieved if leakage is eliminated ⁽⁹²⁾. The natural greensands, used in some municipal softening installations, are not effective in the removal of anions.

Although the ion exchange process offers one of the most promising methods for removing radio-contaminants, the cost may preclude widespread application unless suitable regeneration techniques are developed.

The possibility of using home water softeners, of the ion exchange type, has been discussed in the literature ⁽⁹³⁾.

b. Phosphate Coagulation

Because the conventional method employing alum or iron salt as the coagulant does not effectively remove Sr and many other isotopes, Lauderdale ⁽⁹⁴⁾ investigated phosphate coagulation as a means of increasing removals. A more comprehensive study was made later by Nesbitt, et al ⁽⁹⁵⁾. Based on the theoretical considerations, as well as experimental observations, Nesbitt ⁽⁹⁵⁾ concluded that the mechanisms of the removal of radioactivity are coprecipitation and adsorption. Nesbitt reported a 98% strontium removal. The three variables which were found to exert the greatest influence on coagulation were pH, calcium concentration, and phosphate concentration. Careful control of these variables was necessary to achieve optimum strontium removals.

Tamura and Strumess ⁽⁹⁶⁾ reported that low cost natural phosphates could be used in place of sodium phosphate. The authors reported that over 90% removals were achieved with these minerals.

Removal of 87.8% for Ba, 98% for La and 85% for Ru have been reported by Matsumura ⁽⁹⁷⁾. Cowser et al ⁽⁹⁸⁾ report only 35% removal of Cs using phosphate coagulation.

c. Modified Coagulation and Lime-Soda Ash Softening

At least two modified coagulation processes have been studied, one of which is the continuous addition of clay. One modification of the process is the addition of small amounts of silver nitrate to increase the removal of iodide. The removal of 95.5% I-131 has been reported by Eden, et al⁽⁹⁸⁾.

Lacy and de Laguna⁽⁹⁹⁾ report removals of 99.7% for Ba and Cs, and 97.4% for Ru when coagulation is supplemented by clay addition. Cowser, et al⁽⁹⁷⁾ using a lime-soda ash softening process with the addition of clay, reported ruthenium removals of 76%. The removal of cesium averaged 86% with clay doses of 200 ppm.

d. Metallic Dusts

Lacy⁽¹⁰⁰⁾ conducted laboratory jar-test studies for the removal of radioactive contaminants by employing various concentrations of powdered aluminum, copper, iron and zinc. In general, highest removals were obtained with iron powder. Removals of 37.2% of I were reported⁽⁸⁰⁾. In 1962, a patent was granted to Silker⁽¹⁰¹⁾ for removing P, As, Mn, the rare earth metals, and actinides from aqueous solutions by sorption on particles of aluminum metal.

e. Clay Materials

Straub, et al⁽⁸¹⁾ and others⁽¹⁰²⁾⁽¹⁰³⁾⁽¹⁰⁴⁾ reported the use of various types of clays (kaolinite, montmorillonite and shales) for the removal of specific radioisotopes from water and waste solutions. The clays were found to be especially suitable for the removal of Cs, Zr and Nb. With the addition of 5,000 ppm of clay, removal of over 98% of Cs was reported⁽⁸⁰⁾. Amphlett and Sammon⁽⁹¹⁾ reported 95% removal of Sr. This method can not be economically justified because large volumes of clay must be handled both initially and as a contaminated sludge. This method has its greatest potential use where geologic and hydrologic conditions are such that the ground itself may be used for disposal of the sludge. Studies have also been made^(105,106) on the use of clay for high level waste disposal by fixing specific radioisotopes into clay by means of high temperature treatment.

f. Oxidation-Reduction

This method was especially designed to improve Ru removal. Ruthenium is often present in the form of a nitrosyl-ruthenium complex which is difficult to remove by coagulation procedures. An approach to the problem, described by Amphlett and Sammon (91), involves pre-treatment with an oxidizing agent to destroy the ruthenium complexes, followed by a calcium phosphate-ferrous phosphate floc in the presence of NaHSO_3 to maintain the ruthenium in a reduced form. As high as 99% of ruthenium was removed when 100 ppm NaHSO_3 was used.

g. Foaming

A foam separation technique, based on surface activity phenomena, was recently developed by Radiation Applications, Inc., Long Island City, New York (107). A reduction of the concentration of radioactive strontium-90 and cesium-137 from 10^{-5} to 10^{-12} molar in low-level nuclear waste was claimed. The concentration of the foaming agent is one of the most critical factors in determining the separation factor (surface adsorption factor). A detailed discussion of the theory as well as experimental observations of the foam separation technique was presented by Schoen and Mazzella (108).

Lacy (109) investigated the flotation process in 1957 and reported removals of up to 78% for Ba-140-La-140, 85% for Cs-137, 74% for Ru and 68% for Sr-90. These studies were conducted using cetylpyridinium chloride as the surface-active agent and foaming by aeration.

3. Emergency Methods for the Decontamination of Radioactive Water

According to the literature, very few emergency decontamination units are now available for municipal use, although the U.S. Army has developed several mobile units which could find wide application for public use. Several smaller decontamination units are commercially available, most of which employ ion exchange techniques.

Supplementary treatment to the conventional water treatment processes would probably be the most efficient means of supplying potable water to a large number of people, following radioactive contamination of the water.

a. Municipal Size Decontamination Units

Woodward and Robeck ⁽¹¹⁰⁾ report on an ion exchange process that may be used to supplement the normal water treatment procedure. An ion exchange column in the form of a cartridge is inserted into the system, and is disposed of after breakthrough occurs. The type of resin will vary according to the time after detonation that the water will be put into use. A mixed-bed resin will be necessary for immediate use of the water, whereas a cation resin will suffice for long-term usage, due to the decay of short-lived iodine-131. The life of each ion cartridge will depend upon the total solids present.

Although large, centrally located, decontamination units are more economical, smaller decentralized units would be preferable as the problem of water distribution would be lessened.

b. Field Decontamination Units

The U.S. Army ⁽¹¹¹⁾ ⁽¹¹²⁾ has developed several mobile decontamination units primarily for use by troops in the field, but these could also be used to supply water for small population groups in case of nuclear attack. One such unit is comprised of a flocculator, filters, dual-bed ion exchange column and a chlorinator. The entire unit is mounted on two 2-1/2 ton trucks. A 1,500 gph output is obtainable. Regeneration of the ion exchange resins is effected by hydrochloric acid and soda ash.

c. Miscellaneous Decontamination Units

Lamotte Chemical Company has developed a mixed ion exchange resin bed ⁽¹¹³⁾, which has been found useful for the decontamination of radioactive

water. The unit consists of a bed of Amberlite resin MP-3 (IR-120 and IRA-410) and is capable of producing 10 gallons of water of triple distilled quality.

A unit developed by Lauderdale and Emmons ⁽¹¹⁴⁾ consists of twin columns of steel wool, burnt clay and activated carbon in one column and a mixed bed ion exchange resin in the other. Approximately 30 liters of water can be decontaminated with an efficiency exceeding 99.9%.

Nease ⁽¹¹⁵⁾ and Lacy ⁽¹¹⁶⁾ describe a method of radioactive water decontamination whereby the water is passed through a column of natural materials, such as clay, leaves, humus, gravel and sand. Removals of over 90% were reported. The problem would be to obtain uncontaminated materials from the environment for use in such a column.

4. Discussion and Conclusions

The more important radioisotopes that appear initially in contaminated water are Ba, Cs, I, La, Ru and Sr. Laboratory data indicate that the combination of conventional water treatment methods, namely, chemical coagulation, lime-soda ash softening, and sand filtration, is capable of removing 99% strontium. The removal of 95% iodine can be accomplished by the addition of silver ions. 86% cesium can be removed by the lime-soda ash softening procedure when proper amounts of clay are added.

The efficiency of gross activity removal lies generally between 50 and 75% in plant scale operation ⁽¹¹⁷⁾. The lower plant scale efficiencies, in comparison to the laboratory results, are believed to result from the fact that: (a) only one or two decontamination processes, among those mentioned, are employed by the usual water treatment plant, and the operating conditions may not be optimized; and (b) in the laboratory, the radioactive materials are generally present in the form of simple salts. In contrast, the radioactive

materials reaching the water treatment plant are generally believed to be in chemical forms which are more difficult to remove because the portion which is readily removed has already been eliminated by natural decontamination mechanisms before reaching the water plant. Setter and Russell⁽¹¹⁸⁾ stated that the longer the activity has been subjected to natural purification, the more difficult it is to remove the remaining soluble activity by coagulation.

It should be pointed out here that the decontamination data reported in the literature, both on laboratory and plant scale, are based on one of the following three sources of radioactivity:

- (1) added radioactive salts
- (2) low level radioactivity waste
- (3) long-range (world-wide) fallout from atomic bomb tests

The chemical and physical characteristics of radioactive materials from any of the above sources is different from that present in local fallout. The latter is characterized by its low water solubility of 1% to 2% in comparison to the 50% or higher solubility of radioactive materials of the above three categories. Low water solubility generally will increase the removal of local fallout by conventional water treatment methods which are efficient in dealing with particulate or colloid materials.

The maximum decontamination factor for each of six selected elements above are listed in Table X. These values are based on the best available data in the literature. It is emphasized that the percentage of removal is greatly dependent on the chemical form and physical state of the radioactive element as well as the concentration of the treatment additives and other related conditions such as pH and temperature of the water. As an example of the decontamination factors required to reduce activity to the MPC, based on hypothetical

Table X

Maximum Decontamination Factors Reported in the Literature for Selected Isotopes

Decontami- nation Method	Decontamination Factors (D.F.) and References					
	Ba-140	Cs-137	I-131	La-140	Ru-106	Sr-89,90
1. Chemical Coagulation	3.4 (83)	1.5 (80)	1.8 (83)	3.4 (8f)	12.5 (84)	2.0 (80)
2. Lime-Soda Softening	10^2 (87)	1.3 (88)	NR	10^1 (87)	NR	3.3×10^1 (80)
3. Rapid Sand Filtration	2×10^1 (80)	2 (80)	NR	3.8 (80)	NR	1.04 (80)
4. Ion Exchange	10^4 (80)	10^4 (80)	10^3 (91)	10^3 (80)	NR	3.3×10^3 (80)
5. Phosphate Coagulation	3.2 (84)	1.5 (97)	NR	5×10^1 (84)	6.7 (84)	4.5×10^1 (94)
6. Clay	NR	5×10^1 (80)	1.2 (80)	NR	NR	2×10^1 (91)
7. Metallic Dusts	NR	NR	1.6 (80)	NR	NR	NR
8. Coagulation w/ Silver Ions	NR	NR	2.2 (98)	NR	NR	NR
9. Oxidation- Reduction	NR	NR	NR	NR	10^2 (91)	NR
10. Coagulation with Clay	3.3×10^1 (99)	3.3×10^1 (99)	NR	NR	3.8 (99)	NR
11. Lime Soda with Clay	NR	7.1 (97)	NR	NR	4.2 (97)	NR
12. Foaming (Flotation)	4.5 (109)	6.7 (109)	NR	4.5 (109)	3.9 (109)	3.1 (109)
13. Slow Sand Filtration	NR	NR	2 (90)	NR	NR	NR

Notes:

(1) Percent Removal = $100 - (\frac{1}{D.F.})100$

(2) NR - not reported in literature reviewed

contamination of the Springfield, Mass. watershed (as reported elsewhere in this report), Table XI was prepared. It is apparent from this table that ion exchange is the only single decontamination process that will adequately remove the minimum concentration reported for the six selected isotopes and that no process will adequately remove the maximum radiocontaminant, namely I-131.

TABLE XI

D.F. and Percent Removal Required to Reduce Activity at 5 + 1 Hour to MPC

Isotope	MPC ^(a) ($\mu\text{Ci}/\text{ml}$)	Minimum Contamination		Maximum Contamination		Effective Processes (No. from Table X)	
		D.F.	% Removal	D.F.	% Removal	minimum	maximum
Ba-140 La-140	2×10^{-3}	5.0	80	3.8×10^2	99.74	Ba - 2,3,4,5,10 La - 2,4,5	4
Cs-137	1.5×10^{-3}	6×10^{-3}	None	4.3×10^{-1}	None	None required	None required
I-131	3×10^{-5}	4.7×10^2	99.8	3.7×10^4	99.997	4	None
Ru-106	1×10^{-1}	1.4×10^{-3}	None	1.1×10^{-1}	9	None required	1,2,3,4,5,12
Sr-89	7×10^{-5}	17	95	1.3×10^3	99.93	} 2,4,5,6, }	} 4 }
Sr-90	8×10^{-7}	14	94	1.1×10^3	99.91		

(a) Regulation of Radiation Exposure by Legislative Means", Handbook 61,
National Bureau of Standards (1955)

APPENDIX B

Distribution List

<u>Addressee</u>	<u>No. of Copies</u>	<u>Addressee</u>	<u>No. of Copies</u>
Office of Civil Defense, DOD Pentagon, Washington, D. C. Atten: Director for Research	38	Advisory Committee on Civil Defense National Academy of Sciences 2101 Constitution Ave. N. W. Washington 25, D. C. Atten: Mr. Richard Park	1
Army Library, Civil Defense Unit Pentagon, Washington, D. C.	3	Defense Documentation Center Arlington Hall Station Arlington, Virginia	20
Assistant Secretary of the Army (R & D) Washington 25, D. C. Atten: Assistant for Research	1	Chief, Bureau of Ships Department of the Navy (Code 335)	2
Chief of Naval Research (Code 104) Department of the Navy Washington 25, D. C.	1	Chief, Bureau of Ships (Code 203) Department of the Navy	1
Chief of Naval Operations (Op-07T10) Department of the Navy Washington 25, D. C.	1	Principal Investigator Office of Civil Defense Contract OCD-OS-62-205 General Dynamics Corp. P. O. Box 5 Old San Diego Station San Diego 10, California	1
Chief, Bureau of Naval Weapons (Code RRRE-5) Department of the Navy Washington 25, D. C.	1	Principal Investigator Office of Civil Defense Contract OCD-OS-62-186 Technical Operations, Inc. Burlington, Massachusetts	1
Chief, Bureau of Medicine and Surgery Department of the Navy Washington 25, D. C.	1	Principal Investigator Office of Civil Defense Contract: OCD-CS-62-135 Stanford Research Institute Menlo Park, California	1
Chief, Bureau of Supplies and Accounts (Code 112) Department of the Navy Washington 25, D. C.	1	Principal Investigator Office of Civil Defense Contract: OCD-OS-62-142 Naval Civil Engineering Lab. Port Hueneme, California	1
Chief, Bureau of Yards & Docks Office of Research (Code 74) Department of the Navy Washington 25, D. C.	1		
U. S. Naval Civil Engineering Laboratory Port Hueneme, California	1		

<u>Addressee</u>	<u>No. of Copies</u>	<u>Addressee</u>	<u>No. of Copies</u>
Principal Investigator Office of Civil Defense Contract: OCD-OS-62-193 Isotopes, Incorporated 123 Woodlawn Avenue Westwood, New Jersey	1	Principal Investigator Office of Civil Defense Contract: OCD-OS-62-279 Curtiss-Wright, Incorporated Caldwell, New Jersey	1
Principal Investigator Office of Civil Defense Contract: CDM-SR-59-54 Naval Radiological Defense Laboratory San Francisco, California	1	Principal Investigator Office of Civil Defense Contract: OCD-OS-62-257 Hoff R&D Laboratories, Inc. 1922 East 107 Street Cleveland, Ohio	1
Principal Investigator Office of Civil Defense Research Army Chemical Corps Department of the Army Chemical Center, Maryland	1	Principal Investigator Office of Civil Defense Contract: OCD-OS-62-106 Engineering Science, Inc. 150 E. Foothill Blvd. Arcadia, Calif.	1
Principal Investigator Office of Civil Defense Contract: OCD-OS-62-206 Ionics, Incorporated 152 - 6th Street Cambridge, Massachusetts	1	Principal Investigator Office of Civil Defense Contract: OCD-OS-62-202 Armour Research Foundation 10 West 35th Street Chicago 16, Illinois	1
Principal Investigator Office of Civil Defense Contract: OCD-OS-62-73 U. S. Army Material Office Directorate of Research and Development Washington 25, D. C.	1	Homer J. McConnell, Director Civil Defense Training Program FDA/DHEW Washington 25, D. C.	1
Principal Investigator Office of Civil Defense Cornell Aeronautical Laboratory 4455 Genesee Street Buffalo 21, New York	1	Lt. Col. Converse R. Lewis Office of the Surgeon General Main Navy Building Washington 25, D. C.	1
Principal Investigator Office of Civil Defense Contract: OCD-OS-62-144 Research Triangle Institute P. O. Box 490 Durham, North Carolina	1	Dr. Luna Leopold, Chief Water Resources Division U. S. Geological Survey Washington 25, D. C.	1
		Gordon E. McCallum, Chief Water Supply & Pollution Control Dept. of Health, Education and Welfare Public Health Service Washington 25, D. C.	1

<u>Addressee</u>	<u>No. of Copies</u>	<u>Addressee</u>	<u>No. of Copies</u>
George W. Burke, Jr. Div. of Water Supply and Pollution Control Public Health Service Washington 25, D. C.	1	H. Malcom Childers 708 North West Street Alexandria 14, Virginia	1
Pro. Thomas deS. Furman Civil Engineering Dept. University of Florida Gainesville, Florida	1	Dr. Edward Ray, Director Nuclear Science & Engineering Corp. P. O. Box 10901 Pittsburgh 36, Pennsylvania	1